5-2019

Detection of Larval Aggregations Using a Drone Mounted Thermal Imaging Camera

Megan Descalzi
University of New Haven

Comments

Committee members: Peter Massey, Sasha Voss

THE UNIVERSITY OF NEW HAVEN

DETECTION OF LARVAL AGGREGATIONS USING A DRONE MOUNTED THERMAL IMAGING CAMERA

A THESIS

Submitted in partial fulfillment

of the requirements for the degree of

MASTER OF SCIENCE IN FORENSIC SCIENCE

BY

Megan Descalzi

University of New Haven
West Haven, Connecticut
May 2019

University *of* New Haven

HENRY C. LEE COLLEGE OF
CRIMINAL JUSTICE AND FORENSIC SCIENCES

Department of Forensic Science

ACKNOWLEDGEMENTS

First and foremost, I would like to thank my supervisor, Dr. Chris O'Brien, for his unconditional support and guidance over the past two years. The knowledge I have gained and the experiences I have had in being your student have been far greater than anything I could have ever learned within a classroom. Every single day you have made me a better scientist and a better person by challenging me to "think smarter, not harder," and by pushing me outside of my comfort zone where I have learned, time and time again, that I am capable of anything. Thank you for providing me with such incredible opportunities to learn and grow from, and that have made my time here worthwhile. From our research trips to Horse Island, to traveling to present in Western Australia, to a horse necropsy and to even just sitting around laughing our asses off in the lab at your endless jokes – these moments, and so many more, will be what I remember most from my time in this program. This entire research experience is one of the best things to ever happen to me, and I am so grateful to have had the chance to be your student. While there were many times where I wanted to call it quits throughout this research, I am incredibly thankful that you constantly pushed me to keep working hard because I am now so proud of what I have been able to achieve and how far I have come since the beginning. It is above and beyond what I ever thought I could accomplish two years ago, and it all would not have been possible without you. We make a pretty good team and have accomplished a lot in this short amount of time, and I am excited to see what we continue to accomplish in the future. You are not getting rid of me that easily! Thank you for everything and for giving me the experience of a lifetime. Mad love.

Thank you to Dr. Sasha Voss and Dr. Michael Lee for collaborating with me and allowing me to further their incredible work. Also, a big thank you to Dr. Voss for always being

willing to look at my writing and presentations, and for providing such detailed and thorough feedback. It has been a pleasure working with you and I am so glad that I got the opportunity to meet you in person at the ANZFSS conference.

Thank you to Pete Massey for generously allowing me to use his handheld FLIR throughout the entirety of this research. Also, thank you for all of your moral support over the last two years and for always taking time out of your busy schedule to listen to me when I show up at your office door. I am so grateful to you for everything you have done for me and all of the opportunities you have included me in.

Thank you to all of those who have helped me at various points throughout my research, whether it was helping to maintain my fly colonies or recording data measurements during field experiments. Specifically, thank you to Emily Neverett, Mandy Pascu, Julie Pinto, Sarai Santofimio, Amanda Dye, Laura Jankowski and Bethany Hoschar. This work would not have been possible without all of your time and support.

Thank you to Dr. Robert Powers and Dr. Roman Zajac for being a part of my support team over these past two years and for always encouraging me to continue on in my education. Thank you for always keeping me laughing even through the most difficult times of completing this research. The numerous afternoons we have all spent at the lab were significant moments in my time here and will be something that I never forget. Also, thank you to Dr. Zajac for allowing us to use your boat to get to Horse Island, and to Dr. Powers for helping to teach me the ins and outs of boating.

Thank you to Rich Boardman for allowing us to utilize Horse Island as one of the experimental sites for this research. Thank you to Dr. Jeff Tomberlin, Dr. Amanda Roe and Dr. Christine Picard for donating fly pupae to help get my fly colonies up and running. Thank you to Emily Powers for her time and talent in creating the maggot drawings for this thesis document. Finally, thank you to the University of New Haven and the Henry C. Lee College of Criminal Justice and Forensic Science.

ABSTRACT

When a body's temperature reaches ambient temperature after death, remote detection of the body can become difficult. At this point, useful search tactics include the use of cadaver dogs, search parties and aerial imaging devices, all of which can be costly and time-consuming for every day law enforcement use. This study investigated the potential of a novel search technique in which a small, unmanned aerial system (drone) mounted with a forward-looking infrared radar (FLIR) was utilized to detect decomposing animal carcasses via the heat generated by associated Diptera larval aggregations. Hot water baths were utilized as analogs for larval aggregations in order to simulate varying conditions that could be encountered during a search and recovery mission, such as different sized aggregations and varying differences in temperature between aggregations and the environment. Animal carcasses were also utilized to determine the effectiveness of this search technique within the Connecticut region based on the formation of larval aggregations and the associated detection of the carcass on the days following its placement. While this research demonstrated that a thermal drone could successfully detect larval aggregations associated with a decomposing carcass, it also demonstrated that there are limitations to when or how this technique can be implemented during a search and recovery mission. An increase in drone height limited the capability of detection due to the masking of the hot water analog's and carcass's thermal signature by the surrounding environment, with a smaller heat source experiencing greater masking effects. Detection and accurate location of larval aggregations was also more likely to occur when there was minimal wind and sunlight at the time of deployment, and when ambient temperature was ideal for larval growth and development. Ultimately, the successful detection of larval aggregations was dependent upon the

ability of the drone operator to understand how these factors can affect detection and how to adjust search parameters to optimize the success of this search technique.

TABLE OF CONTENTS

LIST OF TABLES

LIST OF FIGURES

GLOSSARY

Diapause	Physiological state of dormancy during unfavorable environmental conditions
Geosynchronous hovering	Synchronous rotation with the Earth's orbit resulting in a constant position at the same point above the ground
Kariomone	Chemical signals used for interspecific communication which benefit the receiver, but harm the producer
Pheromone	Chemical signals used for intraspecific communication, which can regulate the behavior and/or physiological response of the receiver

CHAPTER 1:INTRODUCTION

University of New Haven
HENRY C. LEE COLLEGE OF
CRIMINAL JUSTICE AND FORENSIC SCIENCES
Department of Forensic Science

Current search methods for missing individuals can be costly and inefficient for every day law enforcement use. Extensive search areas make it difficult for timely detection and often require expensive techniques and/or excessive manpower. Recent research has demonstrated the potential of a more effective search technique by studying the phenomenon of heat generation produced by larval aggregations and the capability of detection using an aerial system equipped with thermal imaging (Amendt et al., 2017; Lee, Voss, Franklin, & Dadour, 2018). Larval aggregations on decomposing pig carcasses were detected by comparing temperature differences between the aggregations and the surrounding environment. Despite the success of the search technique under different climatic conditions, this study relied upon the availability of police helicopters and expensive infrared technology (Amendt et al., 2017; Lee et al., 2018). Recent advances in both unmanned aerial systems (UAS) (drones), in particular small unmanned aerial systems (sUAS), and thermal imaging technology offer a cost-effective alternative to traditional search options with the added benefit of rapid maneuverability. The aim of this study was to investigate the effectiveness of using a small, unmanned aerial system mounted with a forward-looking infrared radar to detect the heat signature of larval aggregations associated with decomposition, and to determine the factors and conditions that would affect the capability of detection when using this device in search and recovery missions.

1.1 Entomology

Entomology, which is the study of insects, provides contextual importance to the presence of insects via the examination of their life history and behavior (Anderson, 2014). One common application is forensic entomology, which applies to the broad study of insects as it pertains to the legal system and can encompass such circumstances as insect damage to buildings (urban entomology), food infestations (stored products entomology), and death investigations

(medicolegal entomology) (Hall, 1990). In these circumstances, insects can provide probative information to aid in the legal proceedings of forensic cases.

1.1.1 Medicolegal Entomology

Insects associated with a crime scene are important to examine, as they can be used to provide probative information about the circumstances surrounding a death. This practice is referred to as medicolegal entomology, and the earliest account of its use dates back to a homicide investigation in thirteenth-century China by the death investigator, Sung Tz'u (Mcknight, 1981). In this case, a body was found near rice fields and the stab wound located on the body was determined to be consistent with a sickle, a tool commonly used by workers in the field (Mcknight, 1981). Sung Tz'u examined all of the workers tools in the village and noticed that flies were located only on and around one sickle (Mcknight, 1981). Sung Tz'u began to question the owner of this sickle and soon after, the worker confessed to the murder (Mcknight, 1981). The presence of flies surrounding the sickle was attributed to trace amounts of blood still present on the blade that was attracting the flies to it (Mcknight, 1981). Additional case work and extensive research has since contributed to a better understanding of the common association between insects and decomposing remains, and how the presence of insects can be utilized for death investigations.

1.1.1.1 Forensically Important Insects

Insect species commonly associated with decomposing remains are classified into four categories (Catts & Goff, 1992; Rivers & Dahlem, 2014; Smith, 1986):

1. Necrophageous species – insects that feed and/or breed on decomposing remains. These insects, which include true flies (Diptera) and beetles (Coleoptera), are typically the most probative species utilized by entomologists for death investigations (Catts & Goff, 1992; Rivers & Dahlem, 2014; Smith, 1986).

2. Predacious and parasitic species – insects that feed on the necrophageous species present on the remains and not on the remains itself. They include rove beetles (Coleoptera: Staphylinidae) and parasitoid wasps (Hymenoptera: Braconidae and Pteromalidae). Some necrophageous larvae, such as *Chrysomya rufufacies* (Calliphoridae), can become predacious on other larvae at later stages in development. Predacious and parasitic species are identified as the second most forensically significant group of insects (Catts & Goff, 1992; Goff, 2010; Rivers & Dahlem, 2014; Smith, 1986; Voss, 2010).

3. Omnivorous species – insects that feed on the remains and on the other associated insects. They include carrion beetles (Coleoptera: Silphidae), ants (Hymenoptera: Formicidae) and yellowjackets (Hymenoptera: Vespidae). It has previously been observed that large populations of omnivorous species can slow decomposition of remains by feeding on, and therefore reducing the number of, the necrophageous species present (Catts & Goff, 1992; Early & Goff, 1986; Rivers & Dahlem, 2014; Smith, 1986).

4. Adventive species – insects and other arthropods that do not feed on decomposing remains or associated insects, but rather use remains as an extension of their environment to hide and protect themselves under. They include spiders, centipedes and springtails (Catts & Goff, 1992; Rivers & Dahlem, 2014; Smith, 1986).

1.1.1.2 Estimating Minimum Postmortem Interval (PMI_{min}) using Entomology

Entomological evidence found at death scenes is most commonly utilized to estimate the minimum postmortem interval (PMI_{min}). PMI_{min} refers to the amount of time that has elapsed since the initial wave of insect colonization, and thus, the minimum amount of time that has passed since death. Estimation of PMI_{min} is important to forensic investigations as it can provide a timeline as to when an individual may have died, which can contribute to the reconstruction of events that occurred and can aid in the exclusion (or inclusion) of a suspect.

There are additional methods that can be utilized to estimate PMI_{min}, including livor, algor and rigor mortis (Rivers & Dahlem, 2014). These factors are associated with the natural changes that occur within the body immediately following death, such as the blood settling (livor), and the body cooling (algor) and stiffening (rigor) (Rivers & Dahlem, 2014). However, approximately 72 hours after death (post mortem), the decay of the body progresses to a state where it becomes more difficult to accurately determine the PMI_{min} using these factors (Rivers & Dahlem, 2014; Sharma, 2015). Comparatively, insects are attracted to remains throughout all stages of decomposition, and therefore can be utilized to estimate PMI_{min} even 72 hours post mortem. In particular, knowledge of the expected arrival time and the predictable development of a species on a body can be utilized to estimate PMI_{min} (Anderson, 2014).

The predictable succession of insects on decomposing remains is one way in which forensic entomologists utilize insect evidence to determine the minimum amount of time that has elapsed since death (Anderson, 2001, 2014; Rivers & Dahlem, 2014). This predictable succession results from the chemical and physical changes a body undergoes throughout the decomposition process, which alters the attractiveness and nutritional value of remains to various decomposers, including insects (Anderson, 2001, 2014). As a result, groups of insects will colonize decomposing remains at different times and in a predictable sequence (Anderson, 2001, 2014). For example, research on insect colonization at the Anthropological Research Facility in Knoxville, TN observed the succession pattern of flies (Diptera) and beetles (Coleoptera) on decaying human remains (Figure 1:1 a-b). Variation in the succession patterns between and within these two insect groups was observed. Flies were present on the remains in greater numbers during the earlier stages of decomposition, with blowflies (Diptera: Calliphoridae) being the first species to arrive, followed by muscid flies (Diptera: Muscidae) and then flesh flies (Diptera: Sarcophagidae) (Rodriguez & Bass, 1983). Beetles were observed at various stages of decomposition depending on the species. Carrion beetles (Coleoptera: Silphidae) were present in the bloated and decay stages while dermestid beetles (Coleoptera: Dermestidae) were most prevalent in the final stage of decomposition (Rodriguez & Bass, 1983).

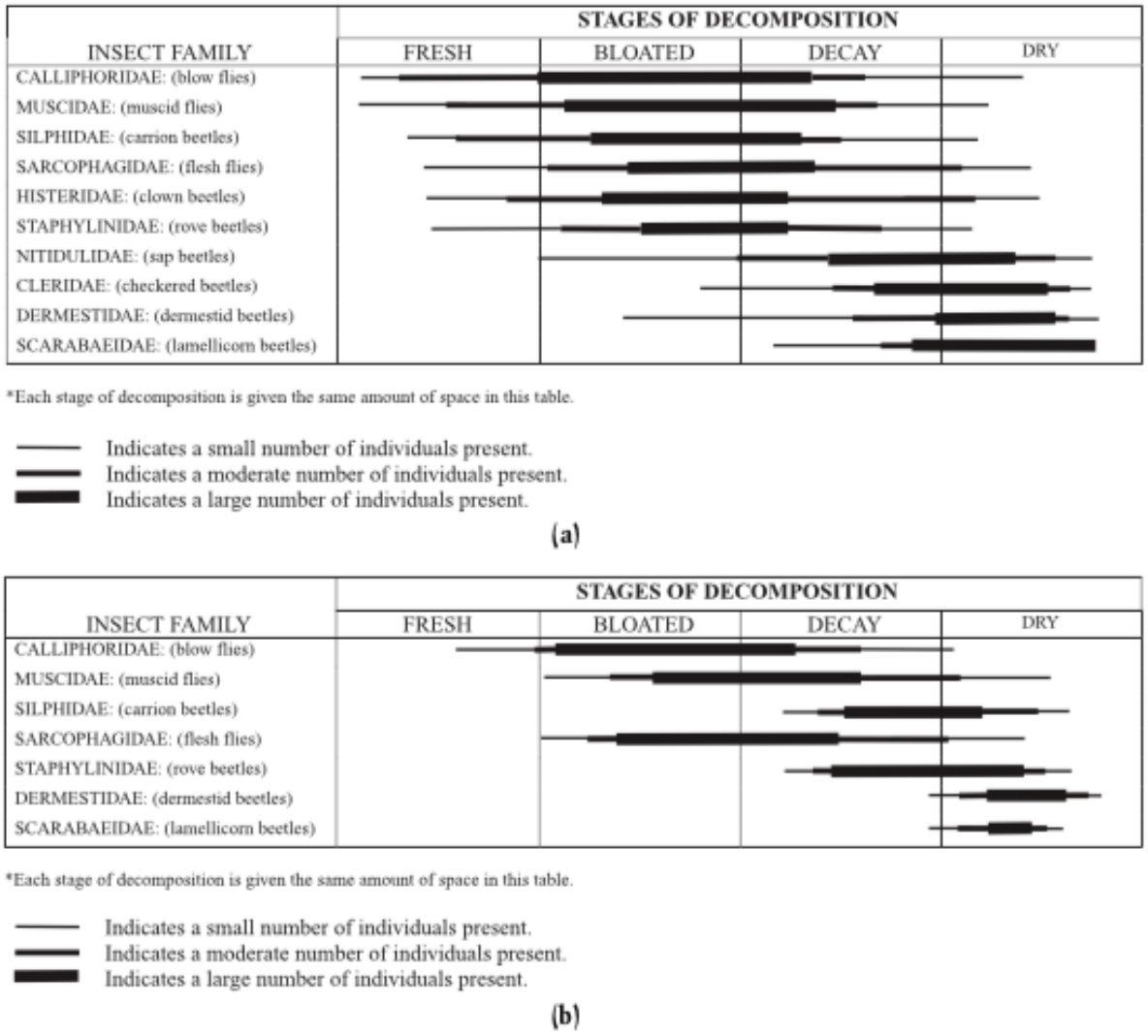

Figure 1:1 - a-b - Insect succession of Diptera and Coleoptera species at the Anthropological Research Facility in Knoxville, TN, a) succession of adults, b) succession of larvae (Rodriguez & Bass, 1983, as adapted in Hall, 2001)

Additional research on insect colonization has demonstrated similar succession patterns of Diptera and Coleoptera species and have also noted the observed patterns of other forensically significant species during different stages of decomposition and within various environmental or climatic conditions (Bornemissza, 1957; Grassberger & Frank, 2004; Johnston & Villeneuve, 1897; Reed, 1958; Voss, Spafford, & Dadour, 2009). For example, research conducted in Perth,

Western Australia observed succession patterns of various Diptera, Coleoptera and Hymenoptera species on domestic guinea pig carcasses (*Cavia porcellus*) over a two year time period (Figure 1:2) (Voss et al., 2009). Replications occurred within seasons and at two different study sites, a bushland wildlife reserve and an agricultural field station, in order to determine the temporal and spatial succession patterns of insects in Western Australia. Diptera were the first insects observed on the carcasses throughout all seasons and between locations, with *Lucilia sericata* (Diptera: Calliphoridae) and *Calliphora dubia* (Diptera: Calliphoridae) consistently being the first to arrive**.** The predatory Hymenoptera species of Diptera, including *Tachinaephagus zealandicus* (Hymenoptera: Encryptidae) and *Nasonia vitripennis* (Hymenoptera: Pteromalidae), were observed on the carcasses soon after Diptera colonization and were present throughout all stages of decomposition. Coleoptera species did not arrive to the carcass until the bloat stage and were represented in greater numbers towards the end of decomposition. This study found that the successional patterns of these three insect species in Western Australia was consistent between sites but not between seasons (Voss et al., 2009).

Agricultural			Days													
Order	Family	Species	0–3 Fresh			4–9 Bloat				10–18 Wet				19–on Dry			
			A	E	L	A	E	L	PP	A	L	PP	P	A	L	PP	P
Diptera	Calliphoridae	*Lucilia sericata*	X	X	X	X		X		X	X	X	X			X	X
		Calliphora dubia	X		X	X		X		X	X	X	X			X	X
		Calliphora albifrontalis	X	X	X	X		X		X	X	X				X	X
		Chrysomya megacephala	X	X				X									
		Chrysomya rufifacies				X	X	X		X	X	X				X	X
		Chrysomya varipes				X				X	X					X	X
	Muscidae	*Hydrotaea rostrata*								X	X			X	X	X	X
		Musca vetustissima								X				X			
		Musca domestica	X			X				X	X			X			
	Sarcophagidae	Not identified beyond family				X				X	X						X
Coleoptera	Dermestidae	*Dermestes ater*								X				X	X		
		Dermestes maculatus								X				X	X		
	Histeridae	*Saprinus* sp.				X				X				X	X		
	Staphylinidae	*Creophilus erythrocephalus*				X				X				X	X		
		Aleochara sp.								X				X			
	Cleridae	*Necrobia rufipes*												X			
Hymenoptera	Pteromalidae	*Nasonia vitripennis*								X				X	X		
	Encryptidae	*Tachinaephagus zealandicus*			X	X		X		X	X				X		
	Braconidae	*Aphaereta* sp.	X			X		X		X	X						
	Diapriidae	*Spilomicrus* sp.								X	X						
	Formicidae	*Iridomyrmex* sp.	X			X				X				X			

Figure 1:2 - Spring succession of insects at the agricultural study site in Perth, Western Australia (Voss et al., 2009)

Research on succession patterns has provided known sequences and timeframes of colonization for various groups of insects, which have been applied by forensic entomologists in death investigations (Anderson, 2001, 2014). The presence (or absence) of certain species on remains at the time of discovery can be compared to these known sequences and timeframes of colonization in order to aid in the estimation of PMI_{min} (Anderson, 2001, 2014).

Rate of larvae development, particularly of fly larvae, is the second approach forensic entomologists use when estimating PMI_{min} (Anderson, 2014; Rivers & Dahlem, 2014). The first known use of development rates for PMI_{min} estimation was in 1850 by Louis Bergeret, when the mummified body of a baby was found behind a fireplace in a house (Greenberg & Kunich, 2002; Hall, 2005). Bergeret found empty pupae of *Sarcophaga carnaria* (Diptera: Sarcophagidae) on the body and used the known development rate of this species to determine that this colonization

event occurred in 1848, soon after the baby's death (Greenberg & Kunich, 2002; Hall, 2005). Bergeret's estimation of when the baby died was used to exclude the tenants who occupied the house at the time of discovery as suspects (Greenberg & Kunich, 2002; Hall, 2005). Since this time, developmental rates have become a key indicator for determining the minimum amount of time that has elapsed since death.

Developmental rates of different fly species have been studied in order to determine the amount of time each species spends in the egg, larval and pupal stages (Anderson, 2000; Donovan, Hall, Turner, & Moncrieff, 2006; Grassberger & Reiter, 2001, 2002). For example, developmental data was collected for the forensically important blowfly, *Calliphora varifrons* (Diptera: Calliphoridae), which is native to Western Australia (Voss, Cook, Hung, & Dadour, 2014). *C. varifrons* was reared at constant temperatures between 12 °C and 30 °C to determine how temperature influenced development time, or the amount of time between larviposition to adult emergence (Voss et al., 2014). The developmental data collected showed that as the temperature increased, the development time also increased. At 27°C the development time of *C. varifrons* was 16.65 ± 0.17 days while at 12°C the time was 49.93 ± 0.26 days (Voss et al., 2014). The results of this study also found that mortality was higher at the temperature extremes, the adult body size was smaller at the temperature extremes and the maximum larval length decreased as temperature increased (Voss et al., 2014).

Developmental data has also been collected by rearing fly species under cyclic temperatures in order to simulate the normal fluctuating temperatures that would be experienced within the environment. Cyclic temperature conditions have varying effects on the rate of development in comparison to constant temperatures as it can accelerate the rate for some fly

species, such as *Calliphora vomitoria, Phormia terraenova* and *Lucilia sericata,* but retard it for others, such as *Calliphora vicinia* (Davies & Ratcliffe, 1994). The collection of developmental data for different fly species under both cyclic and constant temperatures can assist forensic entomologists in making more accurate estimations of PMI_{min} by taking into consideration the various temperature regimes insects may experience during development (Dadour, Cook, & Wirth, 2001)

These two approaches to PMI_{min} estimation are of great value to forensic entomologists in death investigations due to the information they can provide about the circumstances surrounding a death. However, the predictable succession and development of insects are not consistent methods that all forensic entomologists can apply in the same way. For example, the sequence of insect colonization varies depending on factors like geographical region, season and body placement (i.e. indoors vs. outdoor; rural vs. urban) (Anderson, 2001). Development rates of fly larvae are also dependent on both the species and the temperature (Anderson, 2014; Rivers & Dahlem, 2014). Larvae from different species may develop at a different rate, and larvae from the same species may also develop at a different rate if there is a variation in temperature. The success in using both methods for PMI_{min} estimation is dependent on consideration of these factors, in addition to proper species identification, the availability of experimental data for a given area or species, and proper documentation of the crime scene conditions (Anderson, 2014; Rivers & Dahlem, 2014).

1.1.1.3 Other Uses of Insects for Death Investigation

Entomological evidence can provide additional information about the circumstances surrounding a death beyond estimation of PMI_{min}. For example, insects can be an indicator of

drug use. If the victim consumes drugs or poisons preceding death, those toxins will still be present within the tissues of the body post mortem. The insects feeding on these remains, such as blowfly larvae, will ingest and accumulate these toxins into their own tissues, which can then be analyzed by toxicologists to determine what toxins are present. Insects are useful for drug detection, especially when a body is too decomposed for the tissues to be analyzed directly. The analysis of toxins in insects is referred to as entomotoxicology (Anderson, 2014).

Additionally, insects can be used to indicate if a body has been moved postmortem. In this circumstance, a body may have been moved from the initial scene of the crime to another location in an attempt to hide the body and conceal the crime. If the body was left exposed at the initial scene, blowfly species local to that area can colonize the body within minutes. However, these species at the initial scene may not be common to the area where the body was moved to. Therefore, when the entomological evidence is analyzed, it will be noted that some of the species identified were not common in that location, and therefore the body could have been moved. This information is important for investigators to learn as they can focus their investigation on locating the primary scene of the crime, which may possess more key evidence (Anderson, 2014).

Insects can also be used to link a suspect to a scene. Suspects can unknowingly take entomological evidence with them when they leave the scene of a crime or can be affected by the insects located at the scene. For example, in a particular case in Southern California, bites located on the suspect were used to link the suspect to a homicide scene after determining that the bites were from chiggers (Trombidiformes), or mite larvae, which were only located in the region where the crime occurred. In another case, a suspect was linked to the scene of a robbery

and homicide based on the presence of bumble bee (Hymenoptera: Apidae) hairs discovered on a bank note in his possession. These hairs could be linked to the scene as there was a bumble bee located in the drawer where the money stolen was known to be kept. Discovery of entomological evidence associated with a suspect can provide the probative information needed to link the suspect to the scene or the victim (Anderson, 2014).

Insects, particularly blowflies, can be utilized to locate the position of a wound. Blowflies will colonize open wounds, such as a stab wound or a slashed throat, because it is a protein rich site that will promote larval growth and development. Analysis of where larvae are located on the body can indicate the possible presence of wounds. For example, if older larvae are found in the abdominal region and younger larvae are found in a natural orifice it is likely that an open wound is located in the abdominal region. This information is probative for determining cause of death in forensic investigations when wounds do not reach the hard tissue and remains are too decomposed for wound analysis (Anderson, 2014).

1.1.2 Diptera

True flies, which are insects in the Order Diptera, are of considerable forensic significance as they are among the first insects to colonize decomposing remains (Anderson, 2014). Knowledge of the development, behavior and geographic distribution of fly species associated with decomposing remains assists forensic entomologists in evaluating the circumstances surrounding a death (Byrd & Castner, 2001).

Diptera commonly associated with decomposing remains include blowflies (Diptera: Calliphoridae) and flesh flies (Diptera: Sarcophagidae). Blowflies, which appear metallic green or blue in color, are typically the first to arrive at remains, and can do so within minutes after

death (Anderson & VanLaerhoven, 1996). In total, 93 North American blowfly species have been identified, including species in the genus *Lucilia, Calliphora, Phormia, Cochliomyia* and *Chrysomya* (Whitworth, 2017). The distribution and morphological characteristics for many of these species have been defined in order to assist entomologists in identifying each species (Whitworth, 2017). *Lucilia sericata* (Figure 1:3 a) and *Phormia regina* are among the most prevalent blow fly species found in association with decomposing remains, and are both widely distributed throughout North America (Rivers & Dahlem, 2014; Whitworth, 2017).

Flesh flies (Diptera: Sarcophagidae) typically colonize decomposing remains soon after blowflies (J.H Byrd & Castner, 2001; Rivers & Dahlem, 2014). There are approximately 320 species of flesh flies common to North America, many of which are in the genus *Sarcophaga.* Some of the most common species associated with decomposing remains include *Sarcophaga bullata* (Figure 1:3 b), *Sarcophaga haemorrhoidalis, Sarcophaga crassipalpis* and *Blaesoxipha plinthopyga* (Byrd & Castner, 2001; Rivers & Dahlem, 2014). The necrophageous flesh flies are characterized by their red eyes and dark stripes on the dorsal aspect of the thorax and are distinct from other families of flies as they lay live larvae as opposed to eggs (Rivers & Dahlem, 2014). Unlike blowflies, the identification and differentiation of Sarcophagidae species is difficult due to the similarity in morphological features (Byrd & Castner, 2001).

a)  b) 

Figure 1:3 - a-b - Diptera flies, a) *Lucilia sericata* adult fly, b) *Sarcophaga bullata* adult fly (Photographs by Megan Descalzi)

1.1.2.1 Life Cycle

Flies undergo holometabolous development, meaning they progress through multiple stages of life beginning as eggs, developing into larvae and then pupae before becoming adults (Figure 1:4) (Castner, 2001). Once eggs develop into larvae, or maggots, they progress through three stages, or instars, each marked by shedding of the skin and an increase in size (Castner, 2001). The instar of larvae can be determined by examining the number of slits in the posterior spiracles, or respiratory openings (Flores et al., 2016; Liu & Greenberg, 1989). First instar larvae will have one slit in each spiracle, second instar will have two slits and third instar will have three slits (Figure 1:4) (Flores et al., 2016; Liu & Greenberg, 1989). Larvae feed on the substrate where they are laid, and it is the cessation of this feeding and movement away from the substrate that begins the pupae stage of the lifecycle (Castner, 2001). In this stage, the larvae will find a dark and cooler location, usually soil, where they will form a hard, outer casing (puparium) that allow them to develop and later emerge as adult flies (Castner, 2001).

Most fly species are oviparous, meaning they lay eggs (Rivers & Dahlem, 2014). These flies, such as calliphorids, proceed accordingly through the life cycle (Figure 1:4). However,

there are some flies, such as the sarcophagids, that do not lay eggs. These flies are considered larviparous because they lay live larvae instead (Rivers & Dahlem, 2014). While larviparous species proceed through the same life cycle as oviparous flies, the egg stage is absent (Figure 1:4).

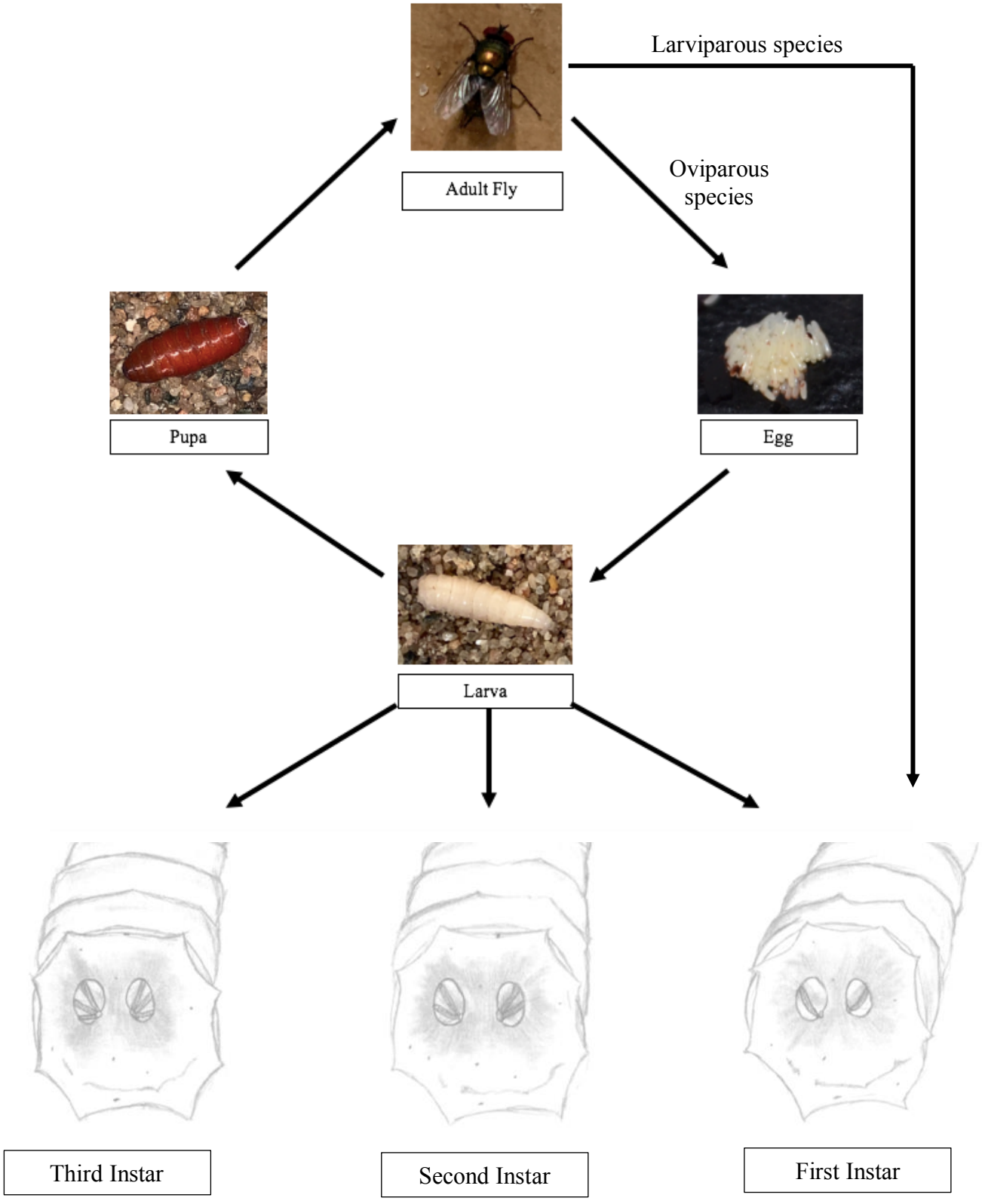

Figure 1:4 - Diptera life cycle (Photographs by Megan Descalzi, Drawings by Emily Powers)

Flies are poikilotherms, meaning that they rely on ambient temperature to regulate their own body heat (Grassberger & Reiter, 2002; Higley & Haskell, 2001; Rivers & Dahlem, 2014). Therefore, the development rate of flies through the stages of the life cycle is dependent on ambient temperature. As temperature increases, the development rate of flies also increases because the enzymatic and metabolic processes that regulate growth work optimally at greater temperatures (Higley & Haskell, 2001). For example, when *Phormia regina* was reared at 19°C, the average minimum duration of the pre-adult stages was 15.6 days (Greenberg & Kunich, 2002). At 35°C, the duration was 10 days (Greenberg & Kunich, 2002). As the rearing temperature increased, the amount of time it took for *P. regina* to develop from eggs to adult flies decreased.

The development rate of flies also varies between species. For example, in comparison to the average minimum duration of the pre-adult stages for *P. regina* at 19°C, the duration at this same temperature for *Phaenicia sericata* was 16.3 days and for *Calliphora vicina* it was 22.8 days (Greenberg & Kunich, 2002). Due to these differences in developmental rates, data has been collected for various species at different temperatures in order to aid forensic entomologists in using development rates for estimation of PMI_{min}.

1.1.2.2 Colonization

Necrophageous flies seek out nutrient-rich sources, such as decomposing remains, that promote growth and development at the adult and larval stages. Decomposing remains are an optimal feeding site for adult flies and larvae because of the abundant amount of protein that is

available (Rivers & Dahlem, 2014). Female flies rely on the consumption of protein for oogenesis, or development of eggs, to occur, and larvae require protein to grow (Rivers & Dahlem, 2014). Therefore, female flies will feed on decomposing remains to consume enough protein to become gravid, and then will oviposit, or lay eggs, on the remains, knowing it is an ideal site for larval growth (Rivers & Dahlem, 2014).

Prior to colonization, adult flies will sense and become attracted to the volatile chemicals released from decomposing remains, such as butane-1,4-diamine (putrescine), pentane-1,5-diamine (cadaverine), indole and dimethyl disulfide (Dekeirsschieter et al., 2009; Eisemann & Rice, 1987; Frederickx, Dekeirsschieter, Verheggen, & Haubruge, 2012). This odor provides a cue, to female flies in particular, that the remains are an optimal site for the consumption of protein and is a suitable host for larval development (Eisemann & Rice, 1987). Then, when oviposition starts to occur, female flies initially attracted to the remains will send chemical signals, such as pheromones or kairomones, to other female flies and additional eggs will be laid (Barton Browne, Bartell, & Shorey, 1969; Eisemann & Rice, 1987; Hammack, 1990). Female flies will oviposit in the moist areas of the organism where sources of protein for development are abundant (Rivers, Thompson, & Brogan, 2011). The areas that will be colonized first include any orifices (i.e. mouth, eyes, anus), folds in the skin and wounds (Rivers et al., 2011).

1.1.2.3 Larval Aggregation

Fly larvae are often found in large aggregations, or maggot masses, on decomposing carcasses during the second or third instar of development (Rivers & Dahlem, 2014). These aggregations can be comprised of one or multiple fly species and may consist of hundreds to

thousands of larvae depending on the size of the remains (Campobasso, Di Vella, & Introna, 2001; Rivers & Dahlem, 2014).

It is unclear as to how these aggregations form, but multiple hypotheses have been developed to explain this behavior. These hypotheses include (i) positive thigmotaxis, (ii) clustered oviposition or larviposition, (iii) random formation, and (iv) foraging (Rivers & Dahlem, 2014).

Positive thigmotaxis is the innate behavior of an organism to seek contact with an object in response to touch or physical stimuli (Gennard, 2007; Rivers & Dahlem, 2014). Fly larvae are characterized as displaying positive thigmotaxis when they seek contact with nearby larvae and form large aggregations (Gennard, 2007; Rivers & Dahlem, 2014). Thigmotaxis explains why larvae continually seek contact with one another and remain aggregated until the end of the third instar. However, thigmotaxis does not explain why larvae are close enough for contact to initially occur (Rivers & Dahlem, 2014). Aggregations do not form until after the first instar, during which some larvae species disperse from the site where oviposition/larviposition occurred and the cluster of eggs were deposited (Greenberg & Kunich, 2002; Rivers & Dahlem, 2014). Larval aggregations produced by thigmotactic behavior will occur if larvae are in close proximity to each other, not dispersed on the carcass. Thigmotaxis is likely a reason for why aggregations persist, but not for how they are initiated (Rivers & Dahlem, 2014).

Clustered oviposition and larviposition results from pheromone and kariomone signaling between and within Diptera species (Rivers & Dahlem, 2014). These chemicals will attract flies to decomposing remains and will stimulate oviposition/larviposition to occur, often at the same location, producing egg clusters. This explanation supposes that clusters of eggs inevitably lead

to aggregation formation and that larvae must therefore feed and grow cooperatively at the site where oviposition/larviposition occurred. Larvae do work together to cooperatively digest the tissues of the decomposing carcass, but similar to the idea of positive thigmotaxis, the limitation in this hypothesis is that species tend to move away from the site of oviposition/larviposition during the first instar (Rivers & Dahlem, 2014).

The explanation of random formation hypothesizes that larval aggregations form by chance, as a result of overcrowding and competition (Rivers & Dahlem, 2014). Decomposing remains are an ephemeral food source, which means that as hundreds to thousands of larvae grow and feed at a single time, they are forced to interact with each other as they compete for food. However, this hypothesis also does not take in to consideration the dispersal of first instar larvae and does not consider that overcrowding may not occur on larger remains, especially for the first wave of colonizers (Rivers & Dahlem, 2014).

The foraging by larvae explanation proposes that aggregations form in response to chemical signals, similar to pheromone trails (Rivers & Dahlem, 2014). This hypothesis supposes that these signals are sensed and then utilized by larvae to detect other larvae feeding on the remains, ultimately leading to the formation of an aggregation. There is little evidence to suggest that chemical cues are the reason for the formation of larval aggregations (Rivers & Dahlem, 2014). However, previous research has supported the presence of chemical cues influencing the foraging behavior of larvae, when second and third instar *S. bullata* larvae were able to locate beef liver from a distance of 33 centimeters using these signals (Christopherson & Gibo, 1997).

It is still unknown as to how larval aggregations form. Although previous research does support some aspects of each hypothesis, there is not enough known to determine if one or more of these hypotheses can explain the formation of larval aggregations.

1.1.2.4 Benefits of forming aggregations

The formation of larval aggregations is beneficial to the survival and development of larvae feeding on decomposing remains. When larvae feed in aggregations, they are able to obtain the nutrients needed to grow more efficiently through cooperative feeding and digestion of tissues. Larvae feed by penetrating tissues with their mouth hooks and by secreting digestive enzymes that assist in breaking down tissues (Figure 1:5 a-b) (Greenberg & Kunich, 2002; Rivers et al., 2011). These physiological adaptations are intended to aid individual larva in obtaining nutrients from feeding on decomposing tissues. However, these adaptations are more beneficial to larvae when utilized in conjunction with hundreds to thousands of other larvae. When larval aggregations form, there is an increased number of mouth hooks being utilized to penetrate tissues and a mass secretion of digestive enzymes on a localized site, resulting in more efficient feeding and assimilation of nutrients (Greenberg & Kunich, 2002; Rivers et al., 2011).

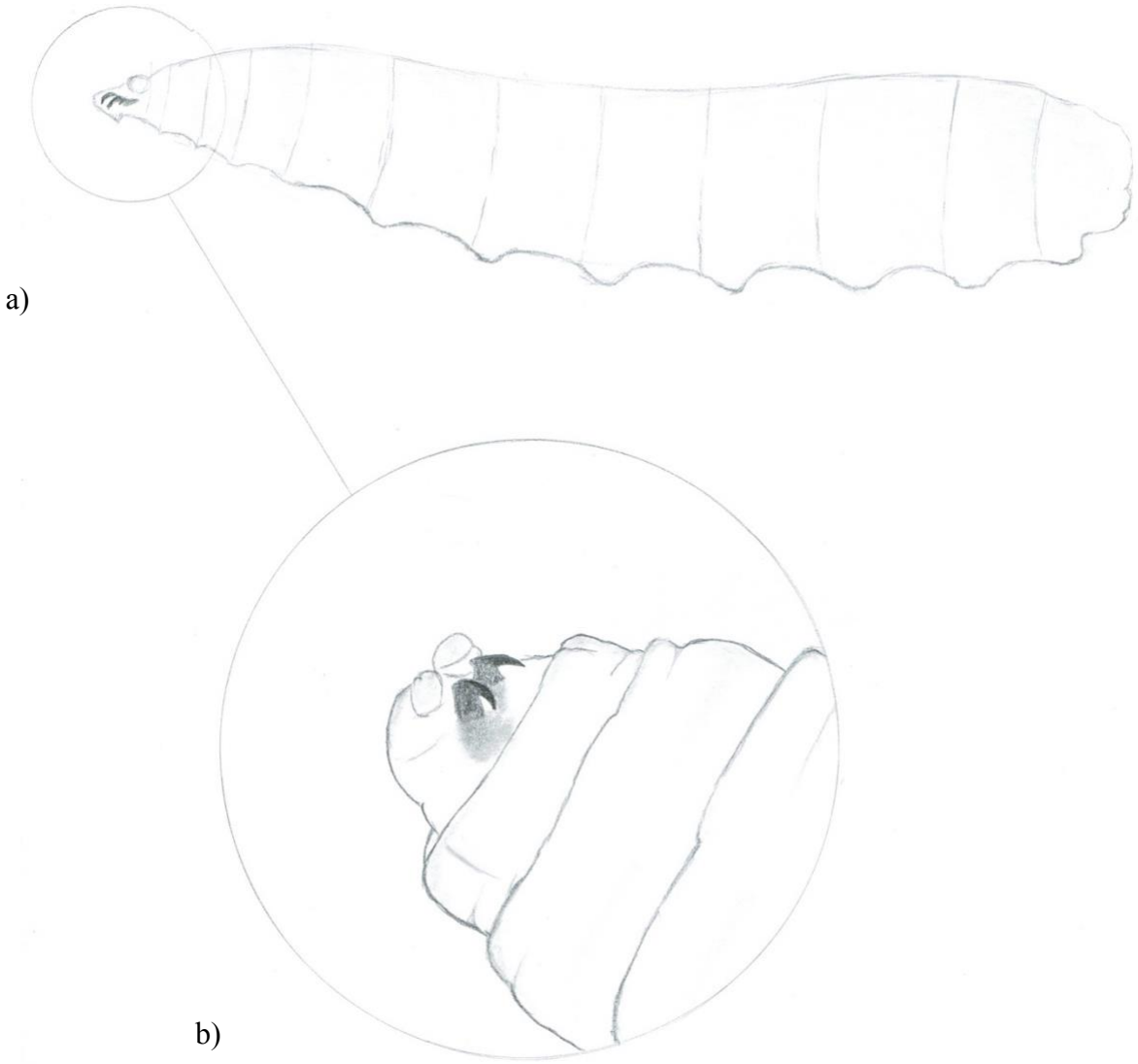

Figure 1:5 - a-b - Diptera larva a) body, b) mouth hooks (Drawings by Emily Powers)

The formation of aggregations also benefits larval development by assisting in the regulation of larval body temperature (Rivers et al., 2011). When larval aggregations form, heat is produced which contributes positively to the developmental rate of larvae. This heat production by larval aggregations is called the larval mass effect and is discussed in more detail in the following section (Charabidze, Bourel, & Gosset, 2011; Rivers & Dahlem, 2014).

1.1.2.5 Larval Mass Effect

It is well reported that larval aggregations produce a significant amount of heat (Charabidze et al., 2011; Deonier, 1940; Turner & Howard, 1992). Larval aggregation temperatures that exceed ambient temperature by more than 30°C have been observed (Anderson & VanLaerhoven, 1996; Slone & Gruner, 2007; Turner & Howard, 1992). However, the reason for this heat production is unknown. It has been hypothesized that heat could be a result of microbiotic activity or a result from the frenetic movement and high metabolism rate of the larvae feeding on the organism (Campobasso et al., 2001; Greenberg & Kunich, 2002).

Although the cause is not well understood, heat production is believed to be necessary for larvae development. In conditions where ambient temperature is not optimal for development, massing behavior and associated heat production elevates the temperature of each larvae in the mass to allow for continued development and food consumption (Rivers et al., 2011). Heat production behavior allows for temperature dependent growth of larvae when conditions are not ideal and hastens development. Faster development during the larval feeding period reduces the time larvae are vulnerable to predation and provides an advantage over other carrion feeding species that are competing for the limited food resource offered by decomposing remains (Rivers et al., 2011).

The amount of heat produced has been reported to be influenced by a variety of intrinsic and extrinsic factors. Slone & Gruner (2007) reported that larger (more dense) and more tightly packed larval aggregations produce the greatest amount of heat, and thus have the highest temperatures. Charabidze, Bourel, and Gosset (2011) reported that heat production is affected by the instar of the larvae and the size of the food source. The older the larvae and the larger the

food source, the greater the amount of heat produced. Additional influences on heat production includes species composition, location of aggregation on remains and surrounding abiotic factors (i.e. ambient temperature and sunlight) (Catts & Goff, 1992; Hall, 2005; Joy, Liette, & Harrah, 2006; Rivers, Ciarlo, Spelman, & Brogan, 2010).

1.2 Decomposition of Terrestrial Remains

Decomposition is continuous process that consists of chemical and physical changes within a body following death (Rivers & Dahlem, 2014). Taphonomy, which is the study of decomposing organisms over time, aims to observe these changes and to observe how various abiotic and biotic factors affect the rate at which the organisms decay (Rivers & Dahlem, 2014).

1.2.1 Chemical Decomposition

Decomposition begins immediately after death when the body's cells become deprived of oxygen, causing a cascade of biochemical events that advance the physical decay of the body. (Rivers & Dahlem, 2014; Vass, 2001). As the condition of the body shifts to an anaerobic state, lysosomes will release enzymes in response to unfavorable intracellular conditions, resulting in the self-digestion of the body's cells, or autolysis, and the release of nutrient rich fluids (Figure 1:6) (Rivers & Dahlem, 2014; Vass, 2001). Autolysis occurs more rapidly in tissues with higher enzyme activity, such as the liver, or higher water content, such as the brain (Rivers & Dahlem, 2014; Vass, 2001). The effects of cell digestion on the body become visible within a few days following death as blisters form on the skin and skin slippage occurs (Vass, 2001).

After a few days, all of the cells in the body will be broken down and the release of nutrient rich fluids will promote microbial activity and subsequently, putrefaction (Figure 1:6) (Vass, 2001). Putrefaction is the process by which bacteria and fungi digest the body's tissues, and in doing so, release volatile gases, liquids and small molecules (Vass, 2001). The effects of putrefaction quickly become visible as the body develops a greenish discoloration and begins to swell as a result of these by-products (Vass, 2001).

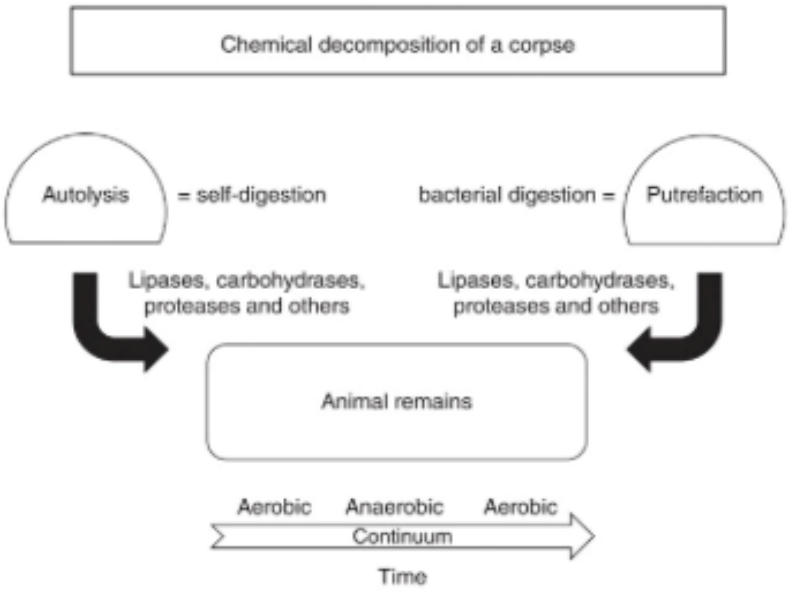

Figure 1:6 - Graph illustrating chemical decomposition (Rivers & Dahlem, 2014)

1.2.2 Stages of Decomposition

Decomposition is typically categorized into discrete stages defined by the visible changes that occur to a body over time and the associated insect activity (Goff, 2010). These stages are utilized by researchers to link decomposition events to expected timeframes, in order to aid in estimating the amount of time that has elapsed since death (Rivers & Dahlem, 2014).

The number of defined stages varies depending on the researcher and the environment in which decomposition is observed (Galloway, 1997; Goff, 2010; O'Brien, 2008; Payne, 1965). The stages proposed by Goff (2010) will be used to define the gross decompositional changes that occur to a body over time.

1.2.2.1 Fresh Stage

The fresh stage of decomposition is consistently defined amongst most researchers as the initial stage of decomposition that begins immediately following death and ends when the body begins to bloat (Galloway, 1997; Goff, 2010; O'Brien, 2008; Payne, 1965). Many of the changes that occur to a body during this initial stage are largely internal as autolysis begins in response to increasing anaerobic conditions. The visible changes that occur to a body during the fresh stage of decomposition can include stiffening (rigor mortis), red/purple discoloration of the skin (livor mortis), black discoloration across the cornea (tache noir) and/or skin slippage (Gill-King, 2006; Goff, 2010; Rivers & Dahlem, 2014).

Insect attraction to the body can occur within minutes after death (Smith, 1986). Primary colonizers include Diptera from the families Calliphoridae and Sarcophagidae, which lay their eggs/larvae within the body's orifices, wounds or folds in the skin (Galloway, 1997; Goff, 2010; Payne, 1965). During this stage, the eggs begin to hatch, and larvae begin to feed on the body. Additional insects have been observed in association with the body during the fresh stage, including beetles from the family Silphidae, yellow jackets (*Vespula maculifrons)* and ants (Hymenoptera: Formicidae) depending on the location and season in which decomposition was studied (Galloway, 1997; Goff, 2010; Payne, 1965; Rivers & Dahlem, 2014).

1.2.2.2 Bloated Stage

The fresh stage ends and the bloated stage begins when the body starts to bloat, or swell (Goff, 2010; Rivers & Dahlem, 2014). A strong indicator that the body is entering the bloat stage is when the abdomen becomes distended due to the accumulation of gases, such as ammonia, methane and hydrogen sulfide, within the gastrointestinal tract (Clark, Evans, & Wall, 2006; Rivers & Dahlem, 2014). These gases are byproducts of the microbiotic activity in which anaerobic bacteria putrefy the body's tissues (Catts & Goff, 1992; Rivers & Dahlem, 2014). Putrefaction will continue throughout the bloated stage, resulting in the continual build-up of gases and bloating of the body.

In addition to bloating, the body will experience marbling, which is a mosaic pattern of purple to greenish discoloration within the blood vessels (Goff, 2010; Rivers & Dahlem, 2014). This discoloration results from the putrefaction of proteins within the body and the subsequent formation of sulfhemoglobin within pooled blood (Gill-King, 2006; Goff, 2010; Rivers & Dahlem, 2014).

Eventually the build-up of gases within the body will lead to an increase in pressure, which will cause some of the internal liquids and gases to slowly seep out of the body through the natural orifices (Rivers & Dahlem, 2014). The chemical odor of these liquids and gases are sensed by Diptera species that then make their way to the body. Additional colonization by Diptera species from the families Calliphoridae, Sarcophagidae, Muscidae and Piophilidae occurs (Goff, 2010; Payne, 1965; Rivers & Dahlem, 2014). Predatory insects also make their

way to the body during the bloated stage in order to feed on the Diptera eggs and larvae present. These predatory insects include beetles from the families Silphidae and Staphylinidae, and ants and wasps from the order Hymenoptera (Goff, 2010; Payne, 1965; Rivers & Dahlem, 2014).

The end of the bloated stage is marked by deflation of the body when all of the gasses and internal fluids are purged as a result of an extreme built-up of pressure and as larvae begin to penetrate the body's skin (Goff, 2010; Payne, 1965; Rivers & Dahlem, 2014).

1.2.2.3 Decay Stage

The decay stage is the stage of decomposition which varies the most between researchers. While Goff (2010) proposes a single stage, others divide the decay stage into two stages (Goff, 2010; Rivers & Dahlem, 2014). For example, Payne (1965) divides the decay stage into the active decay and advanced decay stages. While the number of decay stages may vary between researchers, all agree that the stage begins when the bloated body becomes deflated (Goff, 2010; Rivers & Dahlem, 2014).

The decay stage of decomposition is often characterized by a strong odor due to the release of the liquids and gasses from the body (Goff, 2010; Rivers & Dahlem, 2014). Although most of the moisture within the body's tissue have been lost, it is not yet dry and therefore continues to serve as a nutritional resource for insects and microbes (Goff, 2010; Rivers & Dahlem, 2014).

During the decay stage, Diptera larvae form large aggregations on the body which result in consumption of most of the body's tissues (Goff, 2010; Rivers & Dahlem, 2014). Predatory insects, including beetles from the families Silphidae, Staphylinidae and Histeridae, increase in numbers as larval aggregations form (Goff, 2010; Rivers & Dahlem, 2014).

By the end of the decay stage, the Diptera larvae will complete feeding and will begin to disperse from the body in search of a location to pupate (Goff, 2010; Rivers & Dahlem, 2014). The end of this stage is marked by the removal of most of the body's tissue, leaving just skin, cartilage and bone (Goff, 2010; Rivers & Dahlem, 2014)

1.2.2.4 Post Decay Stage

As the body transitions to the post decay stage, the remaining tissue dries out as all moisture is lost. At this point, the body no longer has nutritional value to some necrophagous insects, such as Diptera. However, the dried tissue does attract other necrophageous species, such as beetles in the family Dermestidae and flies in the family Piophilidae, which remove all remaining tissue (Goff, 2010; Rivers & Dahlem, 2014). The end of the post decay stage is marked by complete removal of the body's tissues (Goff, 2010; Rivers & Dahlem, 2014).

1.2.2.5 Skeletal or Remains Stage

In the final stage of decomposition, only bones and hair are left of the body (Goff, 2010; Rivers & Dahlem, 2014). There is no insect activity that is associated with the body during the skeletal/remains stage as there is no nutritional value left for the insects to feed on (Goff, 2010; Rivers & Dahlem, 2014). However, remnants of the presence of insects, such as puparium, may

provide insight into past insect activity (Goff, 2010; Rivers & Dahlem, 2014). There is no defined end point to this last stage of decomposition (Goff, 2010; Rivers & Dahlem, 2014).

1.2.3 Factors Affecting the Rate of Decomposition

Although predictable in progression, decomposition is a complex process that is influenced by various environmental (abiotic) factors and living (biotic) organisms (Rivers & Dahlem, 2014). The abiotic and biotic factors can affect the chemical and physical changes that occur and the rate at which decomposition proceeds.

1.2.3.1 Abiotic Factors

Abiotic factors associated with the immediate environment in which a body is located can affect the decomposition of a body (Rivers & Dahlem, 2014). Temperature is considered to be the most influential abiotic factor on the rate of decomposition as it directly affects the chemical breakdown of the body's tissues and the activity of living organisms (i.e. microbes and insects) (Rivers & Dahlem, 2014). Warmer temperatures speed up the rate of decomposition, while lower temperatures slow it down, which is why bodies located in direct sunlight decompose faster than those in the shade (Joy et al., 2006).

Environmental moisture can also affect the progression of decomposition (Rivers & Dahlem, 2014). Moisture is needed for autolysis and putrefaction to proceed, and maintains the nutritional value of the body for feeding insects (Goff, 2010; Rivers & Dahlem, 2014). A body located in moist regions, such as tropical environments, can rapidly decompose and become

skeletonized within two weeks (Ubelaker, 2006). However, environments with low moisture can cause mummification, or drying of the body's tissue, which preserves the body and prevents skeletonization from occurring (Galloway, 1997; Goff, 2010). Dry climates with low moisture can occur in regions with high temperatures and subzero temperatures, although the rate of mummification varies between the two (Goff, 2010; Rivers & Dahlem, 2014). A body located in a region with high temperatures and low moisture can become mummified within weeks, but will take much longer to occur when temperatures are low (Goff, 2010; Rivers & Dahlem, 2014). A body can also be preserved in moist environments if it is located in wet, anaerobic conditions, such as being buried in soil (Goff, 2010; Rivers & Dahlem, 2014). In these conditions, adipocere can form, which is a thick, waxy layer that forms on the body when fatty tissues are hydrolyzed during decomposition (Notter, Stuart, Rowe, & Langlois, 2009).

Precipitation in the form of rain can slow the rate of decomposition by deterring insects from colonizing and/or feeding on the remains (Rivers & Dahlem, 2014). Many Diptera species are unable to successfully search for decomposing organism as flying becomes difficult in heavy rains (Catts & Goff, 1992; Rivers & Dahlem, 2014). Additionally, if rain occurs post-colonization, feeding larvae can become disturbed and wander elsewhere (Rivers & Dahlem, 2014). Therefore, rain results in decreased insect activity, which in turn results in slower rates of decomposition.

1.2.3.2 Biotic Factors

Living organisms can also affect the rate of decomposition. These organisms, which include microorganisms, insects and scavengers, feed on the body's tissues, increasing the rate at

which decay occurs (Goff, 2010; Rivers & Dahlem, 2014). Microorganisms, such as bacteria and fungi, play a crucial role in the chemical decomposition of a body, while insects and scavengers affect the physical deterioration of a body (Rivers & Dahlem, 2014).

Research conducted by DesMarais (2014) demonstrated the pivotal role insect activity plays during decomposition. In this research, control carcasses were sprayed with insecticide to prevent insect activity from occurring. An extended bloat stage and an overall slower rate of decomposition was observed for the control carcasses in comparison to the experimental carcasses that were not subjected to insecticide (DesMarais, 2014). Insect activity significantly affects the rate at which decomposition occurs (Rivers & Dahlem, 2014)

Vertebrate scavengers, which can include a variety of avian, mammalian and reptilian species, utilize decomposing bodies as a food source (Goff, 2010; O'Brien, 2008). These scavengers can consume much of the body's tissue, thus decreasing the time to skeletonization (Goff, 2010). Scavenging has been shown to eliminate the difference in decompositional rates between seasons by removing the tissues more quickly during colder seasons than would typically occur by insect and microbial activity alone (O'Brien, 2008)

CHAPTER 2: IMAGING

University of New Haven
HENRY C. LEE COLLEGE OF
CRIMINAL JUSTICE AND FORENSIC SCIENCES
Department of Forensic Science

2.1 Infrared Radiation

In 1800, Frederick William Herschel was the first to discover the infrared (IR) region of the electromagnetic spectrum. Herschel used thermometers and a prism to measure the temperatures of different visible regions of the electromagnetic spectrum. However, Herschel discovered that maximum heat was detected beyond the exposure of the prism to the maximum amount of visible light (i.e. red). Therefore, Hershel concluded that there must be wavelengths of light in the electromagnetic spectrum that is beyond what is visible to the human eye (Herschel, 1800). Soon after this discovery, it was established that any living or non-living body with a temperature above zero does emit IR (Brewster, 1992; Vollmer & Mollmann, 2017).

The electromagnetic spectrum describes the frequencies and wavelengths of both visible and invisible light (i.e. UV and infrared). The IR region is considered low energy due to its low frequencies and long wavelengths (Petersen, 2007). Although these wavelengths are not detectable by the human eye, our senses have evolved to sense IR through its associated heat (Petersen, 2007).

The emissivity of IR by an object is dependent upon the object's properties and ability to absorb infrared. An object with a high emissivity is considered a blackbody, which absorbs all IR placed upon it. Comparatively, a greybody, which has a low emissivity, will reflect some IR. An object will have a greater emissivity the more IR it absorbs (Brewster, 1992; Vollmer & Mollmann, 2017). To put this into perspective, a black vehicle would appear hotter than a silver vehicle using an infrared camera due to its high emissivity (Lee, 2017). Understanding the concept of emissivity is vital in understanding how thermal imaging technology can be used to detect differences in temperature between an object and its surroundings.

Properties of IR radiation have been implemented in thermal imaging techniques to detect components of the world that would otherwise go unnoticed. Some applications of IR imaging techniques include the use in search and surveillance operations for the military, in photographing crime scenes, and in medical diagnoses (Edelman, Hoveling, Roos, van Leeuwen, & Aalders, 2013; Lloyd, 1975)

2.1.1 Forward Looking Infrared Radar (FLIR)

Forward looking infrared radar (FLIR) is a type of thermal imaging often used in aerial operations. The FLIR operates in the far-infrared spectrum with a wavelength of about 20-1000 μm (Petersen, 2007). The field of view will consist of the object of interest (target) and the environment surrounding it (background), all emitting different amounts of IR. There may also be additional objects (clutter) that can obscure the detected radiation (Petersen, 2007). Therefore, the image gathered must be deciphered in order to distinguish the target from its surroundings.

FLIR technology has recently been utilized in two research studies to detect larval aggregations on decomposing pig carcasses (Amendt et al., 2017; Lee et al., 2018). These research studies aimed to determine if the heat produced from larval aggregations was significant enough to be detected by a FLIR mounted on a police helicopter under different climatic conditions (Amendt et al., 2017; Lee et al., 2018). The recent success of these studies supports the need for further research using FLIR technology to detect larval aggregations in different regions and investigate options to improve the techniques with the aim of providing cost-effective and adaptable system for law enforcement agencies when searching for missing individuals.

2.2 Aerial Imaging

Aerial imaging pertains to the capturing or surveillance of the world from an elevated surface above ground. The development of aerial imaging technology began in early 1700's, and has continued to advance for various purposes, such as surveillance, disaster assessment, ecosystem monitoring, and search and rescue missions (Petersen, 2007). Devices used historically and/or presently for such purposes include planes, satellites, helicopters and unmanned aerial systems. Many of these devices use electromagnetic surveillance techniques, such as infrared radars, for greater visualization of the area of interest (Petersen, 2007). With aerial imaging technology, the world can be seen in a way that is not possible through the human eye alone.

2.2.1 Unmanned Aerial Systems (UAS)

Unmanned aerial systems (UAS), or drones, are aircrafts that require no onboard operator and are controlled by computer or remote technology (Perritt & Spraque, 2017). UAS were developed in the early 1900's due to advancements in technology that was driven by military and model-aircraft interests. The initial use of UAS was for anti-aircraft target practice during World War II. However, by the end of the war and during the wars to follow, UAS became involved in additional operations, including surveillance and reconnaissance missions (Perritt & Spraque, 2017).This unique aircraft system allowed the military to save lives and to go places that would otherwise be unreachable. UAS have since become a common technique used for aerial imaging purposes.

Further advancement in technology has allowed for the development of smaller systems with increased aerial imaging capabilities, including capturing photos/videos and live streaming images to operators (Cheng, 2016). Within the past decade, these small, unmanned aerial systems (sUAS) have become a well-known and easily acquired technological device for both business and pleasure. Besides military operations, sUAS are currently being used for landscape photography, movie and T.V. production, search and rescue missions and law enforcement (Perritt & Spraque, 2017).

2.2.1.1 UAS Classification

There is no standard classification system for UAS. As the use of UAS has readily increased for a variety of applications, it has become more difficult to create a classification system that can incorporate all of the different UAS being utilized. Therefore, UAS are typically classified based on a number of performance specifications and/or by mission aspects (Agbeyangi, Odiete, & Olorunlomerue, 2016).

UAS can be classified according to one or more performance specifications, including weight, endurance and range, maximum altitude, wing loading, engine type and power (Arjomandi, Agostino, Mammone, Nelson, & Zhou, 2006). For example, the United States Department of Defense has specified five categories of military UAS based on four of these performance specifications (Table 2:1) (Arjomandi et al., 2006).

Table 2:1 - United States Department of Defense Classification of Unmanned Aerial Systems (adapted in Arjomandi et al., 2006)

Category	Size	Maximum Gross Takeoff Weight (MGTW) (lbs)	Normal Operating Altitude (ft)	Airspeed (knots)
Group 1	Small	0-20	<1200 AGL	<100
Group 2	Medium	21-55	<3500	<250
Group 3	Large	<1320	<18000 MSL	<250
Group 4	Larger	>1320	<18000 MSL	Any
Group 5	Largest	>1320	>18000	Any
AGL = Above Ground Level MSL = Mean Sea Level				

UAS can also be classified according to mission aspects, which are based on functional applications (Agbeyangi et al., 2016; Arjomandi et al., 2006). These functional categories include UAS target and decoy, reconnaissance (surveillance), combat, logistics (delivery), and civil and commercial purposes (Arjomandi et al., 2006). `

2.3 Forensic Implications

The use of sUAS in law enforcement is quickly growing. Aerial imaging by helicopters has historically been used by law enforcement for surveillance, pursuits, incident investigations and accident reconstructions. However, helicopters are expensive and not all agencies have access to one (Perritt & Spraque, 2017). Also, helicopters can be restricted to priority applications due to cost, they are unable to fly over certain areas and compared to sUAS, have less adaptability in

rapid height adjustment and positioning. Therefore, sUAS are becoming incorporated into these situations due to low cost and ease of use. For example, in March 2017, a Maryland police department used a sUAS to fly over a suspected area and capture images of stolen construction equipment worth nearly $400,000 (Warren, 2017). In March 2019, police in Texas used a sUAS to follow and catch a suspect who was on the run ("Arlington police now using drones to catch criminals," 2019). These are just two of the many examples in which the technological advancements of sUAS are providing new possibilities to law enforcement that would otherwise be too expensive or difficult to undertake.

One of the benefits of using sUAS, especially in law enforcement, is that they can be equipped with various types of cameras, including infrared cameras (Cheng, 2016). The combining of aerial and thermal imaging into a single, compatible device has provided law enforcement with greater visualization capabilities in operations like search and rescue missions. The first time a sUAS equipped with an infrared camera was used in a search and rescue mission was in May 2013 by the Royal Canadian Mounted Police. A man's car had flipped over into the snow in a remote, wooded area. He tried calling 911 for assistance but was not able to provide his exact location. Other search methods were used, such as helicopters and search parties, but only the sUAS was able to locate the man, due to the difference in temperature between the man and his surroundings (Franzen, 2013). Since then, many search and rescue organizations have incorporated the use of this technology into their procedures. For example, sUAS with infrared technology have also been utilized by police for detection of suspects in pursuits. In March 2019, Murrysville police used a sUAS with an infrared camera to track two suspects who had fled into the woods after crashing a stolen car. The sUAS operator was able to detect two heat signatures and dispatched officers to the area where the two suspects were hiding (Peirce, 2019).

Despite the increasing use of sUAS by law enforcement agencies, this technology has not yet been utilized in search and recovery missions for missing, deceased individuals. Currently, law enforcement agencies rely on expensive and/or time-consuming search tactics including cadaver dogs, search parties and aerial imaging devices. However, previous research has shown the success of utilizing an aircraft system mounted with a FLIR to detect decomposing carcasses more than four days after death, as a result of the heat produced from associated larval aggregations (Amendt et al., 2017; Lee et al., 2018). Therefore, a smaller aircraft system, such as a drone, mounted with a FLIR could be utilized to detect larval aggregations on decomposing remains, providing a more cost-effective and less-time consuming method to search extensive areas for missing, deceased individuals.

2.4 Research Statement

In an international collaboration with Dr. Sasha Voss and Dr. Michael Lee from the University of Western Australia, this research aims to determine if a sUAS mounted with a FLIR can detect larval aggregations on decomposing carcasses in an effort to develop a more effective search and recovery method for law enforcement agencies.

2.5 Aims and Objectives

This research aims to develop a user-friendly, portable, field adaptable and cost-effective search method for law enforcement by:

1. Determining if a sUAS and a thermal imaging camera are compatible and can be used to detect differences in temperature while in flight.
2. Determining a baseline for the amount of heat generated by *Phormia regina* maggot masses in the Connecticut region.
3. Evaluating the relationship between sUAS height and temperature detection using FLIR technology.
4. Determining if larval aggregations on decomposing carcasses can be detected using a sUAS with thermal imaging technology.

The objectives of this research are to:

1. Integrate the FLIR with the sUAS for real time imaging of thermal differences at varying heights.
2. Record the temperature of different sized maggot masses in a lab-controlled study in order to calculate the daily differences in temperature between each maggot mass and the ambient temperature.
3. Utilize the FLIR and sUAS to detect artificial heat sources that model the temperature of maggot masses.

4. Utilize the FLIR and sUAS to determine if larval aggregations on decomposing organisms can be detected.

CHAPTER 3: MATERIALS AND METHODS

University of New Haven
HENRY C. LEE COLLEGE OF
CRIMINAL JUSTICE AND FORENSIC SCIENCES
Department of Forensic Science

3.1 Drone and Thermal Camera Integration

Drone and thermal camera devices were integrated and tested to determine which set-up would be optimal for the aims of this research. Each system was assessed for compatibility, as well as for individual drone and thermal camera capabilities.

3.1.1 DJI Phantom™ 3 Standard Drone and FLIR Duo® Camera

The DJI Phantom™ 3 Standard drone (Figure 3:1) was the initial sUAS tested for this research. The drone's features included live Global Positioning System (GPS), geosynchronous hovering for stability and ease of control, and a built-in camera to capture images and videos. This drone was also compatible with the DJI© GO mobile application, which provided a live video feed, or first-person view (FPV), and control of the on-board camera during flight.

Figure 3:1 - DJI Phantom™ 3 Standard drone with remote controller and DJI© GO mobile application (Photograph by Megan Descalzi)

The FLIR Duo® (Figure 3:2) was a dual-sensor thermal camera designed for drones. This camera was compact and lightweight, making it suitable for on-board attachment during drone

flight. The FLIR Duo® was controlled via the FLIR UAS™ mobile application, which could be utilized to capture real-time thermal and visual images and videos. These images could then be uploaded to the FLIR Tools® software program for analysis. This program could be utilized to determine the temperature of an area and to optimize thermal signatures by adjusting the color palette and optical parameters, such as emissivity and reflected temperature.

Figure 3:2 - FLIR Duo® thermal camera (Photograph by Megan Descalzi)

While both devices were independently valuable for this research, they could not be integrated into one system. The aim was to remove and replace the built-in camera on the DJI Phantom™ 3 Standard drone with the FLIR Duo®. However, it was not possible to remove the built-in camera as it had been integrated into the drone hardware during manufacturing. Without removing the built-in camera, the thermal camera could not be mounted on to the drone. It was concluded that these two devices were not compatible for drone flight.

3.1.2 DJI Phantom™ 2 Drone and FLIR Duo® Camera

The FLIR Duo® was then tested with the DJI Phantom™ 2 drone, as these devices were advertised by FLIR® as compatible. The DJI Phantom™ 2 drone (Figure 3:3) had GPS and was

capable of geosynchronous hovering, but because it was an earlier model in the DJI Phantom™ series, this drone did not come equipped with a built-in camera. Instead, a gimbal needed to be installed in order to suspend a camera from the bottom of the drone.

For this research, the Zenmuse™ H3-2D gimbal was connected to the DJI Phantom™ 2 drone. This gimbal was customized for the GoPro® Hero3 camera. However, the FLIR Duo® has similar connections and weighed about the same as the GoPro®, which allowed for the thermal camera to be successfully mounted on the Zenmuse™ H3-2D gimbal. Using this gimbal, the camera could be tilted by the drone's remote controller for optimal positioning during flight.

Figure 3:3 - DJI Phantom™ 2 drone and FLIR Duo® camera set-up, with the remote controller (left) and Flysight® Black Pearl Monitor (right) (Photograph by Megan Descalzi)

The DJI Phantom™ 2 drone was not compatible with the DJI© Go mobile application and was therefore not equipped for FPV when purchased. However, after researching FPV set-ups it

was discovered that with the connection of additional drone parts, FPV could be established using the FLIR Duo® and the DJI Phantom™ 2 drone. To accomplish this FPV set-up, the top cover of the drone was removed and a plug and play cable was used to connect the DJI© iOSD Mini On-Screen Display and the ImmersionRC© 600MW 5.8GHz A/V Transmitter to the drone board (Figure 3:4) (Iftirbashir, 2006). A FatShark® ImmersionRC© 5.8GHz Circular Polarized SpiroNET Antenna with SMA connector was attached to the transmitter, and a FatShark® ImmersionRC© 5.8GHz Circular Polarized SpiroNET Antenna with RP-SMA connector was attached to the receiver, a Flysight® Black Pearl Monitor (Iftirbashir, 2006). This FPV set-up transmitted a real time video from the mounted thermal camera to the monitor while the drone was in flight. Flight information, such as height and velocity, was also transmitted to the monitor from the connected DJI© iOSD Mini On-Screen Display (Iftirbashir, 2006).

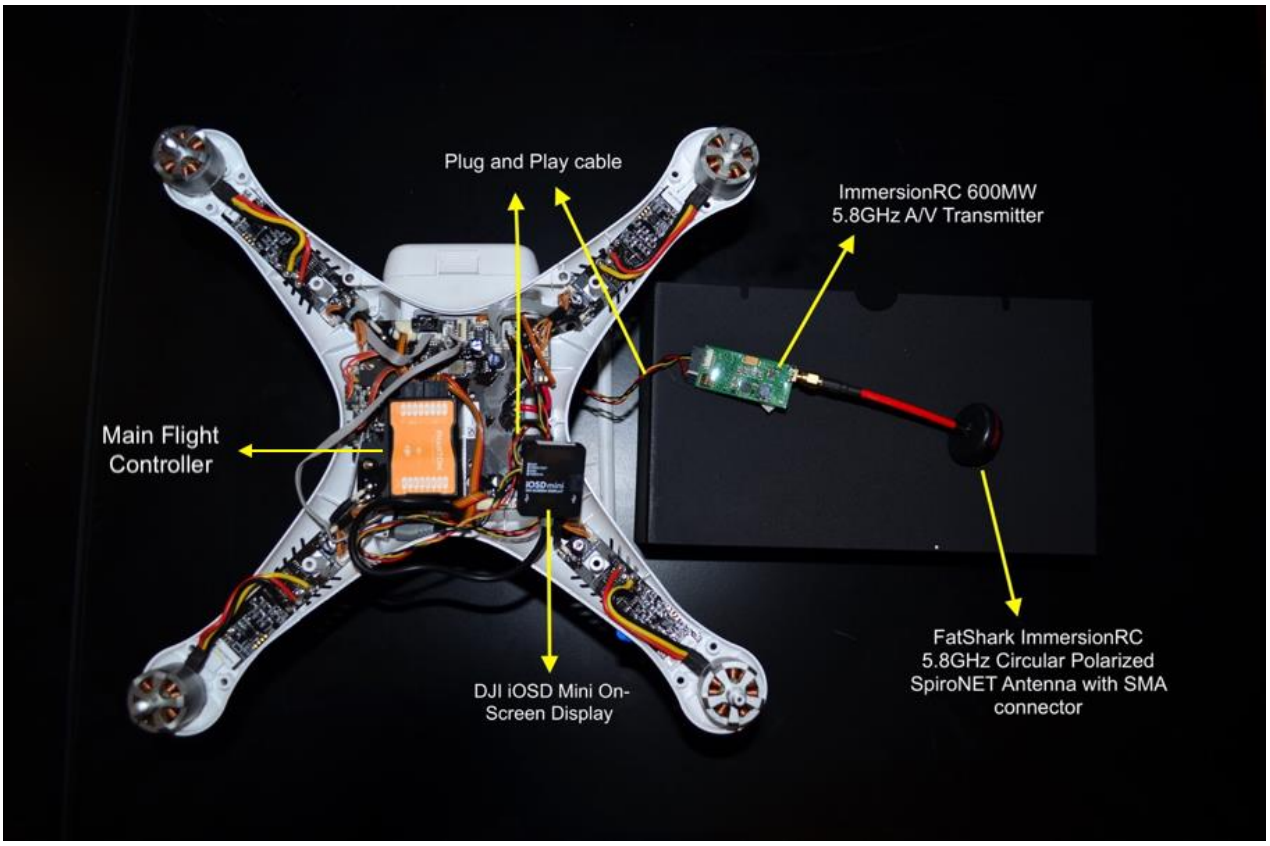

Figure 3:4 - DJI Phantom™ 2 drone connections for FPV set-up (Photograph by Megan Descalzi)

Despite success in integrating the two devices and implementing FPV capability, it was determined that this set-up was not optimal for the aims of this research. There were technological disadvantages with both the drone and thermal camera that became apparent during test flights. The DJI Phantom™ 2 drone was not capable of geosynchronous hovering, which made it difficult to control. The drone maintained its height readily, but the slightest wind disturbance would cause the drone to wander from its designated position. During test flights, the drone crashed to the ground multiple times due to the difficulty in controlling its movement. Experiment protocols for this research required the drone to be flown at heights up to 50 meters and over bodies of water, which would cause substantial damage to the drone if it were to crash

under these conditions. Therefore, it was essential to this research that the drone utilized could maintain its position steadily and be maneuvered easily because if the drone were to wander or crash, further research could be inhibited.

The FLIR Duo® could not be utilized to determine the temperature measurement in real time of a certain area within the field of view. The only way to determine the temperature was to capture an image of an object or area using the FLIR UAS™ mobile application, and then upload the image to the FLIR® Tools program for analysis. This was a time-consuming, multi-step process which prevented efficient analysis of the temperature differences between a targeted object and its surroundings in real time.

Although the FPV set-up was able to display real time video to the monitor during drone flight, the image transmitted was often pixelated and lacked sufficient detail to discern what the FLIR Duo® was detecting in its field of view. FPV is an essential component to this research as it is the visual component needed to detect the temperature differences between the targeted object and its surroundings. The lack of quality in this FPV imaging was problematic for this research as it made it difficult to visualize these temperature differences during drone flight. Additionally, flight information transmitted from the DJI© iOSD Mini On-Screen Display was difficult to read and report during flight. The values displayed on the Flysight® Black Pearl Monitor were sometimes blocked by the edges of the screen, and it was difficult to discern which values corresponded to specific flight information. Drone height in particular was an important value to read and report for this research, but using this drone set-up, it was not always possible to determine the drone's height during flight.

It was determined after multiple test flights that the DJI Phantom™ 2 drone and FLIR Duo® set-up was not efficient or practical for this research. There were too many technological disadvantages needed to be overcome before experiments could begin. Therefore, a new set-up was needed to proceed.

3.1.3 Parrot Bebop-Pro Thermal™ Drone

A search for thermal drones revealed the Parrot Bebop-Pro Thermal™ drone (Figure 3:5), which was released in December 2017. This new thermal drone was advertised for professional use, such as by first responders for search and rescue missions and by builders for roof inspections. This drone had GPS, geosynchronous hovering and was equipped with two built-in cameras, including a visual camera and a FLIR One Pro® thermal imaging camera. The drone was controlled using the Parrot Skycontroller™ 2, in conjunction with the FreeFlight Thermal™ mobile application, which was downloaded on a Samsung Galaxy Tab® A tablet for this research. The FreeFlight Thermal™ mobile application provided a live stream view from the visual and thermal cameras during drone flight. This mobile application was also utilized to capture images and videos, switch between cameras and adjust the thermal color pallet for optimal visualization of thermal signatures.

Figure 3:5 - Parrot Bebop-Pro Thermal™ drone set-up, with Skycontroller™ 2 (top left) and Samsung Galaxy Tab® A tablet (bottom left) (Photograph by Megan Descalzi)

The FreeFlight Thermal™ mobile application was capable of thermal analysis during and after flight. The temperature of an object or area could be determined by simply touching the tablet screen at the location of interest within the image. The detected temperature was then reported on the screen (Figure 3:6). This feature was utilized for this research to analyze and record the temperature of objects and surroundings within captured thermal images after flight.

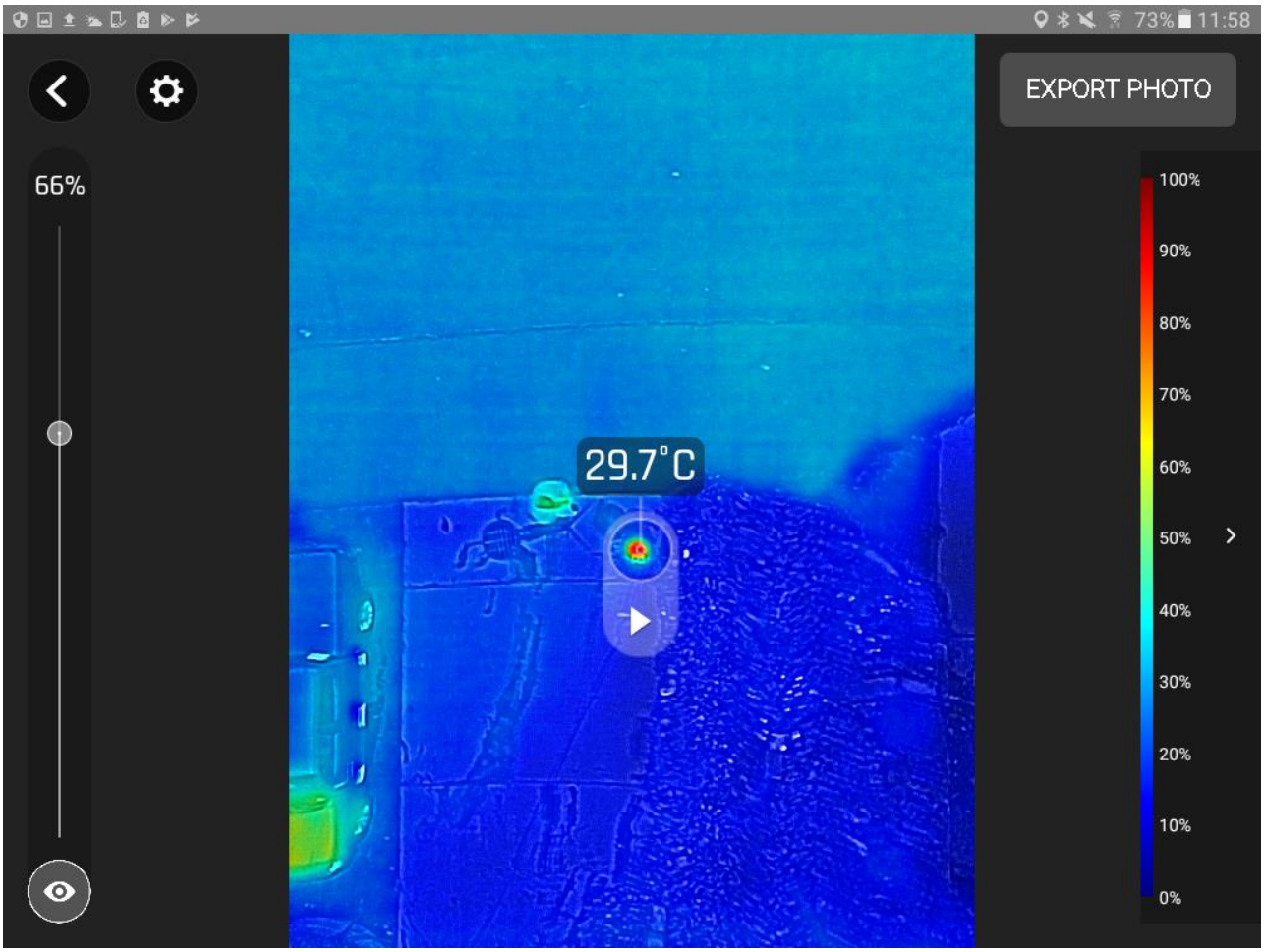

Figure 3:6 - Thermal analysis using the FreeFlight Thermal™ mobile application

Before the Parrot Bebop-Pro Thermal™ drone was utilized for research purposes, test flights (Figure 3:7) were performed in order to learn the features of the drone, such as switching between cameras mid-flight and capturing images and videos. Considerable time was also taken to practice flying the drone at various heights and maneuvering it to a designated position to ensure that operation of the drone was efficient for future research. After multiple test flights, it was determined that the Parrot Bebop-Pro Thermal™ was a more optimal drone for the aims of this research because it was easier to maneuver and provided greater quality imaging to detect differences in temperature between an object and its surroundings

Figure 3:7 - Megan Descalzi flying the Parrot Bebop-Pro Thermal™ drone during a test flight (Photograph by Dr. R. Christopher O'Brien)

Although the test flights and most of the experimental replicates were successful, catastrophic complications were encountered when the Parrot Bebop-Pro Thermal™ drone crashed twice during flight. The first crash occurred in August 2018 due to GPS failure and the second crash occurred in March 2019 because of a battery failure. Damage occurred to the drone in both instances, which prevented continued use of the drone and inhibited additional experimental replicates from being completed until the drone was replaced by Parrot. After the first crash in August 2018, a replacement drone was not received from Parrot until October 2018, which delayed the progress of this research for two months. The drone could not be replaced after the crash in March 2019 because the Parrot Bebop-Pro Thermal™ drone was no longer manufactured.

3.2 Diptera Colonies

Fly colonies were maintained throughout the duration of this research in order to rear the eggs needed for developing maggot masses for laboratory experiments. Colonies of *Lucilia sericata* (Meigen, 1826), *Phormia regina* (Meigen, 1826), *Sarcophaga bullata* (Parker, 1916) and collected wild flies were maintained. *Lucilia sericata* pupae was donated from Dr. Jeff Tomberlin's laboratory at Texas A&M University and Dr. Amanda Roe's laboratory at the College of Saint Mary. *Phormia regina* pupae was donated from Dr. Christine Picard's laboratory at Indiana University-Purdue University Indianapolis and *Sarcophaga bullata* pupae was purchased from Carolina® Biological Supply Company. The larvae of the wild flies were collected from a rabbit (*Sylvilagus floridanus*) (Figure 3:8) carcass placed outside Dr. R. Christopher O'Brien's laboratory at the University of New Haven in West Haven, Connecticut, and were reared to emergence. The wild sample flies were identified as *Phormia regina* (Whitworth, 2017).

Figure 3:8 - Rabbit (*Sylvilagus floridanus*) carcass (Photograph by Megan Descalzi)

3.2.1 Colony room

All fly colonies were located in the colony room within Dr. R. Christopher O'Brien's laboratory in West Haven, Connecticut. The colony room was temperature controlled, but the room temperature would fluctuate depending on the ambient conditions in the Connecticut region, which exposed the flies to varying temperatures throughout the rearing process. During colder seasons, a space heater was used in addition to the heating system, in order to keep the space warm enough for fly rearing and survival. A humidifier was also placed in the room to keep the environment moist for optimal larvae survival.

There were two metal racks in the colony room utilized for fly colony maintenance and breeding. The first rack held all of the fly colony cages and by the end of this research, there was a total of 14 cages located on the first rack (3:9 a). The second rack held all of the rearing dishes for fly larvae (3:9 b). Fly colony and rearing dish consumables were also kept on both racks.

a)  b) 

Figure 3:9 - a-b - Colony room set-up, a) fly colony rack, b) rearing dish rack (Photographs by Megan Descalzi)

The room had one large window, which provided natural light throughout the day. However, due to the onset of diapause in response to increased hours of darkness in November 2018, a light timer was installed and set to a 16:8 hour (light:dark) photoperiod (Heaton, Moffatt, & Simmons, 2014; Ody, Bulling, & Barnes, 2017).

3.2.2 Diptera Maintenance

Colony cages (*12 in ×12 in × 12 in*) were built with ½" PVC pipes, fastened together with PVC side outlet elbows and PVC cement (Figure 3:10 a). Sides of curtain liner were sewed

together and used as mesh to cover the cages. The opened ends of the liner were secured with rubber bands and clamps to keep the flies contained (Figure 3:10 b).

a) 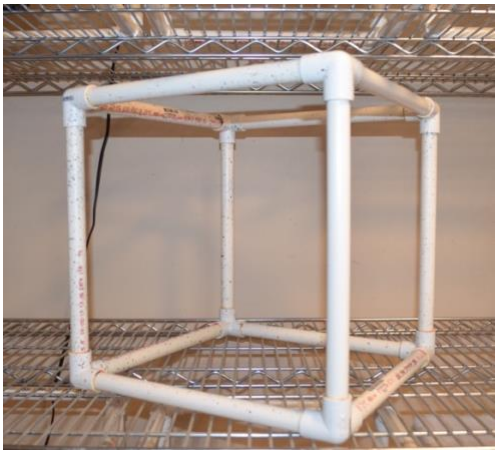 b) 

Figure 3:10 - a-b - Colony cages, a) PVC structure of cage, b) cage covered with curtain liner and secured with rubber bands and a clamp (Photographs by Megan Descalzi)

Each cage was given a continual supply of sugar and water. Sugar cubes were placed on a petri dish and water was contained in a urine collection cup, which had a fabric square placed through a hole cut in the lid (Figure 3:11). The fabric was used to wick the water upward, where the flies could easily drink from it. Sugar and water were monitored daily for replacement. A log was utilized to keep track of when the sugar and water was replaced in each cage (Appendix A).

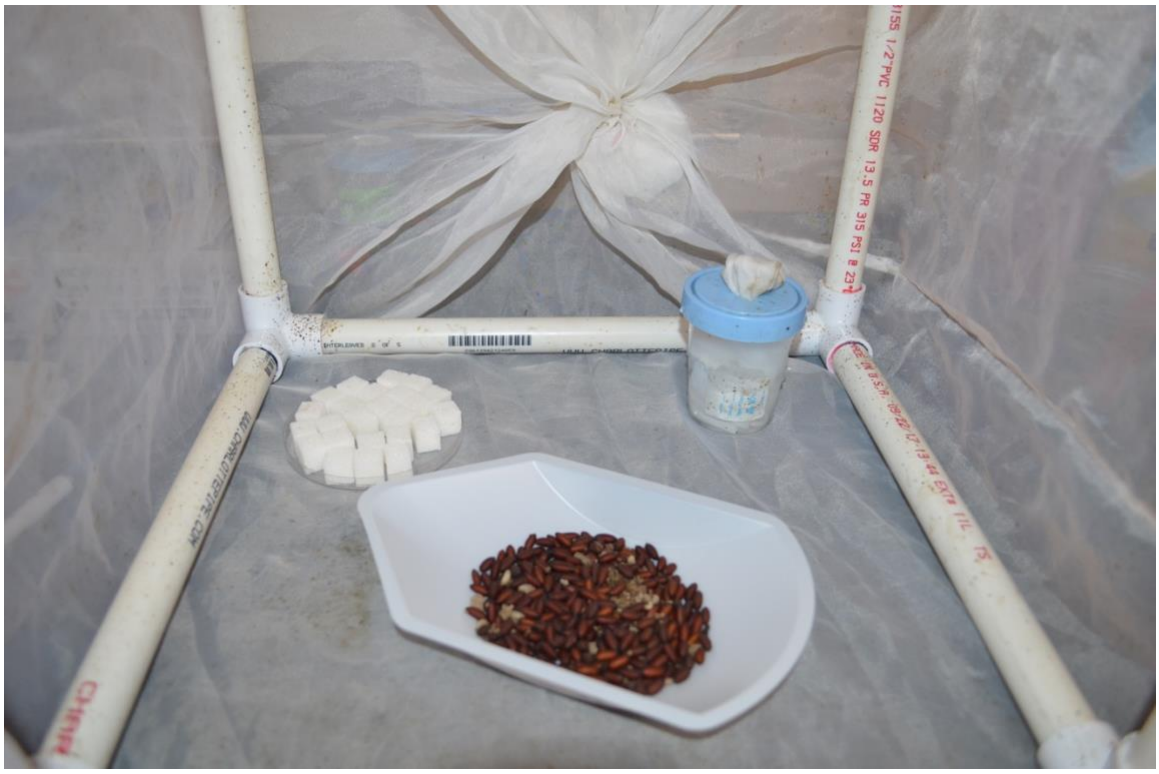

Figure 3:11 - Sugar, water and *Sarcophaga bullata* pupae placed inside colony cages (Photograph by Megan Descalzi)

3.2.3 Diptera Breeding

A blood feed was prepared a minimum of once a week for each cage. A blood feed consisted of either pig liver or ground beef placed in a large weigh boat and covered in pigs blood. After 24 hours, the blood feed was removed and examined for fly eggs or larvae. If present, a rearing dish (Figure 3:12 a) was prepared. An extra-large GLAD® plastic container was filled halfway with sieved sand. Ground beef was placed on a plastic plate or weight boat and was covered in pigs blood. The ground beef placed in the rearing dishes was mixed with water crystals in order to keep the meat moist for optimal larvae growth through all three instars (Johnson, Wighton, & Wallman, 2014).

The fly eggs laid by the oviparous species or the larvae laid by the larviparous species were transferred to the ground beef, and the plate was placed on the sand. A mesh square was placed on top of the plastic container (Figure 3:12 b), and a rubber band was placed over the mesh to secure it, in order to prevent the larvae from leaving the dish. Each rearing dish was sprayed twice a day with water and larvae were monitored for wandering and pupation. Once all larvae had pupated, the meat was removed, and the sand was sieved. The pupae were either placed directly in a new colony to emerge (Figure 3:11) or were placed in a urine collection container in a 4°C refrigerator for preservation. Each colony and rearing dish had an associated log that was maintained to keep track of daily operations and larvae development **(**Appendix A**)**. This process was continually repeated in order to develop a large quantity of pupae that was later used to generate maggot masses.

a.)  b.) 

Figure 3:12 - a-b - Rearing dish, a) ground beef with pigs blood placed on sand, b) dish covered with curtain liner (Photographs by Megan Descalzi)

3.3 Maggot Mass Temperatures in Laboratory

In laboratory-controlled studies, different sized maggot masses were generated, and temperatures were recorded in order to determine a baseline for the amount of heat generated by maggot mass temperatures in the Connecticut region.

3.3.1 Determination of Egg Weight

Egg rafts removed from blood feeds (Figure 3:13) were weighed and counted in order to determine the average weight of an individual egg for each of the oviparous fly species in colony. Five rafts from the *L. sericata* blood feeds and eight rafts from *P. regina* blood feeds were used. The number of egg rafts weighed and counted varied between the species because greater complications were encountered with maintaining the *L. sericata* colonies than the *P. regina* colonies, which reduced the number of egg rafts that were collected from the *L. sericata* blood feeds. The egg rafts from the *L. sericata* flies all came from Colony Three, while the egg rafts from *P. regina* flies came from Colonies One, Four, Five and Eight.

After being removed from the blood feeds, the egg rafts were immediately weighed using a Mettler® B5 analytical scale. The eggs were preserved in 70% ethanol and the number of eggs in each sample were counted. The weight of each egg raft was then divided by the number of eggs counted in order to determine the weight of each individual egg, in micrograms. This same procedure was followed for the *S. bullata* in colony, but a small quantity of larvae from three blood feeds were weighed and counted instead of egg rafts, as it is a larviparous species. The same calculations were made in order to determine the weight of an individual larvae for *S. bullata*.

Figure 3:13 - Egg raft collected from pigs blood feed (Photograph by Megan Descalzi)

3.3.2 Experimental Set-up for Laboratory-Controlled Studies

The average egg weight of *P. regina* flies was used to estimate the weight of different sized egg rafts containing approximately 200, 1,000 and 5,000 eggs. Blood feeds were placed in the *P. regina* species cages and were removed after 24 hours. The eggs laid were used to generate the different egg raft sizes based on the previously calculated weights. These eggs were then placed on carcasses large enough to support the developing maggot masses. The estimated 200 eggs were placed on a chipmunk (*Tamias striatus*) carcass (Figure 3:14 a), 1,000 eggs on a rabbit (*Sylvilagus floridanus*) carcass (Figure 3:14 b) and 5,000 eggs on a coyote (*Canis latrans)* carcass (Figure 3:14 c).

A total of six carcasses were utilized for two experimental replicates. The chipmunks and rabbits were donated from the Veterinary Clinic for Birds and Exotics in New York, and the coyotes were donated from a hunter in Connecticut. Each carcass was previously frozen and was thawed for at least 24 hours prior to the experiment beginning. The carcasses were placed in a plastic bin containing sand and were covered with either curtain liner or aluminum screen mesh,

in order to prevent disturbance and contamination of the experimental set-up. The coyote bin in the first replicate was the only set-up that did not contain sand for maggots to pupate in, which caused the maggots to wander outside of the bin during the third instar. Therefore, sand was added to the coyote bin in the second replicate.

Figure 3:14 - a-c - Experimental set-up (Replicate One), a) chipmunk (*Tamias striatus*) carcass, b) rabbit (*Sylvilagus floridanus*) carcass, c) coyote (*Canis latrans*) carcass (Photographs by Megan Descalzi)

Prior to placing the egg rafts, lacerations were made on each carcass, which provided the eggs with a moist, protected environment, optimal for larval growth. For the first replicate, an egg raft was placed within a laceration that was made with a scalpel in the lateral cervical region of each carcass (Figure 3:15 a). However, larval aggregations only formed in the cervical region, not in the abdominal region where the probe was positioned to measure aggregation temperatures. Therefore, lacerations in the subsequent replicate were made in the abdominal region of each carcass (Figure 3:15 b).

a)

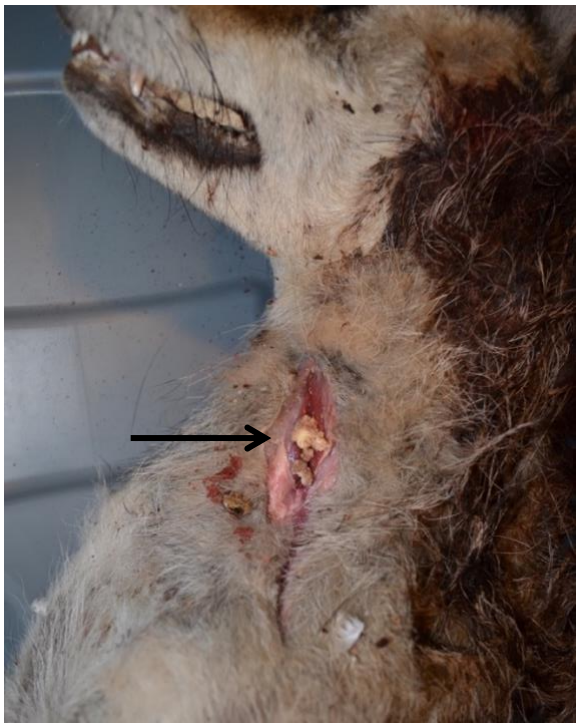

b)

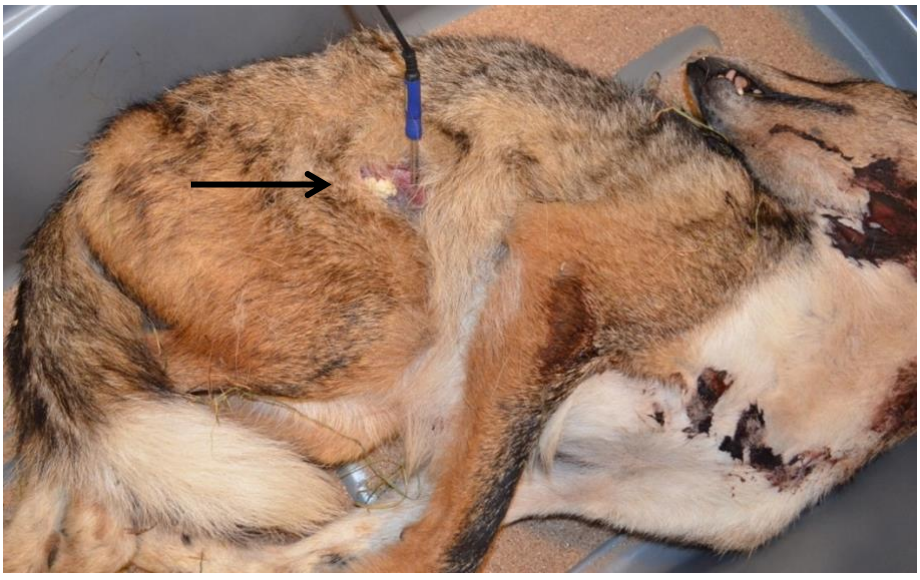

Figure 3:15 - a-b - Egg rafts (indicated by black arrow) placed in lacerations made on coyote (*Canis latrans)* carcasses, a) lateral cervical region (Replicate One), b) abdominal region (Replicate Two) (Photographs by Megan Descalzi)

3.3.3 Data Collection

Temperature readings of the carcasses were recorded using a FLIR® E6 infrared camera (Figure 3:16) and General® IRT207 Infrared Laser Thermometer. The FLIR® E6 camera is capable of visually assessing infrared signatures and was therefore used to locate the warmer regions of the carcasses where maggot masses may have developed and to record the temperature of those regions. Once the warmer regions were identified, the infrared thermometer was utilized to record an additional temperature reading of the area. Both instruments were also used to record the temperature of an area of a carcass unaffected by larval activity. This temperature served as a baseline for the carcass temperature when equivalent to the ambient temperature of the colony room.

Figure 3:16 - FLIR® E6 infrared camera (Photograph by Megan Descalzi)

Additional temperature readings were recorded using a Tinytag® dual external temperature logger with two thermistor probe attachments (TGP-4520) and a Gemini Tinytag® internal/external temperature logger with one thermistor probe attachment (TGP-4510) from Gemini Data Loggers UK Ltd. Each probe was inserted into the abdomen of a carcass used in the experimental set-up (Figure 3:14 a-c). The Tinytag® TGP-4510 temperature logger was also utilized to record ambient temperature of the room in which the experiment was taking place. Temperature readings were recorded daily until larval activity ceased and pupation began to occur.

3.4 Hot Water Analog

A hot water source was utilized as an analog for maggot masses, in order to determine how temperature detection varied with increasing drone height. Hot water sources were placed on and near a variety of substrates at two different locations. The Parrot Bebop-Pro Thermal™ drone was flown at different search heights and was utilized to determine the temperature of the water source and the substrates at those heights.

3.4.1 Hot Water Analog Experimental Set-Up

A plastic container filled with water was placed on a substrate at one of the two locations. A 5-gallon (Figure 3:17 a) and 50-gallon (Figure 3:17 b) plastic container were both utilized in different replicates of this research. Water temperature was kept constant using a PolyScience® Sous Vide® DISCOVERY Circulator and was set between 10°C and 50°C depending on the ambient temperature at the time of each replicate. A Digi-Sense Traceable® Remote Probe Digital Thermometer was placed in the water source, and a Tinytag® internal temperature and

relative humidity logger (TGP-4500) from Gemini Data Loggers UK Ltd was placed near the experimental set-up. A HoldPeak® 866B digital anemometer was not initially used in earlier replicates of this research but was later added to the experimental protocol. The anemometer was assembled on a tripod next to the water source in order to measure wind speed.

a)

b)

Figure 3:17 - a-b - Experimental set-up, a) 5-gallon plastic container on the North-West side of Horse Island, b) 50-gallon plastic container outside Dr. R. Christopher O'Brien's laboratory (photographs by Megan Descalzi)

3.4.2 Experimental Locations

Horse Island is located in the Long Island Sound and is owned by Yale University and managed by the Peabody Museum (Figure 3:18). Two sites on the island were utilized for this research. The hot water source was placed on a rock on the East side of the island and on a concrete dock on the North-West side of the island. The substrates analyzed include rock, marsh and the sound on the East side and rock, concrete and the sound on the west side. Only the hot water source on the North-West side of the island was replicated due to the continued difficulty in accessing the East side of the island with the boat during tide changes.

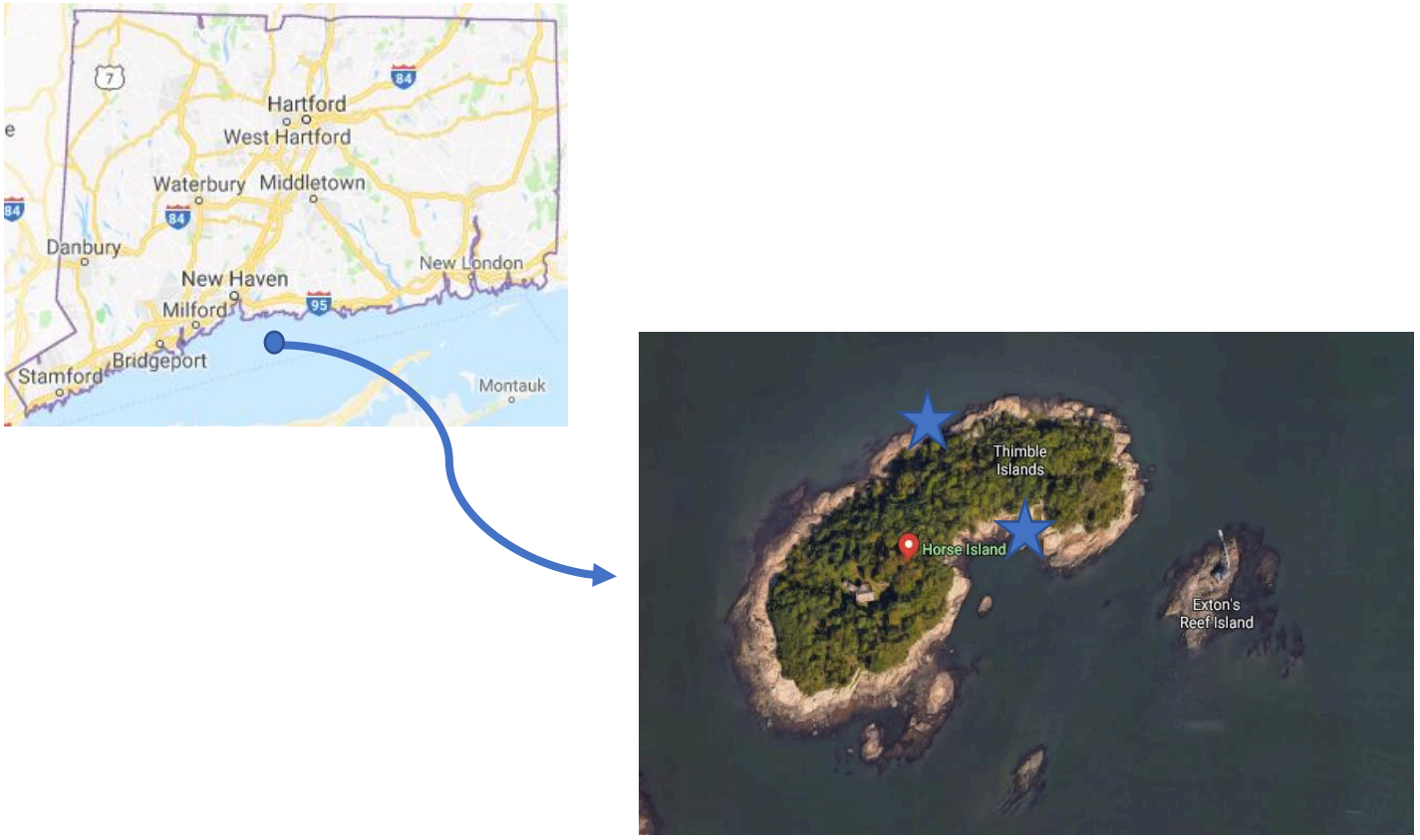

Figure 3:18 - Horse Island (placement of hot water baths is indicated by the blue stars)

Dr. R. Christopher O'Brien's laboratory at the University of New Haven in West Haven, Connecticut was utilized as a second location (Figure 3:19). The hot water source was placed outside on concrete near the East side of the building. The surrounding substrates analyzed also included bitumen and dirt. The hot water source outside the lab was replicated six times, three for each hot water source size.

Figure 3:19 - Dr. R. Christopher O'Brien's laboratory (placement of hot water bath is indicated by blue star) (Photograph by Megan Descalzi)

3.4.3 Data Collection

The Parrot Bebop-Pro Thermal™ drone was utilized to capture thermal images of the hot water source and the surrounding substrates at heights between two and 50 meters. These images were later analyzed using the FreeFlight Thermal™ mobile application to determine the temperature of the water and substrates at each height. During drone flight, the FLIR® E6

infrared camera was also utilized to record the temperature of the water and substrates from a consistent height of about two meters. Two individuals, a drone operator and a data recorder, were needed to carry out these processes. Additional measurements including windspeed using the HoldPeak® 866B digital anemometer, water temperature using the Digi-Sense Traceable® Remote Probe Digital Thermometer and ambient temperature using the Tinytag® TGP-4500 logger were recorded throughout the duration of the experiment. A data collection sheet was created to record all temperature measurements and flight information for each replicate.

3.5 Field-Based Study

The temperature of developing maggot masses on animal carcasses placed outside was analyzed at different drone heights using the Parrot Bebop-Pro Thermal™ drone. Similar experimental protocols used to analyze the hot water sources were followed.

3.5.1 Field-Based Experimental Set-Up

Two carcasses were utilized for this experimental set-up. A coyote (*Canis latrans*) carcass (Figure 3:20 a) was placed at the location on 30 July 2018 and a white-tailed deer fawn (*Odocoileus virginianus)* carcass (Figure 3:20 b) was placed at the same location in 05 November 2018. Both carcasses were secured with rope to prevent scavengers from moving the carcass away from the experimental site. A Moultrie® M-990i Digital Game Camera was set-up to record any scavenging activity that occurred on the carcasses. The Tinytag® TGP-4500 logger was also set-up nearby. The HoldPeak® 866B digital anemometer was added to the experimental protocols following the first replicate and therefore was only utilized to measure windspeed during the second replicate

a)  b) 

Figure 3:20 - a-b - Field-based experimental set-up, a) Coyote *(Canis latrans)* carcass (Day 0), b) White-tailed deer fawn *(Odocoileus virginianus)* carcass (Day 0)

3.5.2 Experimental Location

The University of New Haven has a satellite campus in Orange, Connecticut surrounded by 47 acres of wooded land (Figure 3:21). A site in the south-east corner of the campus was utilized for the purposes of this field research. The ground at this specific site consisted of wood chips and was only partially covered by trees.

Figure 3:21 - University of New Haven, Orange Campus (placement of carcasses indicated by the yellow arrow)

3.5.3 Data Collection

Similar to the hot water sources, the Parrot Bebop-Pro Thermal™ drone was flown above each carcass at heights between two and 50 meters. Thermal images were captured and were later analyzed using the FreeFlight Thermal™ mobile application to determine the temperature of the carcass and wood chips at each height. The drone was utilized on the day of placement to record carcass temperature prior to fly colonization. Each carcass was then monitored daily for the presence of larval activity, and the drone was utilized daily once larvae became visible. The FLIR E6 was again used to record temperature of both the carcass and substrate at a constant

height of about two meters. The Tinytag® TGP-4500 logger recorded ambient temperature and the HoldPeak® 866B digital anemometer recorded wind speed during the time of flight.

3.6 Statistical Analysis

Statistical analysis was conducted using the VSN International GenStat® 19th edition statistical package. Linear regression and analysis of variance (ANOVA) tests were used to determine relationships and differences between different variables and factors from this research. Additional statistical tests were run as necessary.

CHAPTER 4: RESULTS

University *of* New Haven

HENRY C. LEE COLLEGE OF
CRIMINAL JUSTICE AND FORENSIC SCIENCES

Department of Forensic Science

4.1 Drone and Thermal Camera Integration

The compatibility of the DJI Phantom™ 3 Standard drone and DJI Phantom™ 2 drone with the FLIR Duo® thermal camera was tested. The DJI Phantom™ 3 Standard drone was not compatible with the FLIR Duo® because the built-in drone camera could not be removed and replaced with the thermal camera. The DJI Phantom™ 2 drone and FLIR Duo® were successfully integrated using the Zenmuse™ H3-2D gimbal and additional FPV drone parts but was difficult to maneuver and lacked sufficient detail to detect temperature differences between a target and its surroundings. These drone and thermal camera set-ups were not optimal for the aims of this research, and as a result, the Parrot Bebop-Pro Thermal™ drone was tested.

After multiple test flights, it became apparent that the Parrot Bebop-Pro Thermal™ drone was a more practical drone set-up for the purposes of this research. This drone was easier to maneuver as it was capable of maintaining its position even with wind disturbance. This drone was flown in winds recorded up to 3.5 meters per second (mps). It did not wander or crash during these test flights, which provided confidence in the drone's ability to remain stable while being utilized in various conditions during research.

A beneficial feature of this set-up proved to be the integration of the drone, camera and mobile application systems prior to purchasing. Unlike the previous drone set-ups, the Parrot Bebop-Pro Thermal™ drone did not require manipulation to integrate the drone and thermal camera or additional drone parts to provide an FPV set-up. These technologies were manufactured to be compatible, which resulted in the transmission of greater quality imaging and flight information. The image and video transmitted from the thermal camera to the mobile application during flight was of sufficient detail to detect objects within the field of view and to

visualize temperature differences between an object and its surroundings. The flight information was also clearly displayed along the top of the mobile application, making it easier to maneuver the drone to a desired height. This pre-integrated system benefited this research as it reduced the number of technological disadvantages that needed to be overcome and provided more detailed imaging and information that was key for data analysis.

Test flights also provided the opportunity to explore the features of the FreeFlight Thermal™ mobile application (Figure 4:1). During flight, FreeFlight Thermal™ displays flight information and imaging in real time, captures and stores images and videos, and provides the ability to switch between cameras at any time. This mobile application can also be utilized to monitor battery levels of the drone and Skycontroller™ 2, adjust drone speed, and change the thermal color palette for optimal visualization while in flight.

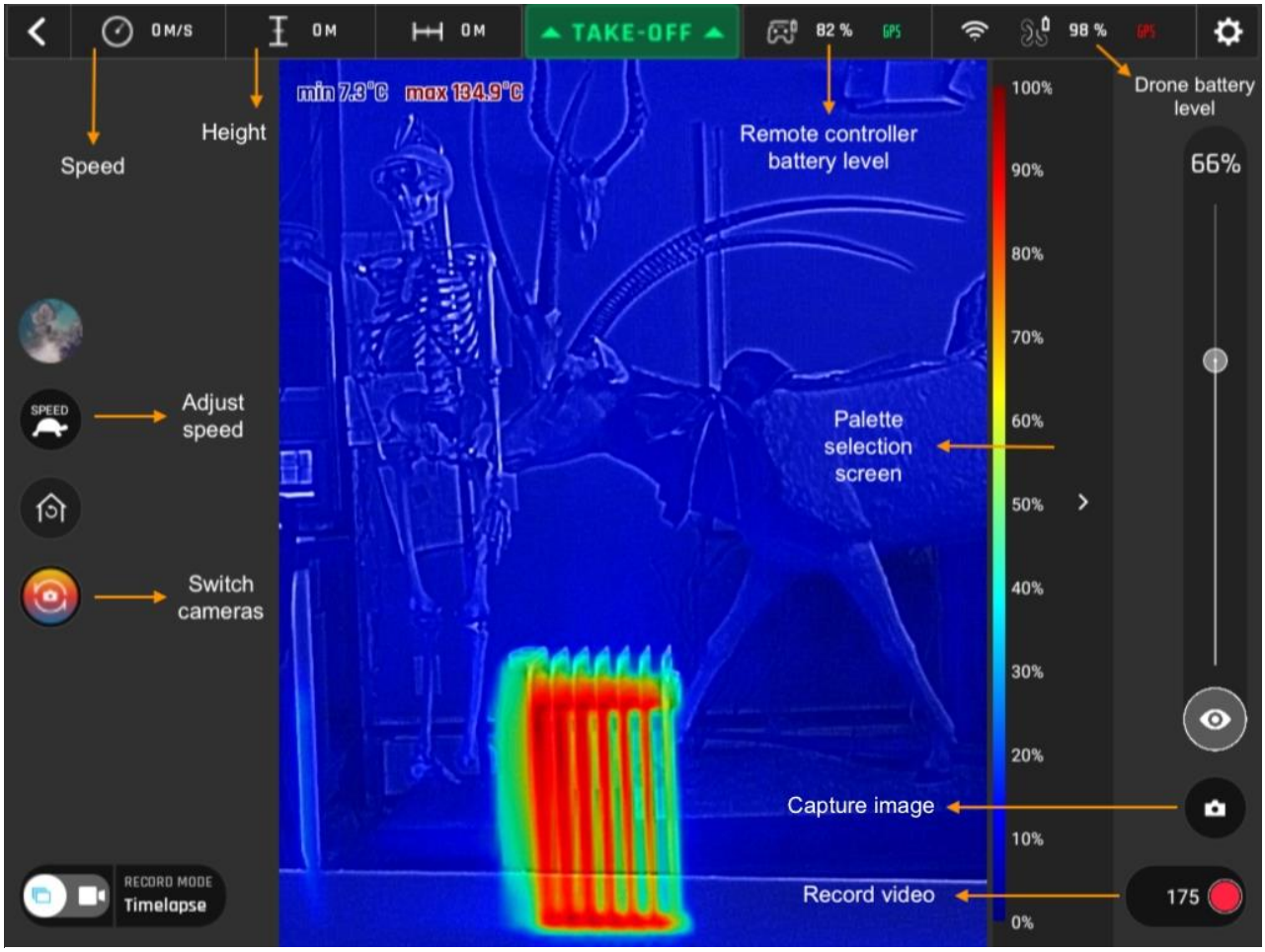

Figure 4:1 - FreeFlight Thermal™ mobile application features

Despite the beneficial features of the Parrot Bebop-Pro Thermal™ drone, there were some complications encountered throughout the course of this research. The first complication was finding a tablet compatible with the FreeFlight Thermal mobile application. Parrot advertised that FreeFlight Thermal™ could be downloaded on an Android™ tablet. However, two Android™ tablets were purchased prior to the Samsung Galaxy Tab® A Tablet that were not compatible with this application. A lot of time and money was spent trying to find a compatible tablet, which impacted the timeline of this research as the drone could not be utilized until the FreeFlight Thermal™ mobile application could be downloaded.

Additional problems occurred with the functioning of the mobile application throughout this research. In one of the first experiments where the drone was used, the images captured by the thermal camera could not be viewed with the thermal color palette after flight. Only visual images could be viewed despite having captured images in the thermal setting. After contacting Parrot customer support and downloading an update for FreeFlight Thermal™, this problem was fixed, and the thermal images could be viewed. A common occurrence also included the mobile application crashing when trying to view and analyze images. After some time, the mobile application would again function properly, but this malfunction inhibited the ability to analyze experimental images in a timely manner.

Major complications occurred in August 2018 (Figure 4:2 a) and March 2019 (Figure 4:2 b-c) when the drone crashed during experiments. In August 2018, the drone was being flown at approximately five meters when it suddenly fell to the ground. Damage did occur to the drone as the platform attaching the thermal camera came loose. After filing a report with Parrot© and sending the drone in for evaluation, it was determined that the GPS associated with the drone malfunctioned and caused the crash. The drone was replaced by Parrot©, but it took about two months for a new drone to be received, which delayed further research from taking place. In March 2019, the drone was flying at 48 meters when it also fell to the ground, causing the thermal camera to detach and the battery to shatter. The thermal camera could not be re-attached because the plastic holding the camera in place broke. According to flight logs, the drone crashed due to a battery failure. This second crash concluded this research as the drone could no longer be flown. In discussing the second crash with Parrot©, it was discovered that the Parrot Bebop-Pro Thermal™ drone is no longer manufactured and therefore could not be replaced by the company.

a) 

b) 

c) 

Figure 4:2 - a-c - Damage to the Parrot Bebop-Pro Thermal™ drone, a) drone damage after crash in August 2018, b) battery damage after crash in March 2019, c) drone damage after crash in March 2019 (Photographs by Megan Descalzi)

4.2 Egg Weight

Prior to generating different sized maggot masses, egg rafts were weighed and counted to determine the weight of an individual egg/larva for the species maintained in colony. The average weight of an individual egg was calculated for *L. sericata* and *P. regina* flies based on the egg rafts weighed and counted from each species (Table 4:1). The average individual larva weight for *S. bullata* flies, a larviparous species, was also calculated from the groups of larvae weighed and counted (Table 4:1).

Table 4:1 - Summary of weights and counts recorded in calculating the average egg weight for *Phormia regina* and *Lucilia sericata* and the average larva weight for *Sarcophaga bullata*

Species	Weight of egg raft (g)	Number of eggs in raft	Individual Egg weight (g)	Average egg weight (g)
Phormia regina	0.030	326	0.00009202	0.00009093
	0.014	130	0.00001077	
	0.013	158	0.00008228	
	0.015	157	0.00009554	
	0.051	631	0.00008082	
	0.012	143	0.00008392	
	0.008	108	0.00007407	
	0.013	117	0.00001111	
Lucilia sericata	0.012	152	78.95	0.00010858
	0.013	117	111.11	
	0.008	106	75.47	
	0.005	58	86.21	
	0.013	68	191.18	
*Sarcophaga bullata**	0.114	66	1727.27	0.00167256
	0.349	213	1638.50	
	0.261	158	1651.90	

*Larviparous species.

There was no difference between the average egg weight of *L. sericata* and *P. regina* flies (Figure 4:3 a). However, there was a difference between the weight of the larviparous and oviparous offspring, with the average larva weight of *S. bullata* flies being greater than the average egg weights of *L. sericata* and *P. regina* flies (Figure 4:3 b). Even though the same amount of time had elapsed between the placement of blood feeds within colonies and the removal of eggs and larvae from blood feeds for all species in colony, the average larva weight of *S. bullata* was more than ten times the weight of the *L. sericata and P. regina* eggs.

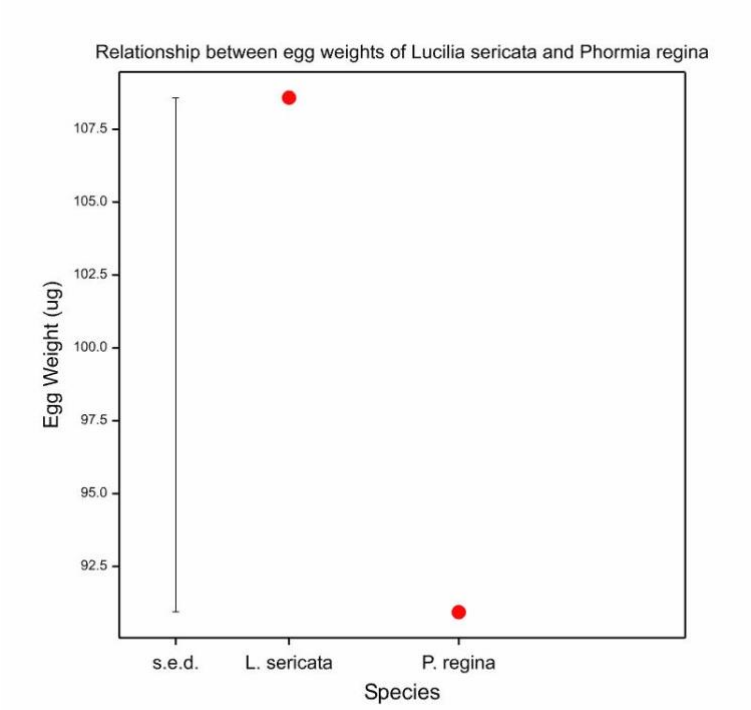

a)

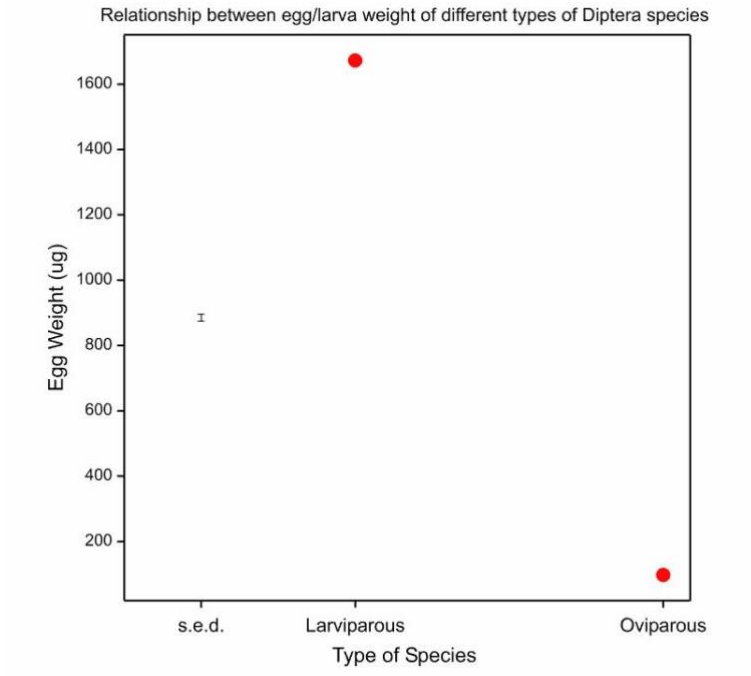

b)

Figure 4:3 - a-b - Differences in means of egg/larva weight by species, a) oviparous Diptera species (ANOVA, $F_{(1,11)} = 1.00$, $p = 0.338$, s.e.d. = standard error of differences), b) oviparous and larviparous Diptera species (ANOVA, $F_{(1.14)} = 5268.62$, $p = <0.001$, s.e.d. = standard error of differences)

Since the nine *P. regina* egg rafts that were weighed and counted originated from four cages, it was necessary to determine if the individual egg weight for *P. regina* varied between cages. In comparing the mean individual egg weight for *P. regina*, there was no difference in the calculated egg weights by cage (Figure 4:4). The five *L. sericata* egg rafts and the three *S. bullata* groups of larvae that were weighed and counted originated from only one colony for each species.

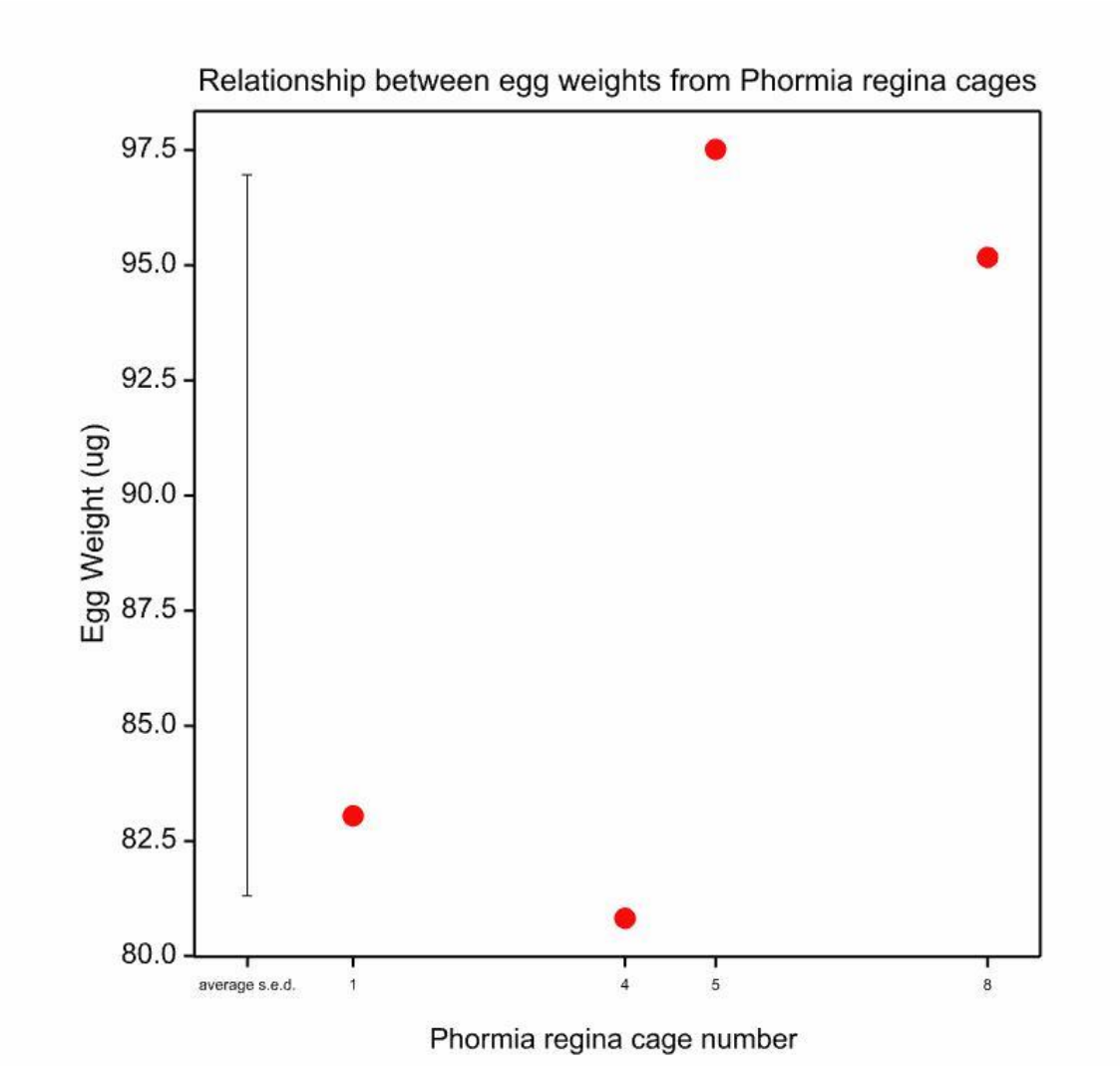

Figure 4:4 - Differences in means of egg weight by *Phormia regina* cage (ANOVA, $F_{(3,4)} = 0.57$, $p = 0.662$, s.e.d. = standard error of differences)

4.2.1 Maggot Mass Temperature

The average egg weight of *P. regina* flies was used to create different sized egg rafts with a varying number of eggs (Table 4:2). The number of eggs placed on each carcass type was similar between replicates.

Table 4:2 - Summary of the estimated number of *Phormia regina* eggs placed on different sized carcasses in both replicates of the lab-controlled study

	Carcass	Weight of egg raft placed (g)	Estimated number of eggs in raft
Replicate 1	Chipmunk	0.020	220
	Rabbit	0.100	1100
	Coyote	0.462	5080
Replicate 2	Chipmunk	0.020	220
	Rabbit	0.097	1070
	Coyote	0.460	5060

The handheld FLIR® E6 infrared camera and General® IRT207 Infrared Laser measured no difference in carcass temperatures throughout both replicates. The temperature measurements of the carcass regions, which included the regions with (hotspot) and without (non-hotspot) larval activity, were similar between instrument type (Figure 4:5).

There was a difference in the temperature measurements of the hotspot and non-hotspot regions (Figure 4:5). This difference was expected as the hotspot regions are emitting more heat than the non-hotspot regions due to larval aggregation activity. The statistical interaction between the instruments and the carcass regions was significant (Figure 4:5). However, this interaction was an anomaly as the handheld FLIR and the infrared laser did not influence each other's temperature measurements of the carcass regions.

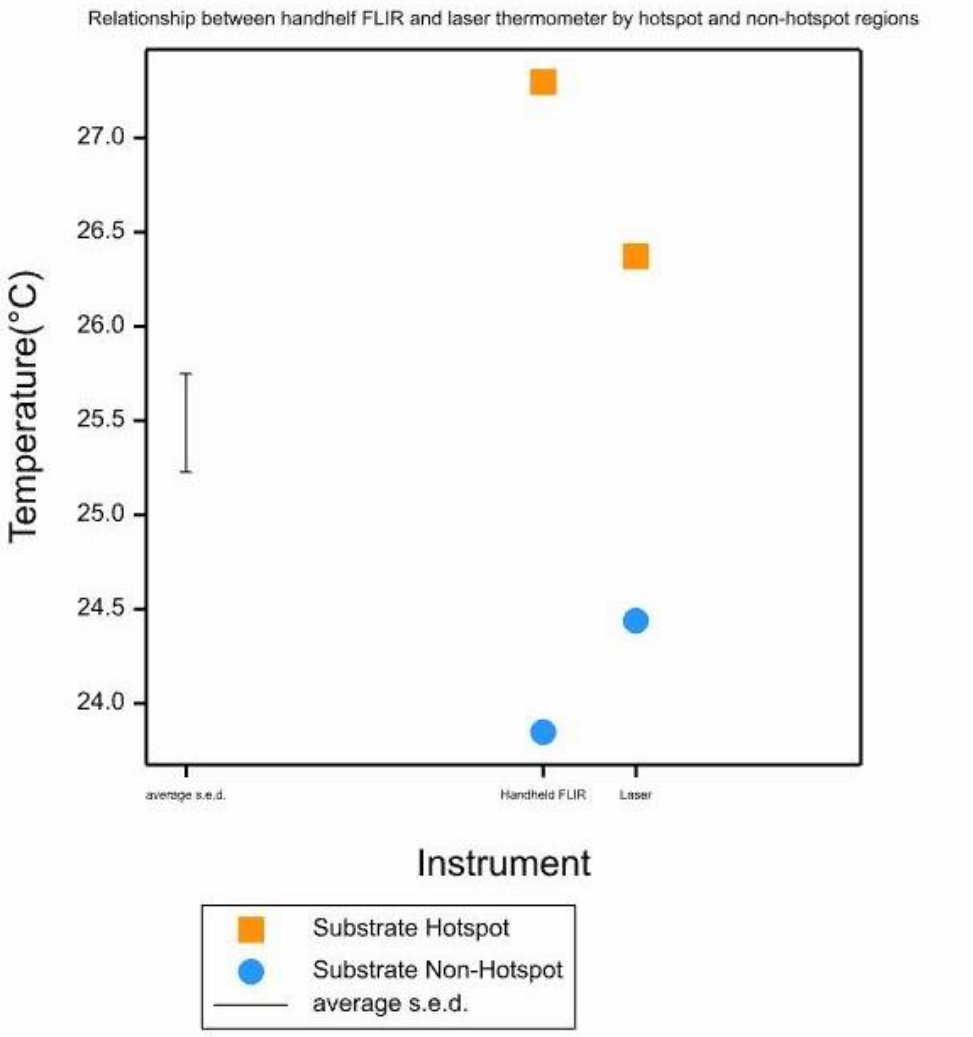

Figure 4:5 - Differences in means of carcass temperatures by instrument (ANOVA, $F_{Inst\ (1,173)} = 0.004$, $p = 0.851$; $F_{Sub\ (1,173)} = 52.91$, $p < 0.001$; $F_{Int\ (1,173)} = 4.17$, $p = 0.043$, s.e.d= standard error of differences)

The greatest temperature recorded by the handheld FLIR of the chipmunk carcass was 2.3°C above ambient temperature on Day Five of Replicate One (Figure 4:6 a-b) and 1.8°C above ambient temperature on Day Eight of Replicate Two (Figure 4:6 c-d). Maggot masses did not form at any point throughout the decomposition process. In Replicate Two, the maggots were wandering from the chipmunk carcass on Day Eight when the greatest temperature difference was recorded. These differences in temperature between the chipmunk carcasses and the ambient temperature were independent of larval aggregations.

a) 

b) 
c) 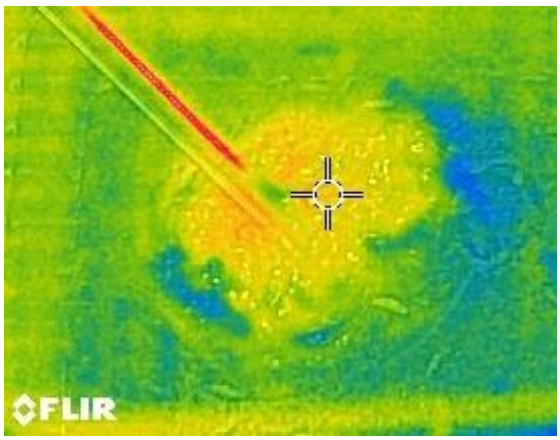

d) 

Figure 4:6 - a-d - Chipmunk carcasses (*Tamias striatus*) on the days when the greatest temperature differences between the carcass and ambient temperature were recorded, a) thermal image of carcass on Day Five for Replicate One, b) real image of carcass on Day Five for Replicate One, c) thermal image of carcass on Day Eight for Replicate Two, d) real image of carcass on Day Eight for Replicate Two

a) 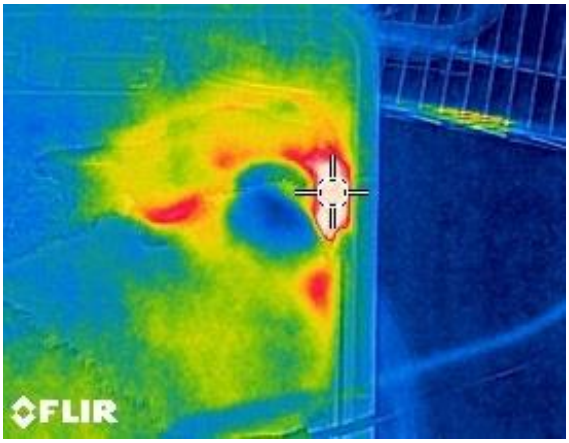

b) 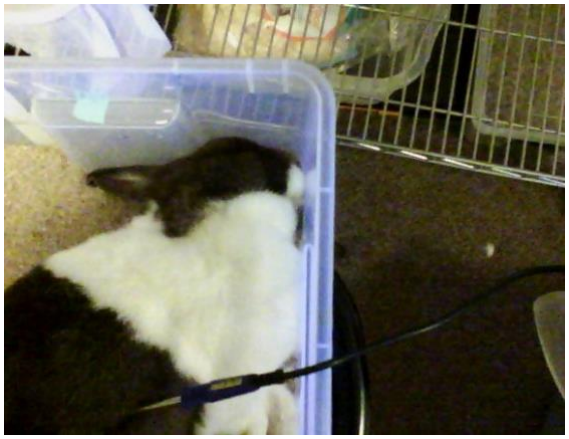

c) 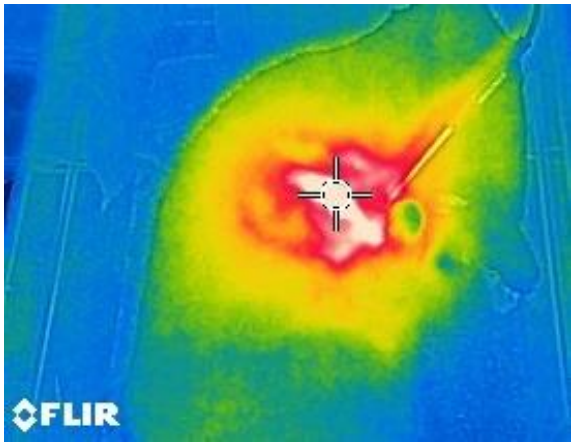

d) 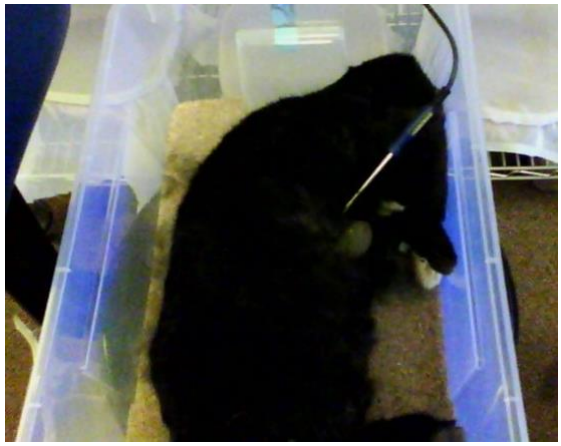

Figure 4:7 - a-d - Rabbit carcasses (*Sylvilagus floridanus)* on the days when the greatest temperature differences between the carcass and ambient temperature were recorded, a) thermal image of carcass on Day Four for Replicate One, b) real image of carcass on Day Four for Replicate One, c) thermal image of carcass on Day Three for Replicate Two, d) real image of carcass on Day Three of Replicate Two

The greatest temperature recorded from the rabbit carcass was 5.5°C above ambient temperature on Day Four for Replicate One (Figure 4:7 a-b) and 8.6°C above ambient temperature on Day Three for Replicate Two (Figure 4:7 c-d). The greatest temperature recorded from the coyote carcass was 15.1°C above ambient temperature on Day Five for Replicate One (Figure 4:8 a-b) and 10.6°C above ambient temperature on Day Four for Replicate Two (Figure 4:8 c-d). Maggot masses were visible on both of the rabbit and coyote carcasses in the regions where this temperature difference was recorded.

a) 

b) 

c) 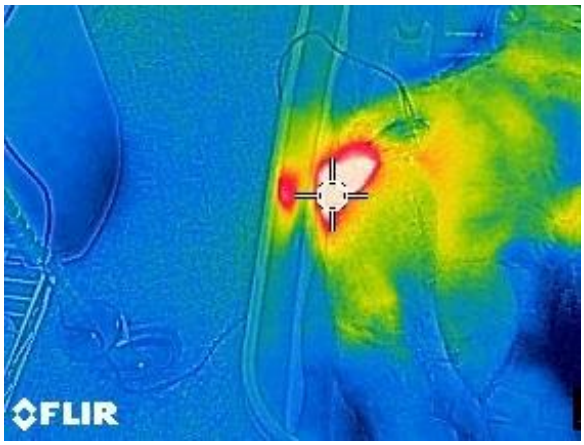

d) 

Figure 4:8 - a-d - Coyote carcasses (*Canis latrans)* on the days when the greatest temperature differences between the carcass and ambient temperature were recorded, a) thermal image of carcass on Day Five for Replicate One, b) real image of carcass on Day Four for Replicate One, c) thermal image of carcass on Day Eight for Replicate Two, d) real image of carcass on Day Four for Replicate Two

There was a difference in the amount of heat generated by the larvae on the chipmunk (200 eggs) carcasses compared to the rabbit (1000 eggs) and coyote carcasses (5000 eggs) (Figure 4:9 a). The mean difference in temperature between the hotspot regions and ambient temperature was lower for the chipmunk carcasses than the rabbit and coyote carcasses. However, there was no difference in the amount of heat generated by larvae between the rabbit and coyote carcasses (Figure 4:9 b). The larvae on both of these carcasses produced similar amounts of heat despite the different egg raft sizes initially placed on the carcasses.

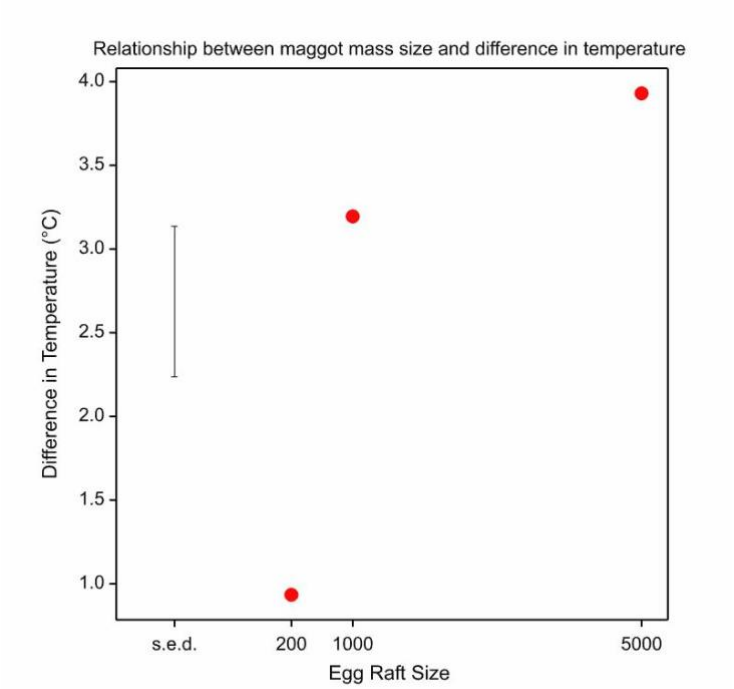

a)

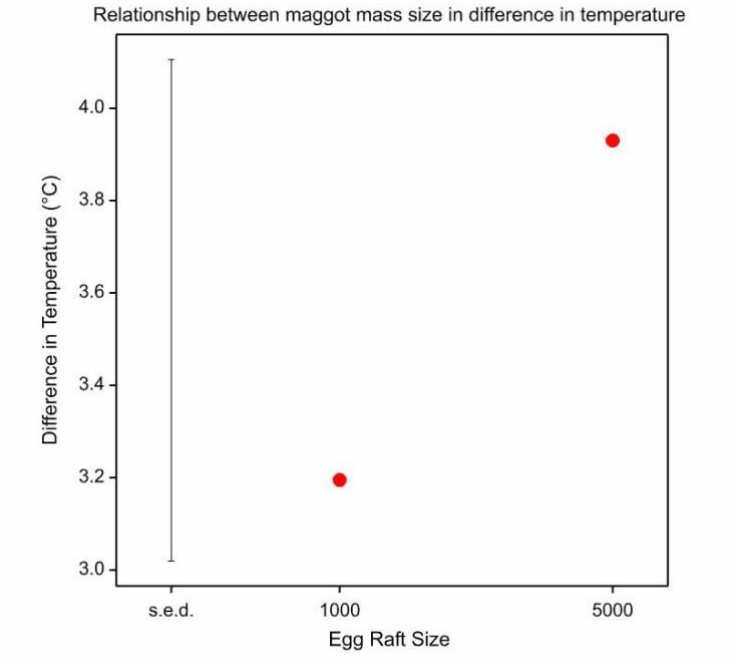

b)

Figure 4:9 - a-b - Differences in means of temperature between the handheld FLIR recordings of developing maggot masses and ambient temperature a) egg raft size placed on each carcass (ANOVA, $F_{(2,57)} = 6.02$, $p = 0.004$, s.e.d. = standard error of differences), b) egg raft size placed on the rabbit (*Sylvilagus floridanus*) and coyote (*Canis latrans)* carcasses (ANOVA, $F_{(1,38)} = 0.46$, $p = 0.503$, s.e.d. = standard error of differences)

4.3 Hot Water Analog

The drone and handheld FLIR measured the temperature of the hot water baths and the surrounding substrates from various heights. There was no difference in temperature between these two FLIR instruments for each substrate, even when the height between the instruments varied (Figure 4:10).

There was a difference in each substrate's temperature (Figure 4:10). However, this difference was expected due to the varying emissivities of the substrates and the ambient conditions at the time of each replicate.

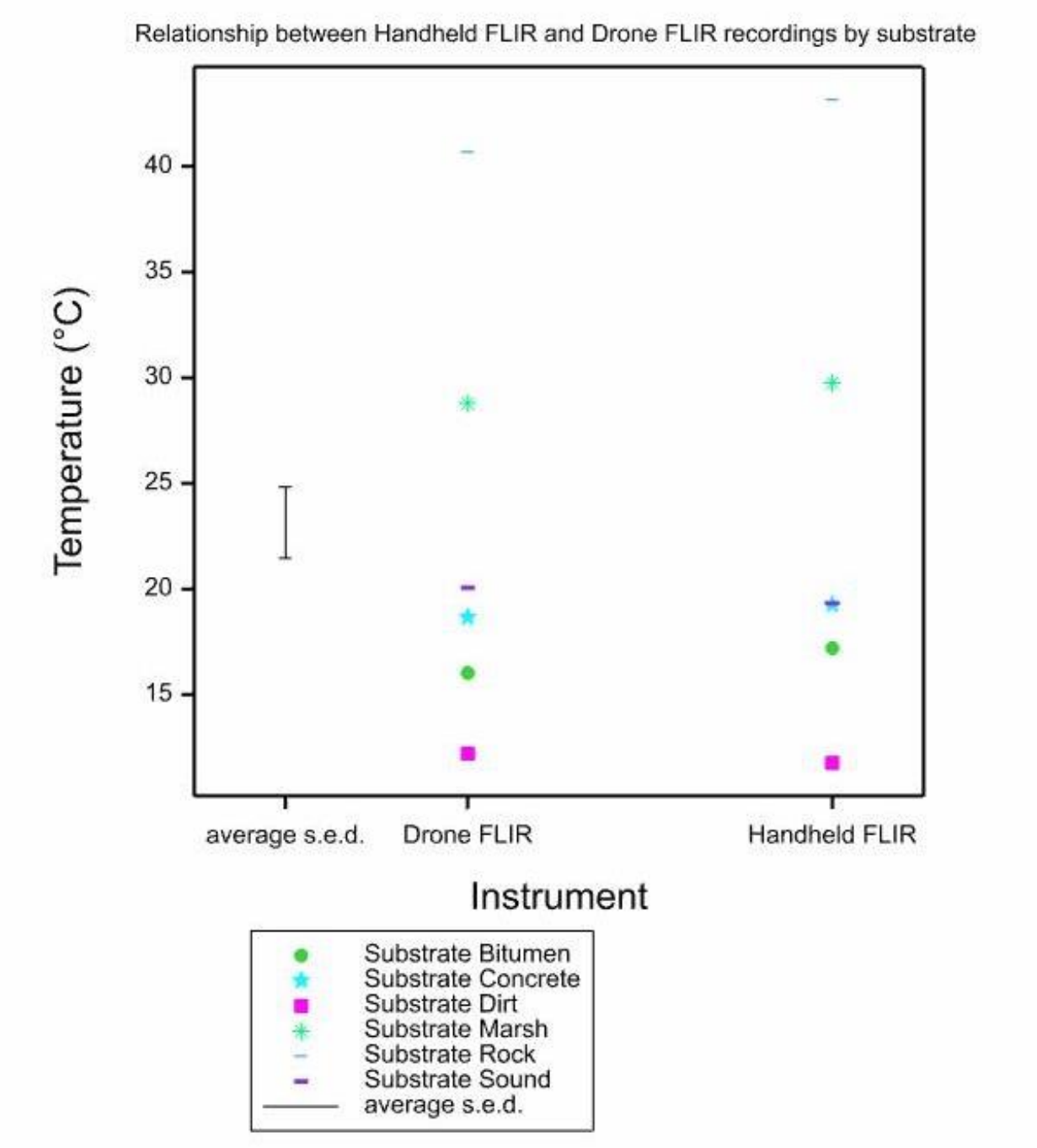

Figure 4:10 - Differences in means of temperature measurements by instrument and substrate (ANOVA,$F_{Inst\ (1,2598)} = 0.02$, $p = 0.896$; $F_{Sub\ (5,2598)} = 39.65$, $p < 0.001$; $F_{Int\ (5,2598)} = 0.40$, $p = 0.850$, s.e.d. = standard error of differences of means)

There was also no difference in the temperature of the hot water bath between the handheld and the drone FLIR at two meters (Figure 4:11).

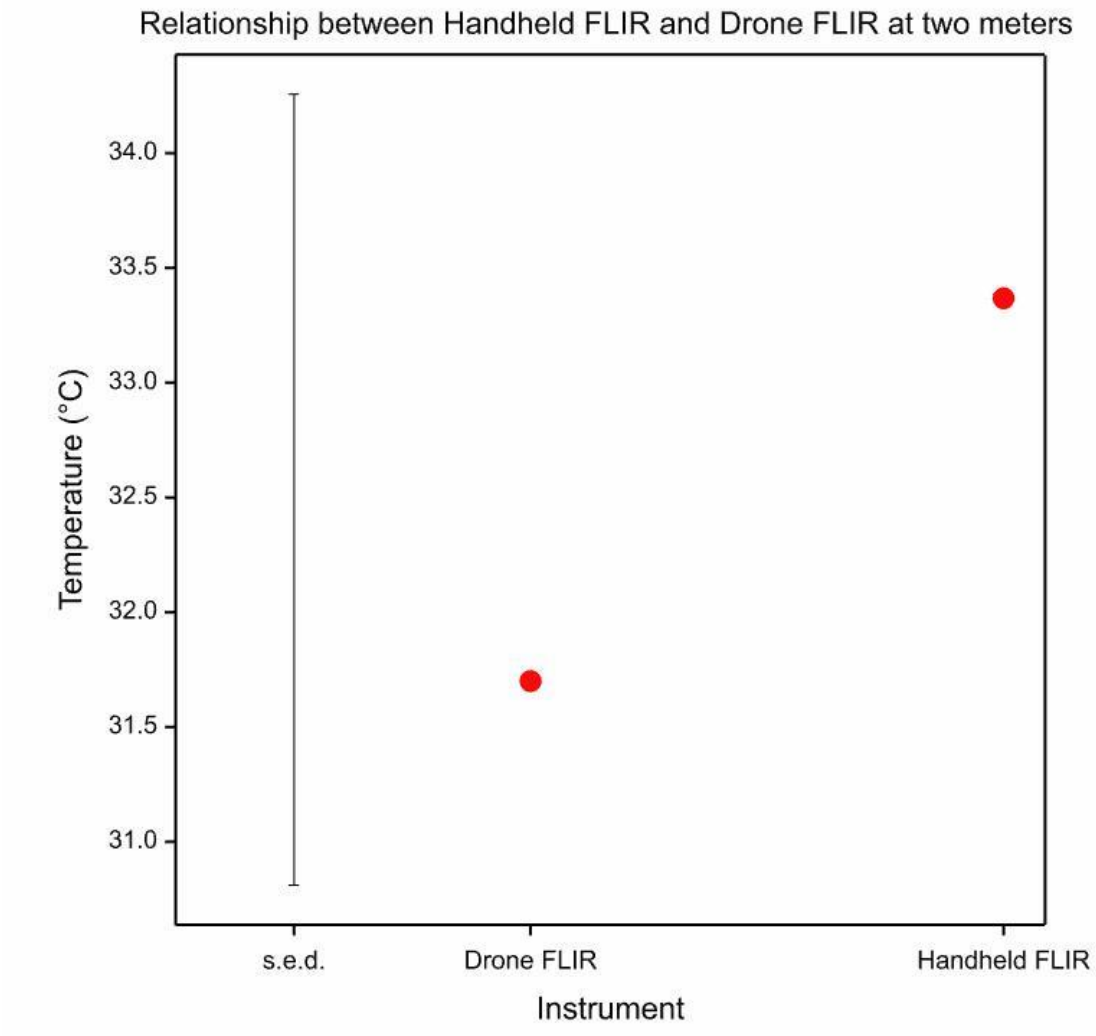

Figure 4:11 - Differences in means of hot water bath temperatures at two meters by instrument (ANOVA, $F_{(1,48)} = 0.23$, $p = 0.631$, s.e.d. = standard error of differences of means)

Visual observations were made to assess the capability of detecting differences in the hot water bath at differing heights. It was difficult to visualize the thermal signature of the hot water bath as height increased (Figure 4:12 a-d). When the drone reached 50 meters, hot water bath was nearly undetectable (Figure 4:12d).

Both FLIR instruments measured the temperature of the hot water bath and the temperature of the substrates at varying heights similarly, therefore the relationship between height and the difference in temperature could be determined. The difference in temperature was calculated by subtracting the handheld FLIR temperature from the drone FLIR temperature at various heights for both the hot water bath and the substrates among all of the replicates completed.

There was a negative relationship between drone height and temperature for the hot water bath (Figure 4:13 b) (Table 4:3 b). As the height of the drone increased, the temperature of the hot water bath measured by the drone FLIR decreased. However, there was no relationship between drone height and substrate temperature (Figure 4:13 b) (Table 4:3 b).

After analysis of the data, it was determined that there were two sets of outliers that were then removed when analyzing the relationship between drone height and the difference in temperature. These outliers displayed an increase in the hot water bath temperature with an increase in drone height (Figure 4:13 a) (Table 4:3 a). Removing these outliers from the data set did not affect the overall negative relationship between drone height and the temperature of the hot water bath by the drone FLIR (Figure 4:13 a-b) (Table 4:3 a-b).

a) 

b) 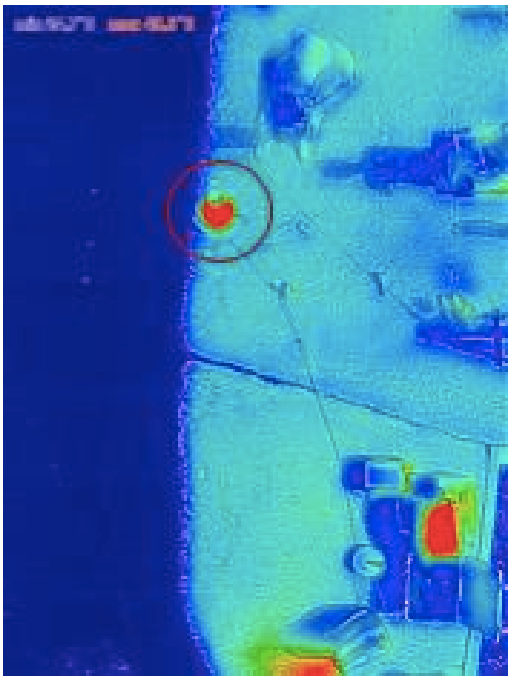

c) 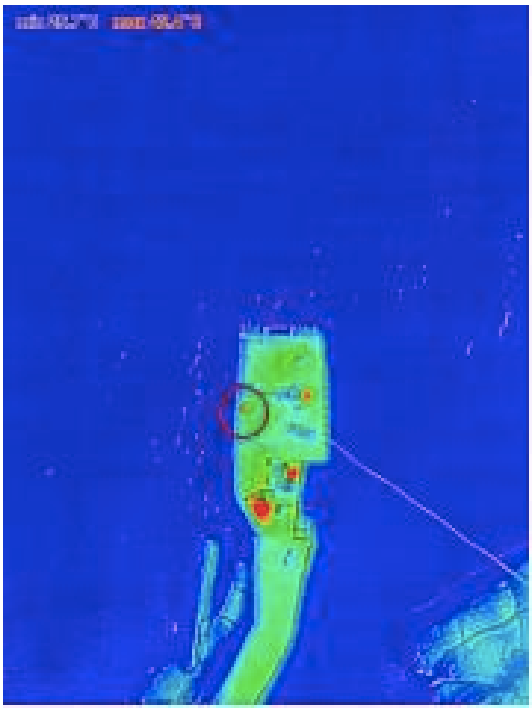

d) 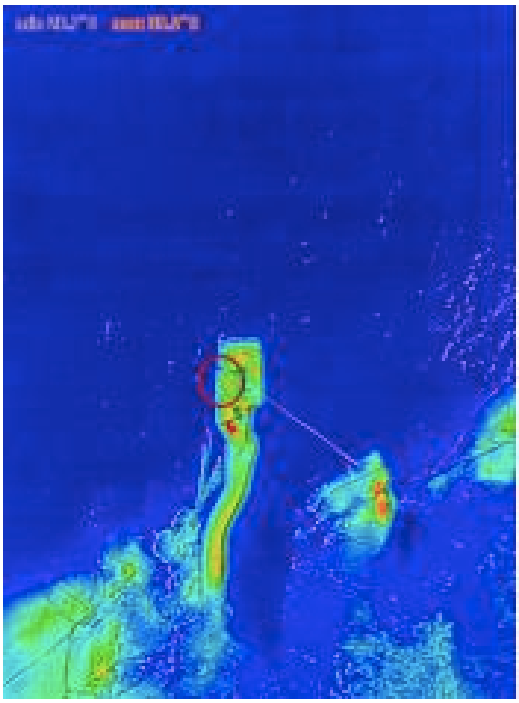

Figure 4:12 - a-d - Small hot water bath (indicated by red circles) at varying drone heights, a) real image at 5 meters, b) thermal image at 5 meters, c) thermal image at 25 meters, d) thermal image at 50 meters

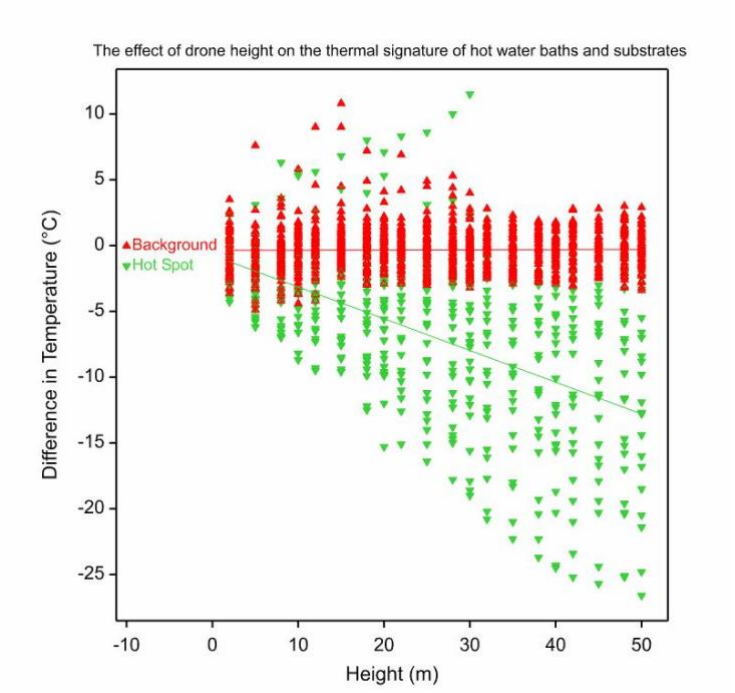

a)

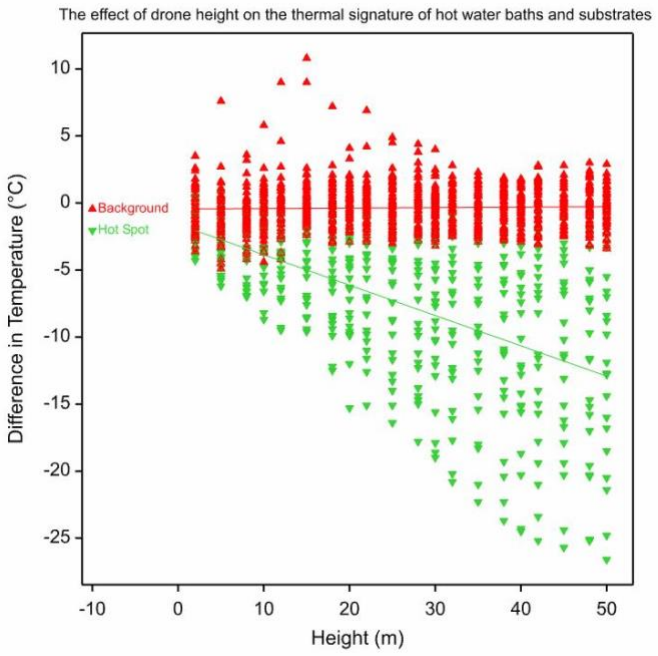

b)

Figure 4:13 - a-b - Relationship between drone height and difference in temperature of the handheld FLIR and drone FLIR readings by hot water baths (hot spot) and substrate (backgrounds), a) with outliers (R^2 = 0.55, p = <0.001, overall with no consideration of groups), b) without outliers [Green nablas above 0°C] (R^2 = 0.61, p = <0.00, overall with no consideration of groups)

Table 4:3 - a-b - Analyses of drone height on the difference in temperature between the handheld FLIR and drone FLIR recordings by hot water baths and substrates a) with outliers, b) without outliers (s.e. = standard error)

a)

Parameter	s.e.	t(1716)	p value
Constant	0.172	-2.11	0.035
Height (m)	0.006	0.24	0.814
Grouping	0.329	-1.14	0.254

b)

Parameter	s.e.	t(1716)	p value
Constant	0.167	-2.73	0.0006
Height (m)	0.00572	0.62	0.538
Grouping	0.318	-3.60	<0.001

4.3.1 Hot Spot Size

The strength of the thermal signatures varied between the small and large hot water baths, even when both hot water baths were set at the same temperature and viewed at the same height. For example, the thermal signature of the 50-gallon hot water bath (Figure 4:14 b) was more readily detected than the 5-gallon hot water bath (Figure 4:14 a) at 15 meters. The larger hot water bath was red, indicating a warmer temperature, which was distinguishable from the surrounding environment. However, the smaller hot water bath was green, indicating a lower temperature, which made it more difficult to differentiate between the hot water bath and the surroundings.

a) 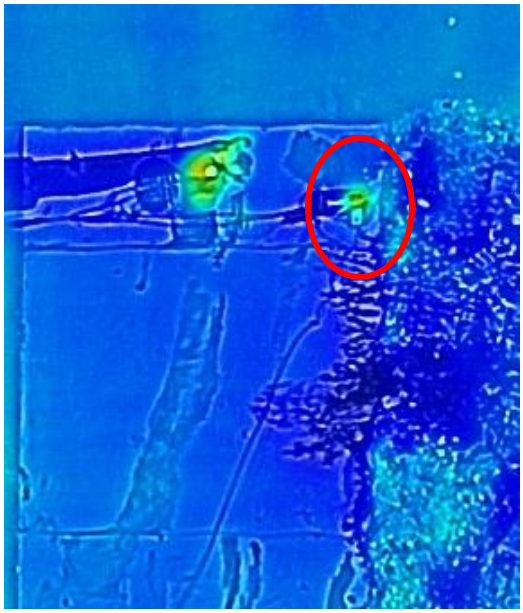 **b)** 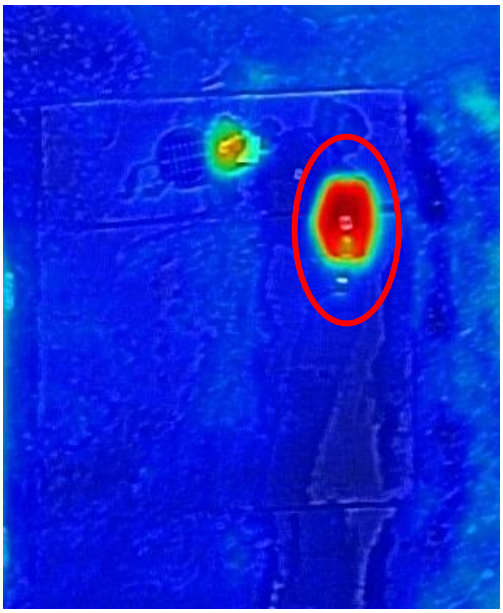

Figure 4:14 - a-b - Visual effects of drone height on the thermal signature of the hot spot for the 5 gallon and 50 gallon hot water bath containers, a) thermal image of 5 gallon hot water bath at 15 meters, b) thermal image of 50 gallon hot water bath at 15 meters

There was a negative relationship between drone height and the difference in temperature for both the large and small hot water baths (Figure 4:15 b). With increasing drone height, the temperature measured of both hot water bath sizes by the drone FLIR decreased. However, the temperature measurement of the large hot water bath was warmer than the small hot water bath at each height (Figure 4:15 b). The two sets of outliers as removed in Figure 4:13, which displayed a positive relationship between drone height and temperature, were removed from this analysis. Removing these outliers did not affect the negative relationship between drone height and temperature for the small and large hot water bath but did eliminate the ability to differentiate between the two (Figure 4:15 a-b) (Table 4:4 a-b).

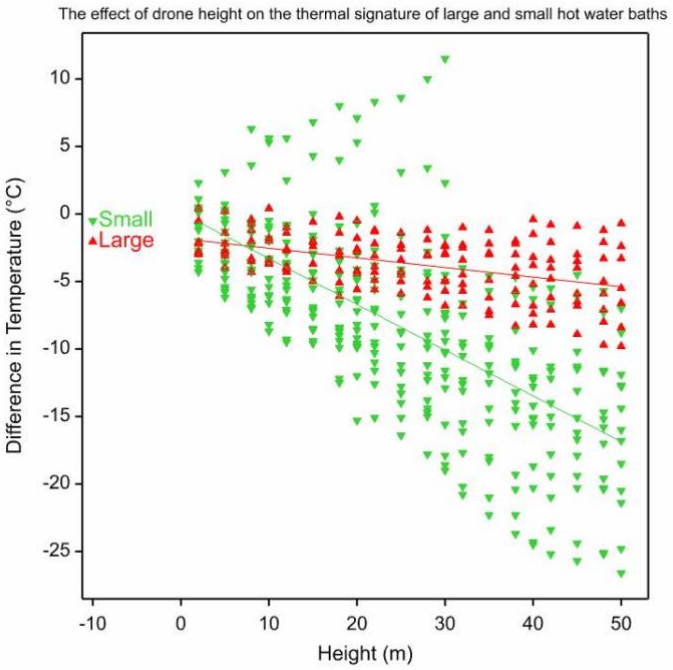

a)

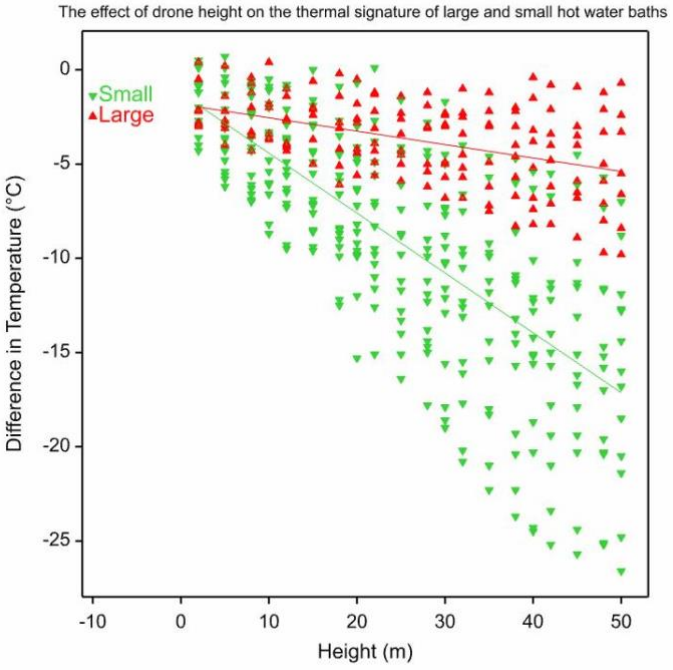

b)

Figure 4:15 - a-b - Relationship between height and difference in temperature between handheld FLIR and drone FLIR readings by hot water bath size, a) with outlier (R^2 = 0.51, p = <0.001, overall with no consideration of groups), b) without outliers [Green nablas above 0°C] (R^2 = 0.61, p = <0.001, overall with no consideration of groups)

Table 4:4 - a-b - Analyses of drone height on the difference in temperature between handheld FLIR and drone FLIR recordings by hot water bath size a) with outliers, b) without outliers (s.e. = standard error)

a)

Parameter	s.e.	t(1716)	p value
Constant	0.726	-2.52	0.012
Height	0.0242	-2.94	0.003
Grouping	0.873	2.18	0.029

b)

Parameter	s.e.	t(1716)	p value
Constant	0.600	-3.05	0.002
Height	0.0200	-3.56	<0.001
Grouping	0.732	0.80	0.425

4.3.2 Wind Effect

Wind had a visual effect on the thermal signature of the hot water bath in the thermal images captured by the drone FLIR. When there was no wind, infrared waves emitted from the hot water bath traveled upward. As a result, the thermal signature of the hot water bath was detected by the drone FLIR at the actual location of the container (Figure 4:16 a). However, when there was wind, the infrared waves were blown downwind, resulting in a displacement of the hot water bath's thermal signature from the location of the container (Figure 4:16 b). Displacement was observed at wind speeds as low as 1.0 mps. Wind affected the accurate detection of the hot water bath's location and indicated a hot spot where there was none (Figure 4:17 a-b).

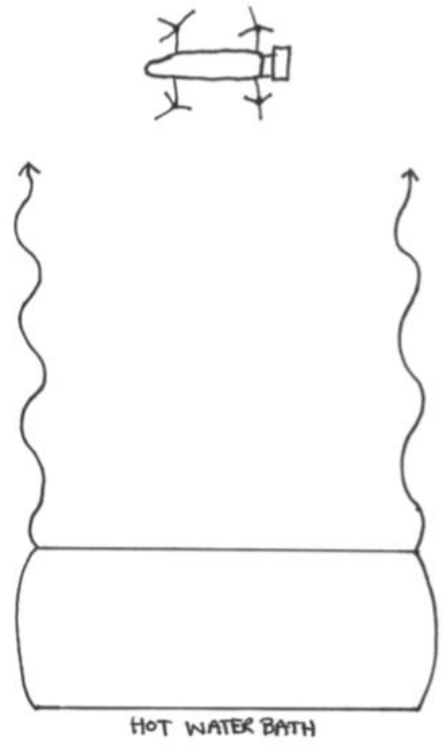

a)

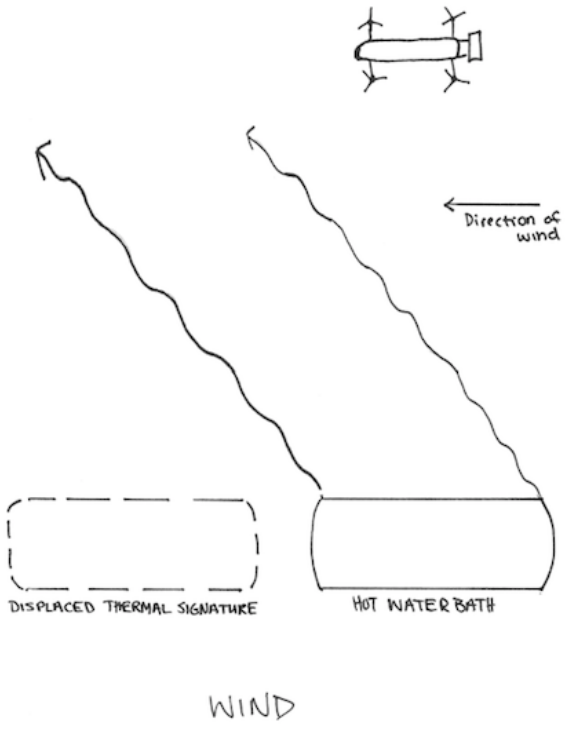

b)

Figure 4:16 - a-b – Direction of emitted infrared waves from the hot water bath, a) without wind, b) with wind (Drawings by Megan Descalzi)

a)

b)

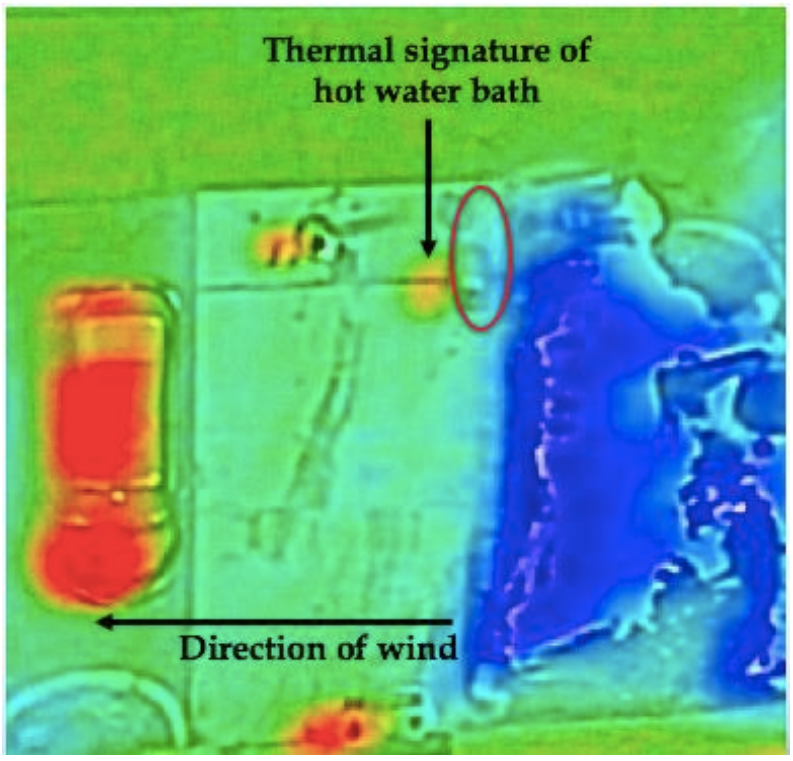

Figure 4:17 - a-b - Visual effects of wind on the thermal signature of the hot water bath (indicated by red circle), a) real image depicting the location of the hot water bath, b) thermal image depicting the thermal signature of the hot water bath

The relationship between wind speed and the difference in temperature for the hot water bath was analyzed, in order to determine if wind speed affected the temperature measurement of the hot water bath by the drone FLIR. The difference in temperature was calculated by subtracting the drone FLIR temperature of the hot water bath at each height from the probe thermometer temperature. The probe thermometer was placed within the hot water bath and was considered to be the actual temperature of the water.

The positive relationship showed that as wind speed increased, so did the difference in temperature between the probe thermometer and drone FLIR of the hot water bath (Figure 4:18). However, wind speed only accounted for 2% ($R^2 = 0.02$) of this difference in temperature (Figure 4:18).

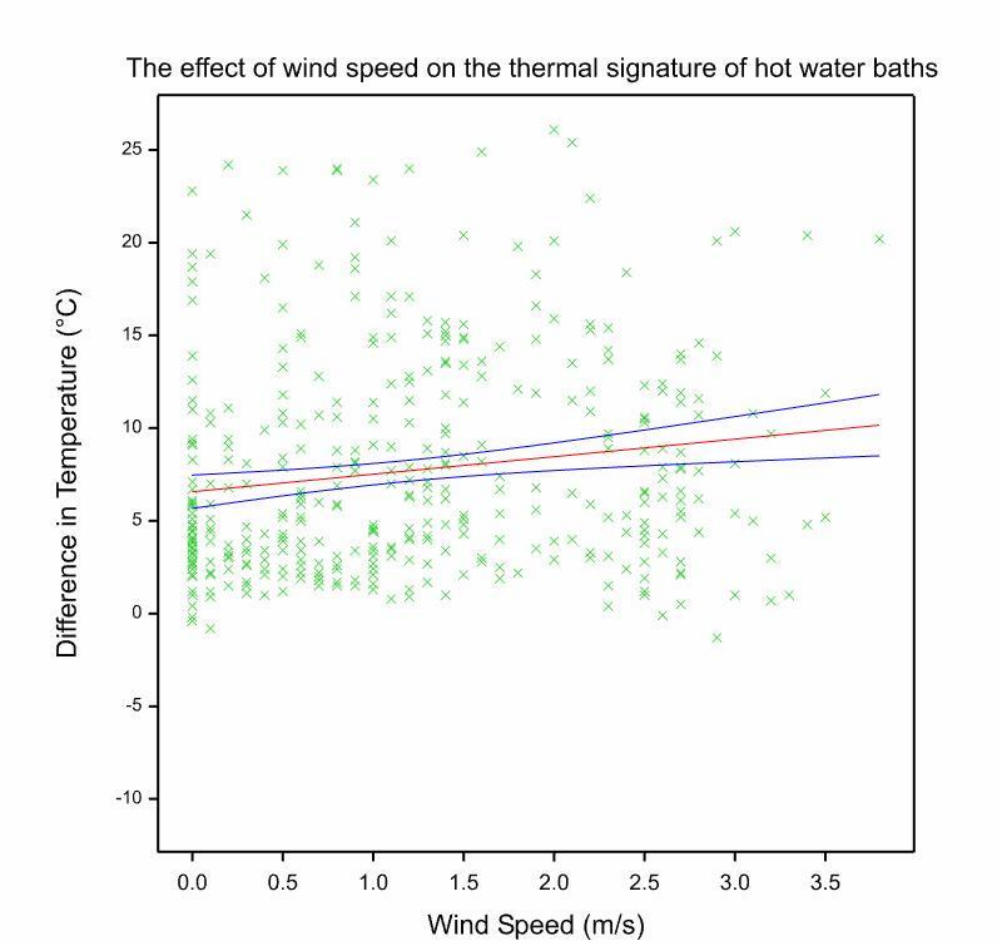

Figure 4:18 - Relationship between windspeed and the difference in temperature between probe and drone FLIR recordings of the hot water baths ($R^2 = 0.02$, $p = 0.002$)

The relationship between wind speed and temperature was compared to the relationship between height and temperature. As the height increased, the difference in temperature also increased between the probe thermometer and the drone FLIR (Figure 4:19). The relationship with height accounted for 33% ($R^2 = 0.33$) of the difference in temperature (Figure 4:19). Therefore, while both wind speed and height affect the measurement of the hot water bath,

height had a greater influence than wind. Wind had a greater effect on the ability to accurately locate the hot water bath than to accurately determine its temperature.

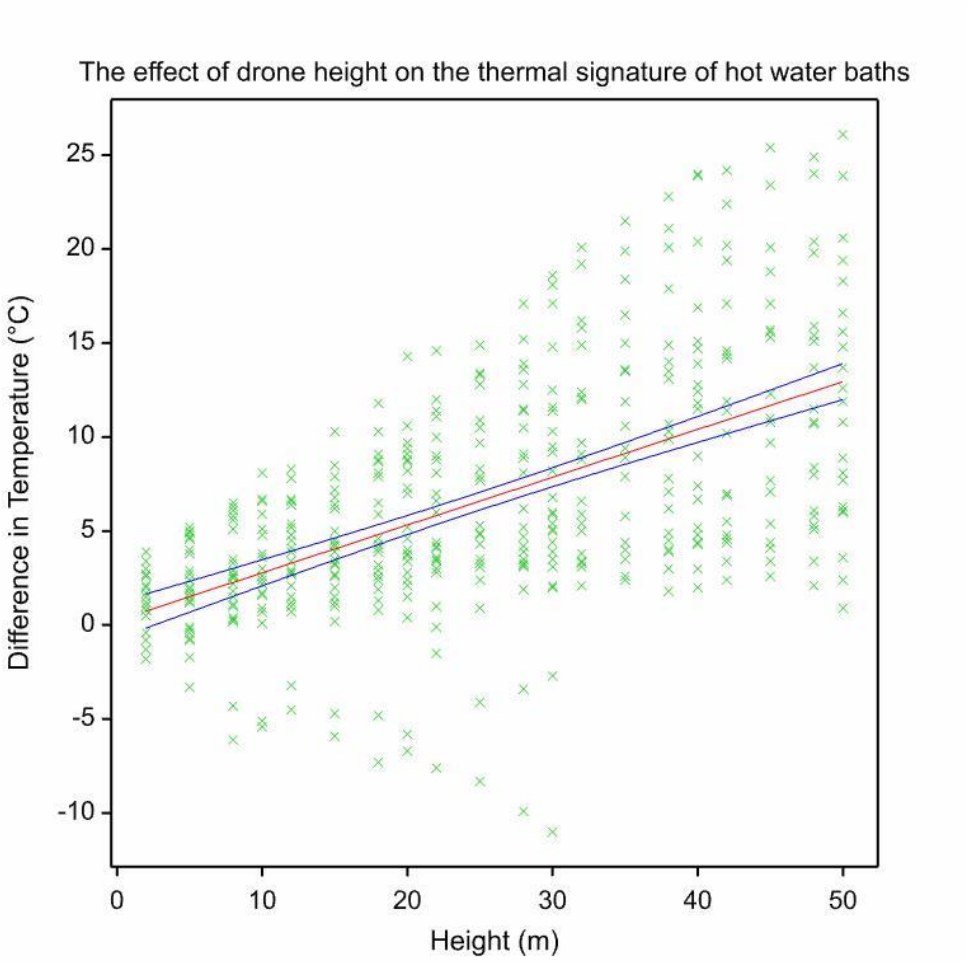

Figure 4:19 - Relationship between drone height and the difference in temperature between probe and drone FLIR recordings of the hot water baths (R^2 = 0.33, p = <0.001)

4.4 Field-Based Study

As the last component to this research, the Parrot Bebop-Pro Thermal™ drone was utilized to analyze the temperature of developing maggot masses on animal carcasses from various heights.

4.4.1 Coyote (*Canis latrans*) Carcass

A coyote (*Canis latrans*) carcass was placed outside on an area of wood chips at the University of New Haven's Orange Campus in August 2018 and was monitored daily for the presence of insect activity.

4.4.1.1 Decomposition and Insect Activity

Within minutes of placement (Day Zero) (Figure 4:20 a), Diptera (true flies) and Hymenoptera (honey bees) were observed on the carcass. On Day One (Figure 4:20 b), there was no change in the gross appearance of the carcass and similar insect activity was observed, including Diptera and Hymenoptera with the inclusion of Araneae (spiders). There was also some larval activity present within the mouth of the coyote. The handheld FLIR temperature of the carcass on Day Zero and Day One was approximately 27°C, similar to that of the surrounding wood chips (~ 26°C) and ambient temperature (~ 24°C).

a)  b) 

Figure 4:20 - a-b - Coyote *(Canis latrans)* carcass, a) Day Zero, b) Day One

On Day Two (Figure 4:21), sloughing of the fur began to occur, exposing the skin on the coyote's legs. In addition to the continued presence of Diptera and Hymenoptera, there were large amounts of larvae observed on the carcass, concentrated near the legs. The handheld FLIR temperature of the carcass on Day Two was approximately 10°C above ambient temperature and the temperature of the surrounding wood chips.

Figure 4:21 - Coyote (*Canis latrans)* carcass on Day Two (yellow arrow indicates area of sloughing)

On Day Three (Figure 4:22 a) and Day Four (Figure 4:22 b), the coyote was mostly skeletonized (approximately 90% soft tissue loss) and was covered with large maggot masses. Additional insect activity on Day Three included Diptera, Coleoptera (beetles) and Lepidoptera (butterflies). The handheld FLIR temperature of the carcass on Day Three was about 18°C above ambient temperature, while on Day Four it had decreased to about 5°C above ambient temperature. Larvae began to wander from the carcass on Day Four, which could have resulted in this decrease in temperature. On the final day of this replicate, Day Five (Figure 4:22 c), the

maggot masses had dissipated, and larvae were wandering away from the carcass. The handheld FLIR temperature of the carcass on Day Five was approximately 26°C, similar to that of the surrounding wood chips (~ 24°C) and ambient temperature (~ 22 °C)

a)  b) 

c) 

Figure 4:22 - a-c - Coyote (*Canis latrans)* carcass, a) Day Three, b) Day Four, c) Day Five

The drone was flown on Day Zero, Day Two, Day Three and Day Four. The drone was not flown on Day One because there was minimal larval activity observed and no difference in the carcass temperature from Day Zero. Additionally, the drone could not be flown on Day Five due to rain.

4.4.1.2 Drone Detection

On Day Zero, the carcass could not be differentiated from the surrounding wood chips and trees due to the similarity in temperature and color (Figure 4:23 a-b). The carcass and trees were blue, and the surrounding wood chips were turquoise.

a) 

b) 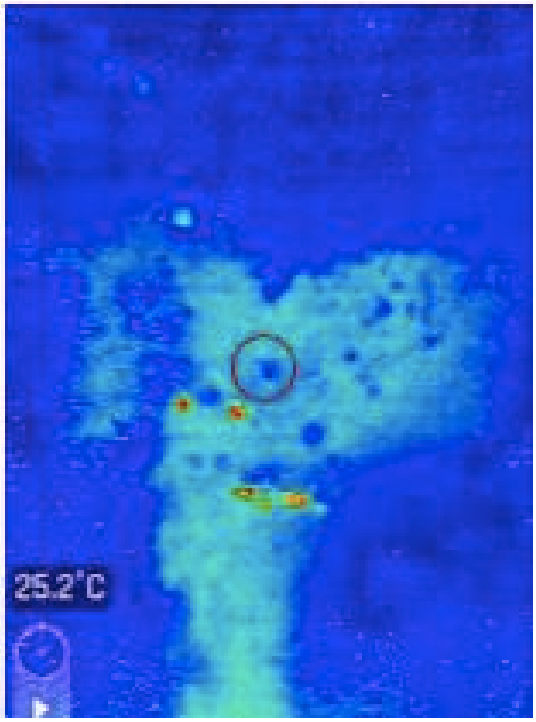

Figure 4:23 - a-b - Coyote (*Canis latrans*) carcass (indicated by the red circle) on Day Zero in August 2018, a) real image at 25 meters, b) thermal image at 25 meters

By Day Two, the carcass could be differentiated from the surrounding environment at a height of 25 meters. The carcass was red, indicating a warmer temperature, while the surrounding trees and wood chips were blue, indicating a cooler temperature (Figure 4:24 b).

a)  b) 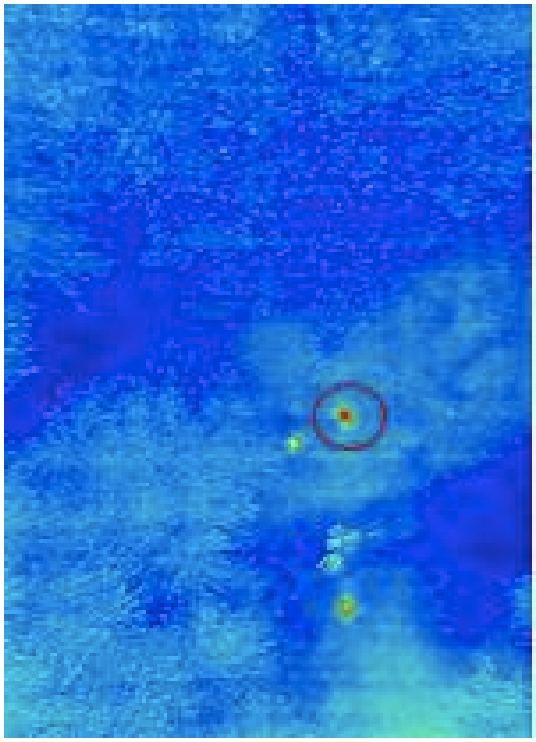

Figure 4:24 - a-b -Coyote (*Canis latrans*) carcass (indicated by red circle) on Day Two in August 2018, a) real image at 25 meters, b) thermal image at 25 meters

On Day Two, the ambient temperature was 23.7°C at the time of flight and there was no direct sunlight on the area where the carcass was located, as conditions were cloudy (Figure 4:24 a). However, on Day Three, ambient temperature increased to 26.3°C and there was sunlight shining directly on an open area of the wood chips (Figure 4:25 a). The carcass was not located in the direct sunlight, but in the shade of the surrounding trees (Figure 4:25 a).

The carcass could be differentiated from the surrounding wood chips in the shade because the difference in the drone FLIR temperature between the two was approximately 10°C. The carcass was green, indicating a warmer temperature, and the wood chips in the shade were blue, indicating a cooler temperature (Figure 4.25 b).

However, the carcass could not be differentiated from the surrounding wood chips in the direct sunlight because the difference in the drone FLIR temperature between the two was approximately 2.5°C. The thermal signature of the carcass and surrounding wood chips in the direct sunlight both displayed a similar green color (Figure 4:25 b). Therefore, although the thermal signature of the carcass was visible at a height of 25 meters, the direct sunlight on the surrounding area made it difficult to differentiate between the carcass and the surrounding wood chips in direct sunlight.

a) 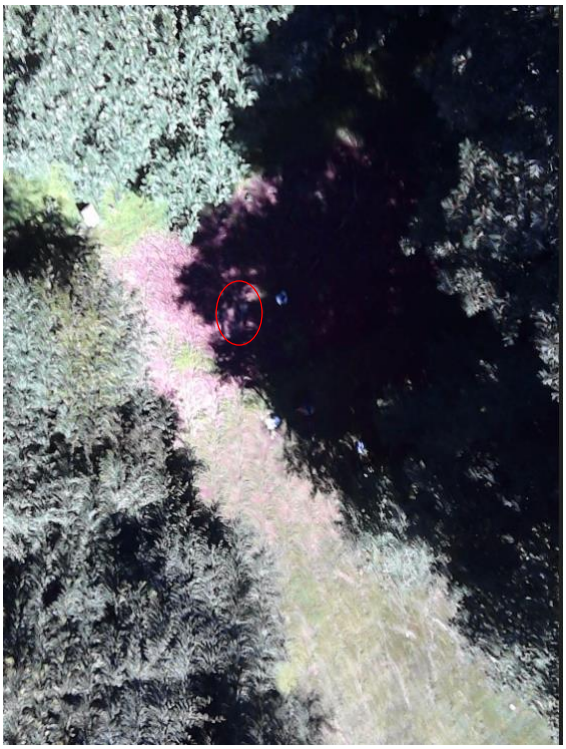 b) 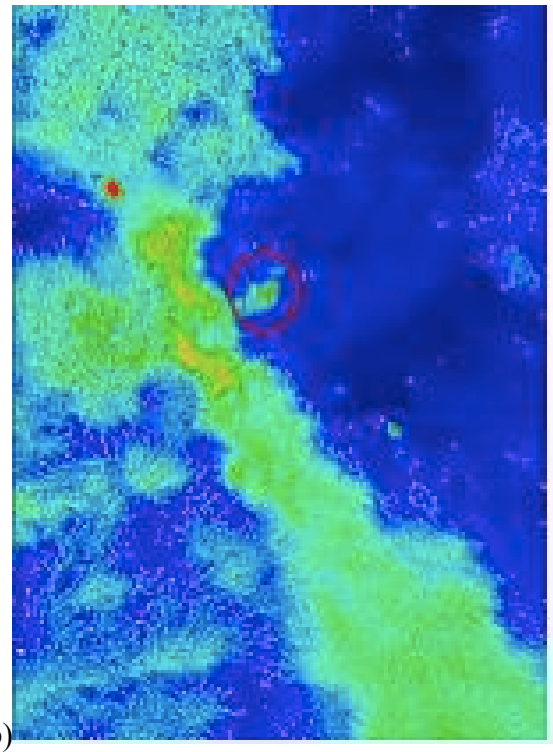

Figure 4:25 - a-b - Coyote *(Canis latrans)* carcass (indicated by red circle) on Day Three in August 2018, a) real image at 25 meters, b) thermal image at 25 meters

On Day Four, ambient temperature decreased to 25°C and there was no direct sunlight in the area where the carcass was located (Figure 4:26 a). The carcass could be differentiated from the surrounding trees and wood chips, which appeared greenish-blue (Figure 4:26 b). Despite only measuring 5°C above ambient and the temperature of the surrounding substrate, the carcass could be detected from a height of greater than 25 meters.

a) 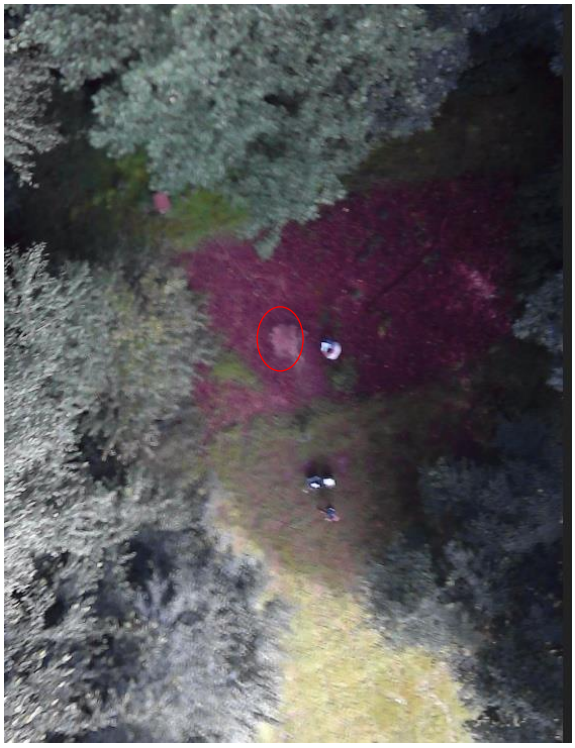 b) 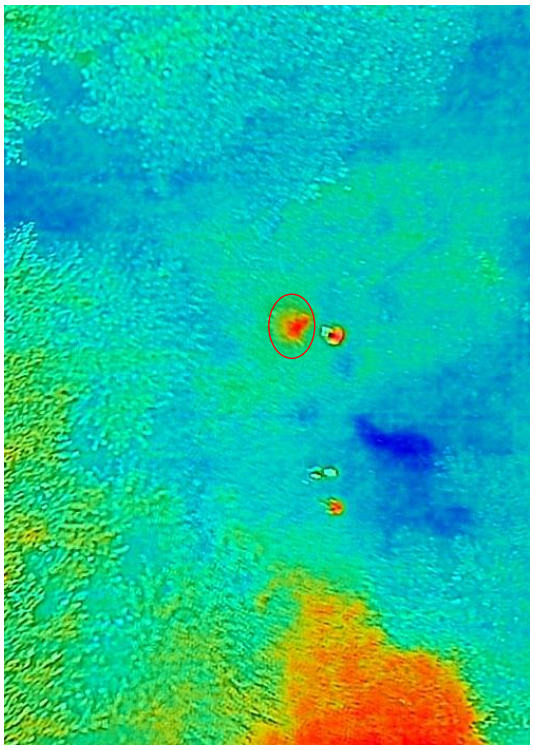

Figure 4:26 - a-b - Coyote *(Canis latrans)* carcass (indicated by the red circle) at on Day Four in August 2018, a) real image at 25 meters, b) thermal image at 25 meters

The relationship between height and the difference in temperature of the coyote carcass was also determined. The difference in temperature was calculated by subtracting the handheld FLIR temperature from the drone FLIR temperature at each height for the carcass and the wood chip substrate. There was a negative relationship between height and temperature for the carcass (Figure 4:27) (Table 4:5). As the height of the drone increased, the drone FLIR measured the hot

spot of the carcass at a lower temperature than the handheld FLIR. However, there was no relationship between height and temperature for the wood chip substrate (Figure 4:27) (Table 4:5). The drone FLIR measured the temperature of the wood chips similarly to the handheld FLIR even with increasing height. The relationship between height and temperature for the carcass and wood chips is similar to that of the hot water bath and corresponding substrates.

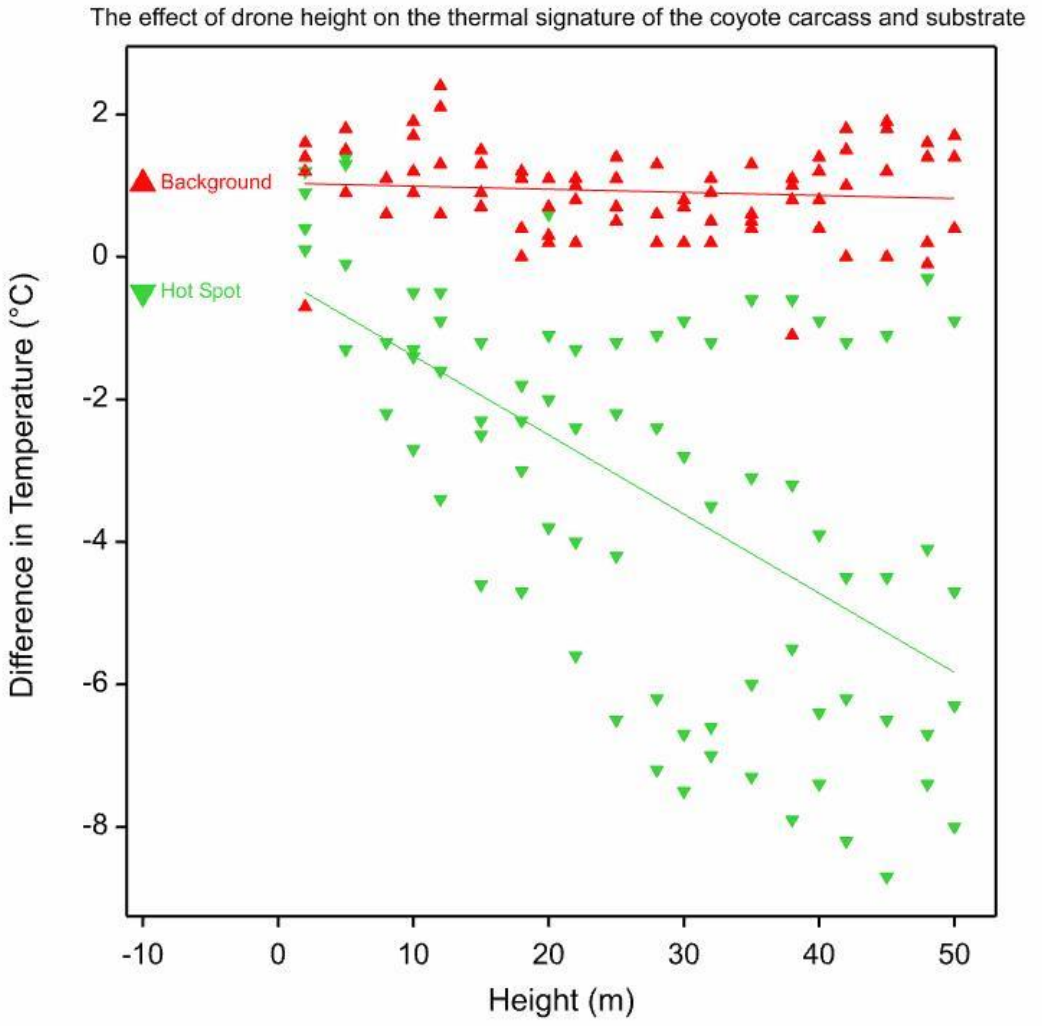

Figure 4:27 - Relationship between height and difference in temperature between handheld FLIR and drone FLIR readings by coyote *(Canis latrans)* carcass (hot spot) and substrate (background) (R^2 = 0.68, p = <0.001, overall with no consideration of groups)

Table 4:5 - Analyses of drone height on the difference in temperature between handheld FLIR and drone FLIR recordings by coyote (*Canis latrans)* carcass and background substrate (s.e. = standard error)

Parameter	s.e.	t(1716)	p value
Constant	0.390	2.66	0.009
Height	0.0129	-0.34	0.736
Grouping	0.552	-2.38	0.018

4.4.2 White-Tailed Deer Fawn *(Odocoileus virginianus)* Carcass

The white-tailed deer fawn (Odocoileus virginianus) carcass was placed at the same location at the University of New Haven's Orange Campus in November 2018 and was monitored for 11 days. The average ambient temperature over this time period was 10°C. Although some Diptera were seen on the carcass on Day Two and Day Six, no larvae were ever observed. The temperature of the fawn carcass was never greater than 2.0°C above ambient temperature or the temperature of the surrounding substrates. The experiment was ended when the carcass was covered by more than 10 centimeters of snow on Day 11.

The drone was flown on Day Two, Day Four and Day Eight. The fawn carcass could not be differentiated from the surrounding substrate on any of these days due to the similarity in temperatures (Figure 4:28 a-c).

a)

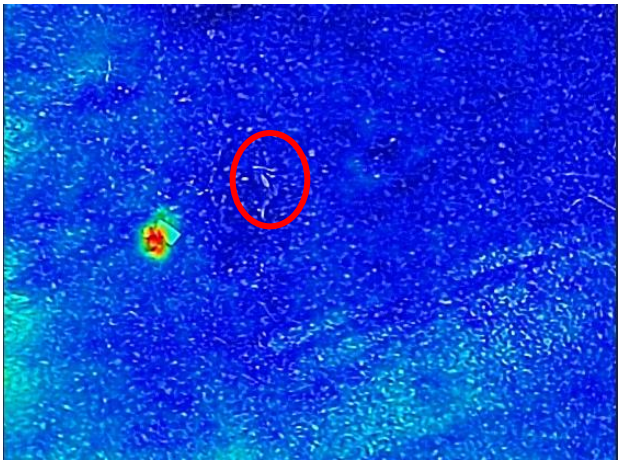

b)

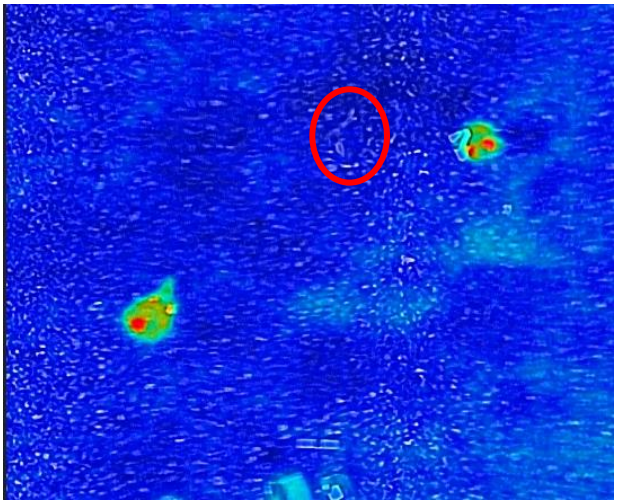

c)

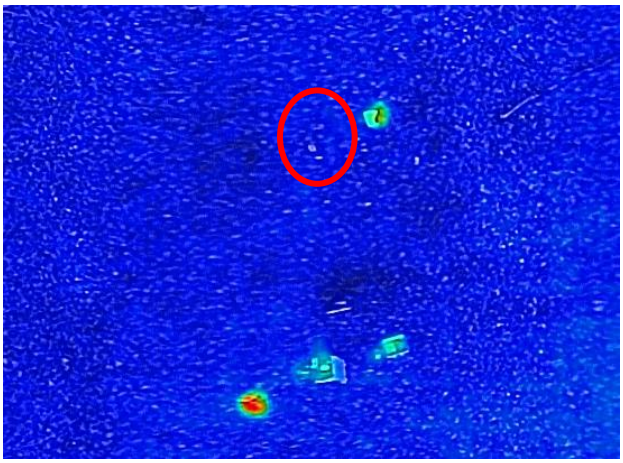

Figure 4:28 - a-c - White-tailed deer fawn (*Odocoileus virginianus*) carcass (indicated by the red circle) in November 2018, a) Day Two, b) Day Four, c) Day Eight

Additional replicates could not be completed in this field-based study due to the drone crashing in August 2018 and March 2019. The drone crashed soon after the coyote replicate was completed in August 2018 and was not replaced until two months later. Therefore, no additional replicates could be completed during this time period. When the replacement drone was received, the fawn replicate was immediately placed at the experimental site, but the ambient temperature was too low for larval aggregations to form. The ambient temperature did not become warm enough for another replicate to be completed before the drone crashed for the second time in March 2019.

CHAPTER 5: DISCUSSION

University of New Haven
HENRY C. LEE COLLEGE OF
CRIMINAL JUSTICE AND FORENSIC SCIENCES
Department of Forensic Science

When a body reaches ambient temperature after death, remote detection of the body can become difficult. At this point, useful search tactics include the use of cadaver dogs, search parties and aerial imaging, all of which can be expensive and/or time consuming for law enforcement agencies. This research presented a novel search and recovery technique by utilizing a drone mounted with a thermal imaging camera to successfully detect larval aggregations on a decomposing carcass.

5.1 Maggot Mass Temperatures

The lab-controlled study aimed to determine a baseline for the amount of heat generated by larval aggregations within the Connecticut region. Different sized larval aggregations were generated using the *Phormia regina* flies that were collected outside Dr. R Christopher O'Brien's laboratory in West Haven, Connecticut. In completing two experimental replicates, this study confirmed previous research in that different sized larval aggregations did produce varying amounts of heat (Slone & Gruner, 2007). Additionally, this study established that within the laboratory alone, the temperature of larval aggregations in the Connecticut region can reach greater than 15°C above ambient temperature. This temperature difference between larval aggregations and ambient temperature also verifies previous research, which have reported similar differences in temperature (Anderson & VanLaerhoven, 1996; Slone & Gruner, 2007; Turner & Howard, 1992).

The consistency in reported larval aggregation temperatures between researchers allows for differences in temperature to be estimated between larval aggregations and ambient conditions during search and recovery missions (Anderson & VanLaerhoven, 1996; Slone & Gruner, 2007; Turner & Howard, 1992). Drone operators can use previously collected

aggregation temperatures to determine the likelihood of detecting a larval aggregation on a decomposing body, when also taking into consideration circumstances of the case, such as the size of the missing individual, and the environmental conditions of the suspected area.

5.2 Factors Affecting the Capability of Detection of Larval Aggregations

The capability of detecting the hot water analogs and the carcasses using a drone mounted with a thermal imaging camera varied depending on different factors. These factors can include drone height, maggot mass size, wind, sunlight and ambient temperature.

5.2.1 Drone Height

This study demonstrated that the detection of the hot water baths and coyote (*Canis latrans*) carcass was affected by the height of the drone. As the drone height increased, the thermal signature of the hot water baths and carcass became masked, or overwhelmed, by the thermal signature of the surrounding substrates (O'Brien, pers. comm., September 2018). This thermal masking resulted in decreased temperature measurements and decreased visibility of the hot spots by the drone FLIR. At greater heights, the thermal signature of these hot spots became indistinguishable from its surroundings due to this masking effect. Thermal drones should therefore be flown at the lowest height possible in order to limit the effect of thermal masking and to optimize the detection of larval aggregations on decomposing remains during search and recovery missions.

Due to the lack of research pertaining to optimal drone search heights, this study aimed to determine at what heights the thermal drone was capable of detecting larval aggregations. Based

on the thermal images captured from this study, a drone search height greater than approximately 25 meters can subject the thermal signature to greater masking and can prevent detection of the hot spot. While lower drone heights are optimal for greater detection of heat signatures, it may not always be possible for drone operators to maneuver the drone at lower heights, such as if the search area contains tall objects such as trees or buildings. Therefore, when flying the drone at heights above 25 meters in search and recovery missions, drone operators should be aware that decomposing remains may be located within the search region but could be undetectable due to this thermal masking effect.

Height had a greater impact on the detection of larval aggregations when utilizing a thermal drone than a helicopter mounted with a FLIR. In the research conducted by Lee et al. (2018), a helicopter mounted with a FLIR successfully detected larval aggregations on decomposing pig (*Sus scrofa)* carcasses at heights greater than 1000 meters. In comparison, the thermal drone had difficulty in detecting the coyote carcass at a height of 50 meters. The discrepancy in the capability of detection at different heights demonstrates one of the limitations of this search technique. Although the helicopter mounted with a FLIR is more expensive and time-consuming to utilize, this more advanced technology does have greater capabilities for detection and, therefore, may be more successful in locating larval aggregations than a thermal drone.

5.2.2 Maggot Mass Size

The different sized hot water baths utilized for this research demonstrated that a smaller heat source yields greater thermal masking potential, making it more difficult to detect at each height. The hot water baths were utilized as analogs for maggot masses, which produce specific

amounts of heat depending on the size of the mass and the amount of food source available (Charabidze et al., 2011; Slone & Gruner, 2007). Therefore, the smaller the size of the remains, the smaller the larval aggregations that can form and the more difficult it will be to detect the remains at increasing drone height.

In search and recovery missions, the size of the missing person should be taken into consideration in order to determine the optimal drone height for detection. For example, a child will be more difficult to detect at a drone search height of 20 meters than that of a grown adult, as the larval aggregation is likely to be smaller in size. This smaller aggregation will not only emit less heat but will also be subjected to greater thermal masking effects.

5.2.3 Wind

This research demonstrated that while the ability to detect the thermal signature is not affected by wind, the ability to detect the exact location of the hot spot can be. Even when wind speeds were mild (1.0 mps) and did not affect the stability of the drone platform, thermal signatures of the hot spots were displaced within the drone images by approximately a meter. Therefore, during search and recovery missions, this wind effect may mislead the drone operator in determining the exact location of the detected hot spot and may require additional ground searching of the surrounding area to successfully locate the body.

In this study, the effect of wind on the location of the hot water bath's or carcass's hot spot was overcome by removing the thermal filter and viewing the area as a real image. By removing the thermal filter when wind was suspected to affect the thermal signature, the true location of

the heat source was identified. The limitation to this methodology is that these experiments were not conducted blind, meaning that the true location of the heat source was known, therefore making it easier to determine its exact location within the image. However, in search and recovery missions, this may not be as efficient as the location of the body is not known and may not be detectable even when removing the thermal signature.

Drone operators should therefore be aware that when wind seems to be affecting the drone's thermal imaging, caution should be taken in providing exact coordinates for the location of the thermal signature. Drone operators should make personnel conducting a ground search aware that the true location of the body may not be where the hot spot was detected, but rather in the surrounding area.

5.2.4 Solar Radiation

This research demonstrated that on days when sunlight is shining directly on an area of interest, a thermal drone may not be the most effective search technique for law enforcement to utilize. The thermal signature of the larval aggregations associated with decomposing remains will likely be overlooked by the drone operator if it is located within or near the area in direct sunlight, as thermal equilibrium will be reached between the aggregation and the area absorbing the solar radiation (O'Brien, pers. comm., May 2019). The larval aggregations will become similar in temperature to the surrounding environment, therefore limiting the capability of detection by the thermal drone.

Lee et. al (2018) observed similar effects on the capability of detection as sunlight prevented the helicopter mounted FLIR from differentiating between the larval aggregations and the areas warmed by sunlight. Based on the observations made during this research, it was suggested that the optimal time of day for detection is pre-dawn (Lee et al., 2018). It is during this time that the solar radiation absorbed from sunlight during the day has dissipated and the ambient temperature is lowest, contributing to a greater temperature difference between the larval aggregations and the surrounding substrates (Lee et al., 2018).

Therefore, based on the current and previous research, a thermal drone would be more effective in detecting larval aggregations in the hours preceding sunrise or on days when direct sunlight is minimal (i.e. cloudy conditions).

5.2.5 Ambient Temperature

The lack of fly colonization on the white-tailed deer fawn *(Odocoileus virginianus)* carcass in November 2018 displayed the limitation of using this search technique in temperate regions experiencing seasonal changes in temperature. The survival of Diptera is strongly influenced by temperature, and as ambient temperature becomes low, survival decreases (Rivers & Dahlem, 2014; Voss et al., 2014). Minimum developmental temperatures for forensically significant fly species have been reported between 10°C and 15°C (Byrd & Allen, 2001; Nabity, Higley, & Heng-Moss, 2006). Any temperature below the minimum developmental temperature will negatively affect the growth and survival of fly species, limiting the success of this search technique.

Throughout the time the fawn carcass was placed at the experimental site, the average ambient temperature was approximately 10°C, which was too low for larvae to survive. Therefore, a thermal drone would not be successful in detecting decomposing remains below ambient temperatures of at least 10°C in the Connecticut region, as no larval aggregations will form, and the body will be indistinguishable from the surrounding substrates. This search technique could only be utilized by law enforcement for search and recovery missions when ambient conditions were optimal for Diptera growth and development.

The low temperatures (~ 10°C) that occurred in November 2018 prevented Diptera growth and development entirely. However, when temperatures are low but above the minimum developmental temperature, larval development does occur, just at a slower rate. The research conducted by Lee et al. (2018) demonstrated that lower temperatures can actually benefit the use of this search technique in missing person cases. During the winter trial, the lower ambient temperatures (average of 19.3°C during the day and 4.9°C at night) resulted in a longer duration of larval aggregation activity and therefore an increase in the time window for detection by the helicopter FLIR (Lee et al., 2018). Lower temperatures can provide law enforcement with a greater timeframe in which they can utilize this search technique to locate larval aggregations on decomposing remains.

The capability of detection can also be affected if ambient temperature becomes too warm, as was reported in the research by Lee et al. (2018). High temperatures during the autumn trial (average of 33.4°C during the day and 13.1°C at night) led to larval death on the pig carcasses, which resulted in decreased visibility by the helicopter FLIR. In this current research, ambient

temperatures did not become high enough for larval death to occur, and therefore did not affect the capability of detection within the Connecticut region.

The current and previous research demonstrates that the implementation of this search technique can vary between geographic regions due to the varying climatic conditions, such as ambient temperature, that affected the capability of detection. These two regions experienced opposite extremes in temperature which affected the capability of detection. In this current study, ambient temperature in Connecticut became too low for larval aggregations to form, while in the previous research conducted by Lee et al. (2018) in Western Australia, ambient conditions became too high for larvae to survive. Therefore, in order to successfully implement this search technique into search and recovery missions, drone operators need to become aware of the temperature thresholds of Diptera species, which will require collaboration with entomologists that have developmental data of forensically significant species within each region

5.3 Operator ability

In completing this research, it became apparent that successful detection of larval aggregations will ultimately be dependent on the ability of the drone operator. Lee et al. (2018) came to the same conclusion when the success of locating the pig carcasses was limited by the ability of the FLIR operator to calibrate the instrument. When the helicopter FLIR was poorly calibrated, larval aggregations associated with the pig carcasses went undetected. Lee et al. (2018) demonstrated that the success of this search technique is dependent on the ability of the operator to utilize the equipment properly and to optimize the technology for successful detection. Therefore, drone operators not only need to possess the skills to maneuver the drone,

but also need to be aware of the factors that can affect the capability of detection, such as drone height, maggot mass size, wind and direct sunlight.

Through multiple replicates and utilization of different drones, the primary investigator in this research acquired the skills needed to successfully detect larval aggregations associated with a decomposing carcass. Therefore, drone operators need to undergo training in order to enhance their understanding of how these factors can affect detection, and to learn how search parameters can be adjusted to optimize the success of locating larval aggregations. This research demonstrated that hot water baths work well as an analog for larval aggregations, with the added ability to adjust the temperature and size in order to simulate various circumstances that may be encountered during a search mission. Thus, operators could utilize hot water baths to practice maneuvering the drone and adjusting search parameters to enhance detection of the hot spots. It is also important for drone operators to become aware of and keep up to date on research and concepts related to larval aggregations and developmental thresholds of forensically significant fly species in each region.

5.4 Applicability in Forensic Science

. Thermal drones are increasingly being used by law enforcement agencies in every day operations, such as for surveillances and pursuits (Perritt & Spraque, 2017). This technology has also been incorporated in search and rescue missions but has not yet been utilized in circumstances when a missing individual is believed to be deceased.

In missing persons cases, law enforcement can search a suspected area, which is often remote and extensive, for an extended period of time in hope of locating a body. More often than not, these search tactics fail to locate the missing individual. For example, in the case of Mollie Tibbetts, who disappeared on 18 July 2018, search parties and helicopters scoured the area near where she was living for a month after her disappearance, looking for any clues to her whereabouts (Earl, 2018). However, Mollie Tibbetts's body was not located until 21 August 2018, when the primary suspect in the case led police officers to the cornfield where he had hidden her body (Earl, 2018).

The disappearance of Mollie Tibbett is an example of when a thermal drone would have been useful for searching a large area for a body. Having disappeared in summer when ambient temperatures are ideal for insect development, larval activity would have been prevalent on the body soon after death. A thermal drone could have easily been deployed in an attempt to detect the thermal signature of larval aggregations that would have been present on the body. This technique, if successful, could have led to the discovery of the body sooner. Cases like Mollie Tibbett's hinder law enforcement due to the amount of time and money that is spent searching for a body. Thus, this novel search technique provides law enforcement with an alternative search tactic that is more cost effective, less time-consuming and easier to use.

However, while this research demonstrates that a thermal drone can detect larval aggregations on a decomposing carcass, it also demonstrates that there are limitations to when or how this technique can be implemented during search and recovery missions. Different factors including drone height, maggot mass size, wind, sunlight and ambient temperature were shown

to limit the capability of detecting heat sources. Therefore, operators need to be trained for detecting dynamic heat sources like larval aggregations, in order to learn how to adjust search parameters to enhance the success of this search technique during search and recovery missions

5.4.1 Suggested Search Parameters

The following are suggested search parameters to optimize the success of using a thermal drone to detect larval aggregations on decomposing remains:

- Prior to deployment, drone operators should gather important information to guide the search such as:
    - Size of the missing individual (i.e. child vs. adult)
    - Ambient temperature and environmental conditions
    - Layout of suspected area
- The thermal drone should be deployed prior to sunrise or on days when conditions are cloudy
    - The thermal drone should not be utilized when there is direct sunlight in the suspected area as the hot spot could go undetected
- The thermal drone should be flown at the lowest height possible to increase the likelihood of detecting a hot spot region.
    - In areas where heights below 25 meters cannot be achieved, ground searches should continue as hot spots could become indistinguishable from the surrounding substrates due to thermal masking
    - The smaller the size of the individual, the lower the height of the drone should be

- Light winds should be assumed to affect the displacement of the thermal signature within the drone images.
    - Drone operators can attempt to locate the exact location of the thermal signature by removing the thermal filter and viewing the area as a real image

5.5 Limitations

The greatest limitation of this study was the technological complications encountered with the drones and thermal cameras throughout the course of this research. A considerable amount of time was spent attempting to integrate the FLIR Duo™ thermal imaging camera with the DJI Phantom™ 3 Standard drone and DJI Phantom™ 2 drone, before determining that the technologies were not viable or optimal for the aims of this research. Although the Parrot Bebop-Pro Thermal™ drone was optimal for the aims of this research, having both an integrated thermal imaging camera and first-person view (FPV) capability, there were complications encountered with the drone which delayed the progress of this research. These complications included finding a tablet that was compatible with the FreeFlight Thermal™ mobile application, the mobile application frequently quitting and not connecting to the drone, and the drone crashing twice due to a GPS and battery failure. These complications delayed this research for variable amounts of time, which ultimately limited the number of hot water bath and carcass replicates that could be completed.

An initial aim of this research was to conduct a blind experiment in which the thermal drone would be utilized to search for a carcass in an unknown location. However, the drone complications encountered also inhibited this blind detection experiment from being conducted.

The ability to replicate the field-based study was limited due to the low ambient temperatures that occurred during the winter season in the Connecticut region. This low temperature prevented larval aggregations from forming on the white-tailed deer fawn (*Odocoileus virginianus)* that was placed outside in November 2018. When ambient temperature remained below the developmental threshold for Diptera species, which was approximately a five month time period, no data could be collected from the formation of larval aggregations.

Another limitation in this study was the difficulty in maintaining viable fly colonies during the transition to the winter months between November 2018 and February 2019. Daylight from a window in the colony room was the only source of light for the flies, and as the hours of daylight decreased during this time period, the flies did not have enough light throughout the day and entered diapause. Diapause prevented some of the flies in colony from laying eggs, while other flies did lay eggs, but the eggs were not viable. By February 2019, many of the fly colonies had died off and the stock of fly pupae needed to be replenished in order to replenish the colonies. This difficulty severely suppressed the success of the fly colonies and prevented additional replicates from taking place in the lab-controlled study of this research.

5.6 Further Research

In order to conduct further research, a more reliable drone and thermal camera set-up would be needed. The Parrot Bebop-Pro Thermal™ drone is no longer manufactured and can therefore not be utilized for any future research or by law enforcement for search and recovery missions. Parrot© is currently manufacturing a new thermal drone, Anafi™ Thermal. However, based on experience with the Parrot© company and their manufactured products, this new thermal drone is not suggested as a viable option for search and recovery purposes. Additional

research needs to take place to determine if there are any new thermal drones being manufactured that is still cost effective and efficient for law enforcement use.

Blind detection experiments could be conducted in order to simulate an experience similar to that encountered by law enforcement in search and recovery missions. Carcasses would be placed in a location unknown to the drone operator. The operator would then utilize the drone with the thermal camera to attempt to determine the location of the carcass via the heat signature of associated larval aggregations.

Further research could also aim to understand how the capability of detection is affected by concealment of a carcass. In homicide cases, the perpetrator may attempt to conceal the body in order to prevent its discovery. Attempts at concealment could include covering the body with debris or fabric, placing the body within a bag or container, and/or placing the body in a remote, wooded area with dense tree coverage. These circumstances could further mask the thermal signature of the larval aggregations associated with the body, potentially limiting the success of the drone and thermal camera in search and recovery missions. To investigate this aim, the same experimental protocols as utilized in this research could be followed, but with the added component of covering the hot water bath and/or carcasses.

CHAPTER 6: CONCLUSIONS

University of New Haven
HENRY C. LEE COLLEGE OF
CRIMINAL JUSTICE AND FORENSIC SCIENCES
Department of Forensic Science

6.1 Conclusions

The research conducted for this thesis had the following conclusions:

- The success of the drone technology to detect thermal signatures was dependent on several factors.
    - The DJI Phantom™ 3 Standard drone was unable to be used for this research as the built-in camera was completely integrated into the flight system and could not be replaced with the FLIR Duo® thermal camera. Additionally, the drone's payload limit prevented an external thermal camera from being mounted to it.
    - The DJI Phantom™ 2 drone was configured to have a thermal camera with first person view capabilities. However, due to the instability of the flight platform and pixelated imaging, it was not found to be a viable search and recovery instrument.
    - The Parrot Bebop-Pro Thermal™ drone was an initially viable flight platform as it had a real time camera and thermal camera installed.
        - The Parrot Bebop-Pro Thermal™ drone was eventually found to be flawed in its design as both GPS and battery malfunctions occurred, leading to catastrophic failures.
        - This drone is no longer manufactured, therefore its applicability to search and recovery personnel is irrelevant.

- The lab-controlled study established that different sized larval aggregations produce different amounts of heat.

    - The temperature of larval aggregations in the Connecticut region can reach greater than 15°C above ambient temperature.
- The sensitivity of detection of hotspots decreases with increasing drone height.
    - The thermal signature of the hot spot becomes masked by the thermal signature of the surrounding environment.
    - The effect of thermal masking is impacted by both the size of the hot spot and the height of the drone.

- A drone mounted with a thermal imaging camera can be utilized to detect larval aggregations on decomposing carcasses and could therefore be implemented by law enforcement for search and recovery missions.
    - Detection depends on the height of the drone, size of the maggot mass, ambient conditions and operator ability.

References

Agbeyangi, A. O., Odiete, J. O., & Olorunlomerue, A. B. (2016). Review on UAVs used for Aerial Surveillance. *Journal of Multidisciplinary Engineering Science and Technology*, *3*(10), 2458–9403.

Amendt, J., Rodner, S., Schuch, C. P., Sprenger, H., Weidlich, L., & Reckel, F. (2017). Helicopter thermal imaging for detecting insect infested cadavers. *Science and Justice*, *57*(5), 366–372.

Anderson, G. S. (2000). Minimum and maximum development rates of some forensically important Calliphoridae (Diptera). *Journal of Forensic Sciences*, *45*(4), 824–832.

Anderson, G. S. (2001). Chapter 5: Insect succession on carrion and its relationship to determining time of death. In J.H Byrd & J. Castner (Eds.), *Forensic entomology: the utility of arthropods in legal investigations* (pp. 143–175). Boca Raton: CRC Press.

Anderson, G. S. (2014). Chapter 7: Forensic entomology. In S. H. James, J. J. Nordby, & S. Bell (Eds.), *Forensic science: An introduction to scientific and investigative techniques* (Fourth, pp. 171–199). Boca Raton, FL: Taylor & Francis Group.

Anderson, G. S., & VanLaerhoven, S. L. (1996). Initial observations on insect succession on carrion in British Columbia. *Journal of Forensic Sciences*, *41*(4), 613–621.

Arjomandi, M., Agostino, S., Mammone, M., Nelson, M., & Zhou, T. (2006). *Classification of unmanned aerial vehicles*. Adelaide, Australia.

Arlington police now using drones to catch criminals. (2019). Retrieved March 29, 2019, from http://www.fox4news.com/news/arlington-police-now-using-drones-to-catch-criminals

Barton Browne, L., Bartell, R. J., & Shorey, H. H. (1969). Pheromone-mediated behaviour leading to group oviposition in the blowfly *Lucilia cuprina*. *Journal of Insect Physiology*, *15*(6), 1003–1014.

Bornemissza, G. F. (1957). An analysis of arthropod succession in carrion and the effect of its decomposition on the soil fauna. *Australian Journal of Zoology*, *5*, 1–12.

Brewster, M. Q. (1992). *Thermal radiative transfer and properties*. Canada: John Wiley & Sons, Ltd.

Byrd, J.H, & Castner, J. (2001). Chapter 2: Insects of forensic importance. In J. Castner & J. Byrd (Eds.), *Forensic entomology: the utility of arthropods in legal investigations* (pp. 43–75). Boca Raton.

Byrd, Jason H., & Allen, J. C. (2001). The development of the black blow fly, *Phormia regina* (Meigen). *Forensic Science International*, *120*(1–2), 79–88.

Campobasso, C. Pietro, Di Vella, G., & Introna, F. (2001). Factors affecting decomposition and Diptera colonization. *Forensic Science International*, *120*(1–2), 18–27.

Catts, E. P., & Goff, M. L. (1992). Forensic Entomology in Criminal Investigations. *Annu. Rev. Entomol.*, *37*, 253–272.

Charabidze, D., Bourel, B., & Gosset, D. (2011). Larval-mass effect: Characterisation of heat emission by necrophageous blowflies (Diptera: Calliphoridae) larval aggregates. *Forensic Science International*, *211*(1–3), 61–66.

Cheng, E. (2016). *Aerial photography and videography using drones*. Berkley, CA: Peachpit Press.

Christopherson, C., & Gibo, D. L. (1997). Forgaing by food deprived larvae of *Neobellieria bullata* (Diptera: Sarcophagidae). *Journal of Forensic Sciences*, *42*(1), 71–73.

Clark, K., Evans, L., & Wall, R. (2006). Growth rates of the blowfly, *Lucilia sericata*, on different body tissues. *Forensic Science International*, *156*(2–3), 145–149.

Dadour, I. R., Cook, D. F., & Wirth, N. (2001). Rate of development of *Hydrotaea rostrata* under summer and winter (cyclic and constant) temperature regimes. *Medical and Veterinary Entomology*, *15*, 177–182.

Davies, L., & Ratcliffe, G. G. (1994). Development rate of some pre-adult stages in blowflies with reference to low temperatures. *Medical and Veterinary Entomology*, *8*, 245–254.

Dekeirsschieter, J., Verheggen, F. J., Gohy, M., Hubrecht, F., Bourguignon, L., Lognay, G., & Haubruge, E. (2009). Cadaveric volatile organic compounds released by decaying pig carcasses (Sus domesticus L.) in different biotopes. *Forensic Science International*, *189*(1–3), 46–53.

Deonier, C. C. (1940). Carcass Temperatures and Their Relation to Winter Blowfly Populations and Activity in the Southwest. *Journal of Economic Entomology*, *33*(1), 166–170.

DesMarais, A. M. (2014). Detection of cadaveric remains by thermal imaging cameras. *Journal of Forensic Identification*, *64*(5), 489–512.

Donovan, S. E., Hall, M. J. R., Turner, B. D., & Moncrieff, C. B. (2006). Larval growth rates of the blowfly, *Calliphora vicina*, over a range of temperatures. *Medical and Veterinary Entomology*, *20*(1), 106–114.

Earl, J. (2018). Mollie Tibbetts, University of Iowa student, found dead: A timeline of events.

Early, M., & Goff, M. L. (1986). Arthropod succession patterns in exposed carrion on the island of O' ahu, Hawaiian Islands, USA. *Journal of Medical Entomology*, *23*, 520–531.

Edelman, G. J., Hoveling, R. J. M., Roos, M., van Leeuwen, T. G., & Aalders, M. C. G. (2013). Infrared imaging of the crime scene: Possibilities and pitfalls. *Journal of Forensic Sciences*, *58*(5), 1156–1162.

Eisemann, C. H., & Rice, M. J. (1987). The origin of sheep blowfly, *Lucilia cuprina* (Wiedemann) (Diptera: Calliphoridae), attractants in media infested with larvae. *Bulletin of Entomological Research*, *77*(2), 287–294.

Flores, D., Miller, A. L., Showman, A., Tobita, C., Shimoda, L. M. N., Sung, C., Turner, H. (2016). Fluorescence Imaging of Posterior Spiracles from Second and Third Instars of Forensically Important *Chrysomya rufifacies* (Diptera: Calliphoridae). *Journal of Forensic Sciences*, *61*(6), 1578–1587.

Franzen, C. (2013). Canadian mounties claim first person's life saved by a police drone. Retrieved March 29, 2019, from https://www.theverge.com/2013/5/10/4318770/canada-draganflyer-drone-claims-first-life-saved-search-rescue

Frederickx, C., Dekeirsschieter, J., Verheggen, F. J., & Haubruge, E. (2012). Responses of *Lucilia sericata* Meigen (Diptera: Calliphoridae) to Cadaveric Volatile Organic Compounds. *Journal of Forensic Sciences*, *57*(2), 386–390.

Galloway, A. (1997). The process of decomposition: A model from the Arizona-Sonoran desert. In W. D. Haglund & M. H. Sorg (Eds.), *Forensic taphonomy: The postmoretm fate of human remains* (pp. 139–150). Boca Raton, FL: CRC Press.

Gennard, D. E. (2007). *Forensic entomology: An introduction*. Chichester, UK: John Wiley & Sons, Ltd.

Gill-King, H. (2006). Chapter 6: Chemical and ultrastructural aspects of decomposition. In W. D. Haglund & M. H. Sorg (Eds.), *Forensic taphonomy: The postmortem fate of human remains* (pp. 93–108). Boca Raton, FL: CRC Press.

Goff, M. L. (2009). Early post-mortem changes and stages of decomposition in exposed cadavers. *Experimental and Applied Acarology*, *49*(1–2), 21–36.

Goff, M. L. (2010). Chapter 1: Early postmortem changes and stages of decomposition. In J. Amendt, C. Pietro Campobasso, M. L. Goff, & M. Grassberger (Eds.), *Current Concepts in Forensic Entomology* (pp. 1–24). Springer.

Grassberger, M., & Frank, C. (2004). Initial study of arthropod succession on pig carrion in a central European urban habitat. *Journal of Medical Entomology*, *41*(3), 511–523.

Grassberger, M., & Reiter, C. (2001). Effect of temperature on *Lucilia sericata* (Diptera: Calliphoridae) development with special reference to the isomegalen- and isomorphen-diagram. *Forensic Science International*, *120*(1–2), 32–36.

Grassberger, M., & Reiter, C. (2002). Effect of temperature on development of the forensically important holarctic blow fly *Protophormia terraenovae* (Robineau-Desvoidy) (Diptera: Calliphoridae). *Forensic Science International*, *128*(3), 177–182.

Greenberg, B., & Kunich, J. C. (2002). *Entomology and the law: Flies as forensic indicators*. New York: Cambridge University Press.

Hall, R. D. (2005). Chapter 1: Medicocriminal entomology. In E. P. Catts & N. H. Haskell (Eds.), *Entomology & death, a procedural guide*. Clemson: Joyce's Print Shop, Inc.

Hammack, L. (1990). Protein Feeding and Oviposition Effects on Attraction of Screw worm Flies (Diptera: Calliphoridae) to Host Fluids. *Ann Entomol. Soc Am.*, *83*(1), 97–102.

Heaton, V., Moffatt, C., & Simmons, T. (2014). Quantifying the temperature of maggot masses and its relationship to decomposition. *Journal of Forensic Sciences*, *59*(3), 676–682.

Herschel, W. (1800). To Heat and Illuminate Objects; With Remarks , That Prove. *Phil. Trans. R. Soc. Lond.*, *90*(January), 255–283.

Higley, L. G., & Haskell, N. . (2001). Chapter 9: Insect development and forensic entomology. In J.H Byrd & J. . Castner (Eds.), *Forensic entomology: the utility of arthropods in legal investigations* (pp. 287–300). Boca Raton, FL: CRC Press.

Iftirbashir. (2006). #7: DJI Phantom 2 - Complete FPV Setup Guide & Test - Step-By-Step! Retrieved February 21, 2018, from https://www.youtube.com/watch?v=hMxXQE_UAyQ

Johnson, A. P., Wighton, S. J., & Wallman, J. F. (2014). Tracking Movement and Temperature Selection of Larvae of Two Forensically Important Blow Fly Species Within a "Maggot Mass." *Journal of Forensic Sciences*, *59*(6), 1586–1591.

Johnston, W., & Villeneuve, G. (1897). On the medico-legal application of entomology. *Montreal Medical Journal*, *26*, 81–90.

Joy, J. E., Liette, N. L., & Harrah, H. L. (2006). Carrion fly (Diptera: Calliphoridae) larval colonization of sunlit and shaded pig carcasses in West Virginia, USA. *Forensic Science International*, *164*(2–3), 183–192.

Lee, M., Voss, S. C., Franklin, D., & Dadour, I. R. (2018). Preliminary investigation of aircraft mounted thermal imaging to locate decomposing remains via the heat produced by larval aggregations. *Forensic Science International*, *289*, 175–185.

Lee, M. J. (2017). *Utilising aircraft mounted forward looking infrared radar to locate decomposing remains via the heat signature of blowfly larval aggregations*. University of Western Australia.

Liu, D., & Greenberg, B. (1989). Immature stages of some flies of forensic importance. *Ann Entomol. Soc Am.*, *82*(1), 80–93.

Lloyd, J. M. (1975). *Thermal imaging systems*. New York: Springer Science + Business Media.

Mcknight, B. . (1981). *The washing away of wrongs: Forensic medicine in thirteenth-century china*. University of Michigan, Ann Arbor.

Nabity, P. D., Higley, L. G., & Heng-Moss, T. M. (2006). Effects of temperature on development of *Phormia regina* (Diptera: Calliphoridae) and use of developmental data in determining time intervals in forensic entomology. *Journal of Medical Entomology*, *43*(6), 1276–1286.

Notter, S. J., Stuart, B. H., Rowe, R., & Langlois, N. (2009). The initial changes of fat deposits during the decomposition of human and pig remains. *Journal of Forensic Sciences*, *54*(1), 195–201.

O'Brien, R. C. (2008). *Forensic animal necrophagy in the South-West of Western Australia : species, feeding patterns and taphonomic effects*. The University of Western Australia.

Ody, H., Bulling, M. T., & Barnes, K. M. (2017). Effects of environmental temperature on oviposition behavior in three blow fly species of forensic importance. *Forensic Science International*, *275*, 138–143.

Payne, J. A. (1965). A Summer Carrion Study of the Baby Pig Sus Scrofa Linnaeus. *Ecology*, *46*(5), 592–602.

Peirce, P. (2019). Murrysville police make 1st arrests using drone to tack suspects. Retrieved March 28, 2019, from https://triblive.com/local/westmoreland/murrysville-police-use-drone-to-track-2-suspects-after-rt-22-crash/

Perritt, H. H., & Spraque, E. O. (2017). *Domesticating drones: The technology, law, and economics of unmanned aircraft*. New York, NY: Routledge.

Petersen, J. K. (2007). *Understanding surveillance technologies: Spy devices, privacy, history & applications* (2nd ed.). Boca Raton, FL: Taylor & Francis Group.

Reed, H. B. (1958). A study of dog carcase communities in Tennessee, with special reference to the insects. *The American Midland Naturalist*, *59*, 213–245.

Rivers, D. B., Ciarlo, T., Spelman, M., & Brogan, R. (2010). Changes in Development and Heat Shock Protein Expression in Two Species of Flies *Sarcophaga bullata* [Diptera: Sarcophagidae] and *Protophormia terraenovae* [Diptera: Calliphoridae] Reared in Different Sized Maggot Masses. *Journal of Medical Entomology*, *47*(4), 677–689.

Rivers, D. B., & Dahlem, G. A. (2014). *The Science of Forensic Entomology* (First). John Wiley & Sons, Ltd.

Rivers, D. B., Thompson, C., & Brogan, R. (2011). Physiological trade-offs of forming maggot masses by necrophagous flies on vertebrate carrion. *Bulletin of Entomological Research*, *101*, 599–611.

Rodriguez, W. C., & Bass, W. M. (1983). Insect activity and its relationship to decay rates of human cadavers in east Tennessee. *Journal of Forensic Sciences*, *28*, 423–432.

Sharma, R. (2015). Various methods for the estimation of the post mortem interval from Calliphoridae : A review. *Egyptian Journal of Forensic Sciences*, *5*(1), 1–12.

Slone, D. H., & Gruner, S. (2007). Thermoregulation in Larval Aggregations of Carrion-Feeding Blow Flies (Diptera: Calliphoridae). *Journal of Medical Entomology*, *44*(3), 516–523.

Smith, K. G. V. (1986). *A Manual of Forensic Entomology*. London: Trustees of the British Museum (Natural History) and Cornell University Press.

Turner, B., & Howard, T. (1992). Metabolic heat generation in dipteran larval aggregations: a consideration for forensic entomology. *Medical and Veterinary Entomology*, *6*(2), 179–181.

Ubelaker, D. H. (2006). Chapter 5: Taphonomic applications in forensic anthropology. In W. D. Haglund & M. H. Sorg (Eds.), *Forensic taphonomy: The postmortem fate of human remains* (pp. 77–90). Boca Raton, FL: CRC Press.

Vass, A. A. (2001). Beyond the grave - understanding human decomposition. *Microbiology Today*, *28*, 190–192.

Vollmer, M., & Mollmann, K. . (2017). *Infrared thermal imaging: Fundamentals, research and applications* (2nd ed.). Weinheim, Germany: John Wiley & Sons.

Voss, S.C. (2010). *Investigation of hymenopteran parasitoids of forensic importance: indicators of post-mortem interval*. University of Western Australia.

Voss, S.C., Cook, D. F., Hung, W. F., & Dadour, I. R. (2014). Survival and development of the forensically important blow fly, *Calliphora varifrons* (Diptera: Calliphoridae) at constant temperatures. *Forensic Science, Medicine, and Pathology*, *10*(3), 314–321.

Voss, S.C., Spafford, H., & Dadour, I. R. (2009). Annual and seasonal patterns of insect succession on decomposing remains at two locations in Western Australia. *Forensic Science International*, *193*(1–3), 26–36.

Warren, P. (2017). Md. police dept. drone helps find $394K in stolen construction equipment from multiple states. Retrieved March 29, 2019, from https://baltimore.cbslocal.com/2017/03/16/md-police-dept-drone-helps-find-394k-in-stolen-construction-equipment-from-multiple-states/

Whitworth, T. (2017). Keys to the Genera and Species of Blow Flies (Diptera: Calliphoridae) of America, North of Mexico. *Proceedings of the Entomological Society of Washington*, *108*(3), 689–725.

APPENDICES

APPENDIX A: Protocol for Fly Colony Maintenance and Breeding

Fly Colony Maintenance

- New cage set-up:
    - Place the previously cut mesh over the PVC cage.
    - Ensure that there is enough mesh on both sides so they can be closed. Close one side with a rubber band → this will be the back of the cage.
    - The other side can be closed with a clip → this will be the front of the cage.
    - **It is very important that you make sure both sides are closed completely so the flies don't escape!**
- Each fly colony will need:
    - A petri dish of **sugar cubes**. These cubes will need to be changed about once a month depending on the size of the colony. You will know they need to be changed when they are crumbling and falling apart.
    - **Water**. A hole should be made in the lid of the urine collection cup. Then a square from a T-shirt (previously cut in one of the baskets) should be put through the hole. Some of the shirt should be sticking out the top, while most should be sitting inside the cup. Fill the cup with water and ensure that the water is wicked up before placing inside the colony.
        - The water probably needs to be changed about once a week. Again, this change depending on how large the colony is. I recommend checking this daily to ensure that they have water.
- To begin the colony:
    - If pupae are in refrigerator: put contents from urine collection cup on a petri dish and place in colony. Wait to emerge.
    - If using pupae directly from a rearing dish: remove meat and place dish (with sand and pupae) directly into colony. Wait to emerge.
    - If using a fly trap: place trapped flies into the colony

Blood Feed Instructions

- A blood feed should be done a minimum of once a week, sometimes twice depending on the colony. This can be based off of how many eggs are being laid.
- Liver should be cut up into cubed form and placed in a large weigh boat (there is a sharp knife and cutting board to do this)
    - Use a pipette to transfer blood from the bottom of the liver container to the weigh boat. Place a good amount of blood onto the liver, but do not saturate it as you do not want to drown the eggs. You can also spray the liver meat with a little bit of water, but also do not saturate it. There should not be a pool of liquid at the bottom.
- Place the weigh boat in the colony.
- Make sure to wash the knife, pipette and cutting board after finishing. When the blood dries it is difficult to wash off.
- Another thing to keep in mind is the amount of liver you have in the fridge. If you are running low, make sure to take out another liver far enough in advance so that it has time to thaw. You can stick the liver in a plastic container and place it into the fridge.

Rearing Dish Preparation and Maintenance

- The liver should be in the fly colony for about 24 hours. A rearing dish needs to be prepped the following day after the protein feed.
- If the flies did not lay, you can throw the weigh boat away. If the flies did lay, do the following,
    - Fill the plastic container with sand (about 1⁄2 full)
    - Place a good amount of ground beef on a plate or weigh boat. Place on top of the sand.
    - Similar to the protein feed, use a pipette to transfer some of the blood (from the liver container) on to the ground beef. Again, this is not to saturate it.
    - Place the liver cubes that have eggs laid on them on top of the ground beef. Try to get as many eggs as possible on to the beef.
    - Spray the beef with water. Hold the spray bottle about a foot away from the meat, and spray about 3 or 4 times. Again, we do not want to saturate them, just keep them moist!
    - Place a mesh square (already pre-cut) on top of the plastic container. Place a rubber band over the rearing mesh. You should make sure that there are no holes where wandering maggots can escape from. The rubber band should be tight and close to the rim of the container.
    - Place the rearing dish on the shelf and label with correct number for binder keeping.
- The rearing dishes need to be sprayed **TWICE A DAY**
    - Make sure to take the mesh off and spray the meat directly (as directed above)
    - Again, make sure to put it on correctly so there are no holes for the maggots to escape
    - If the maggots are wandering to the outer rim of the plastic, be careful when taking the mesh off as the maggots will fall onto the table. At this point they are probably about to pupate so you can just leave the mesh on and just spray through the mesh.
- Once the maggots pupate, remove the meat and throw away.
    - Sieve the sand
    - Either put the pupae in a urine container and place in fridge (with species name, date and initials) or place directly into a fly colony
- Again, be aware of how much ground beef you have in the fridge. When you run low you need to take some out in advance so that it has time to thaw before you need it again
    - We are putting water crystals in the beef to keep it moist. When the meat you have taken out thaws completely, mix the water crystal beads with water. Wait for the beads to absorb the water and then mix in with the meat.

Other Important Information to Know

- You must fill out the binder each time you do something! This is so you and everyone else knows what has been done and which colony/dish is which.
- The binder consists of tabs for: Colony Sheets, Rearing Dish Sheets, Old Colony Sheets and Old Rearing Dish Sheets
- The codes for these sheets for what you have done are located on the wall next to the whiteboard
- On the top right of each sheet be sure to put which species is present in the colony/rearing dish (if known)
- Numbering system for Rearing Dishes:
    - This will be based off of which colony the eggs came from and how many rearing dishes are going.
    - Number = cage number; Letter = how many rearing dishes are already going
    - For example, if you set up a rearing dish for the first eggs laid in your colony, which is cage #4, your rearing dish number would be 4A. However, if you do a few more blood

feeds and you have two previous dishes from Cage #4 going, your new rearing dish number would be 4C.